N/?

Analysis of Major River Systems and Their Deltas: Procedures and Rationale, With Two Examples

by

J. M. Coleman and L. D. Wright

LOUISIANA STATE UNIVERSITY PRESS
BATON ROUGE
1971

ABSTRACT

The great river and delta systems of the world are considered as complex, interacting systems. All components are causally interrelated. Salient process and response parameters have been identified, and procedures for acquiring and generating parameter values have been standardized. Geological, geomorphological, climatological, pedological, biological, and hydrological factors in the drainage basin, alluvial valley, deltaic plain, and receiving basin are being systematically measured, computed, and tabulated for each of 55 of the world's major rivers and deltas.

Means of accurately describing the morphometry of large drainage basins by rapid electronic techniques have been devised. Values obtained are considered in relation to the water balance, soils, vegetation, and river regime. In the alluvial valley similar factors are measured. In addition, a comprehensive descriptive classification of alluvial valley landscapes has been devised.

In the delta such geomorphic and environmental parameters as the relative areas of various deltaic provinces, distributary patterns, landform types, river mouth and bar types, and deltaic bulge subaerial and subaqueous geometry are determined. Process parameters, including discharge, flood peakedness, sediment load, discharge efficiency, climate, etc., are considered as in the basin and alluvial valley.

The oceanographic regimes of the receiving basin are treated in detail. In addition to tides, winds, coastal currents, and continental shelf topography, wave climate and wave power variations along a delta coast are analyzed by a computer program which was developed for that purpose. This program takes into account the effects of wave refraction, shoaling, and frictional attenuation over varying subaqueous topographies.

Applications of these techniques and concepts to river systems analyzed to date have indicated that some process variables exert profound control over the delta morphology, whereas other effects are less conspicuous. The wave power and river discharge climates appear to be among the more important process factors.

The parameters measured have been arranged in a hierarchical fashion to facilitate input into a retrieval-comparison computer program. When data from all river systems have been compiled, this program will be used to compare process-response interactions and associations both within and between river systems.

Technical report obtained under Project No. ONR 1575 (03, Task Order No. NR388-002) of the Geography Branch, Office of Naval Research

ISBN 0-8071-0946-0

Printed in the United States of America Price $4.00

ACKNOWLEDGMENTS

This study was supported by the Coastal Studies Institute, Louisiana State University, under contract with the Geography Programs of the Office of Naval Research, Task Order No. N00014-69-A-0211-0003, Project No. NR 388 002.

The writers are indebted to Drs. W. G. McIntire, Director, R. J. Russell, S. M. Gagliano, and C. J. Sonu, Coastal Studies Institute, for advice and criticisms. Mrs. Romaine Kupfer conducted the literature survey. Mr. James McIntire rendered technical assistance in data acquisition. Programming assistance was given by Mrs. Nancy Roques and Dr. Myron Young of Louisiana State University and by Mr. John Dooley.

CONTENTS

Page
ABSTRACT. iii
ACKNOWLEDGMENTS iv
FIGURES vii
TABLES. viii
INTRODUCTION. 1
DEFINITION OF PARAMETERS. 7
Definitions and Methodology 7
SIGNIFICANCE OF PROCESS AND MORPHOLOGIC PARAMETERS. 51
The Drainage Basin. 51
GEOLOGY 51
GEOMORPHOLOGY 53
CLIMATE 55
PEDOLOGY AND VEGETATION 56
HYDROLOGY 56
The Alluvial Valley 56
GEOLOGY 57
GEOMORPHOLOGY 57
CLIMATE 59
HYDROLOGY 59
The Deltaic Plain 60
GEOLOGY 60
GEOMORPHOLOGY 60
CLIMATE AND VEGETATION. 64
HYDROLOGY 64
The Receiving Basin 65
GEOLOGY AND GEOMORPHOLOGY 65
CLIMATE 65
HYDROLOGY (PHYSICAL OCEANOGRAPHY) 66
APPLICATIONS OF TECHNIQUES TO THE NIGER AND SAO FRANCISCO DEL NORTE RIVER SYSTEMS 68
The Niger and São Francisco River Systems: A Comparison 88
BASIN GEOLOGY AND GEOMORPHOLOGY 88
BASIN CLIMATE AND HYDROLOGY 88
ALLUVIAL VALLEY CHARACTERISTICS 89
DELTAIC PLAIN MORPHOLOGY AND THE OCEANOGRAPHIC REGIME 89
CONCLUSION. 92
REFERENCES. 95
Appendix 1. FORTRAN IV LISTING FOR MAPCAL PROGRAM. 101
Appendix 2. WAVE ANALYSIS. 107

FIGURES

Figure		Page
1.	Major components of river systems	3
2.	Simplified structure diagram for organizing the data tabulated for each river system.	4
3.	Diagram illustrating definitions of terms used in hypsometric calculations.	12
4.	Examples of different drainage densities.	13
5.	Types of stream channels.	22
6.	Aerial photographs of the three major channel types	23
7.	Types of landforms in alluvial valleys.	24
8.	Aerial photographs of alluvial valley landforms	26
9.	Examples of common types of discharge curves.	28
10.	Components of deltaic plain	30
11.	Diagram illustrating distributary index	31
12.	Examples of interdistributary landform types.	32
13.	Aerial photographs of interdistributary types	35
14.	Examples of river mouth types	37
15.	Aerial photographs illustrating four river mouth types.	39
16.	River mouth bar types	40
17.	Diagram defining parameters used in deltaic bulge morphometry	41
18.	Diagrammatic representation of some parameter interactions in a river system	52
19.	Niger and São Francisco drainage basins	89
20.	Hypsometric curves for Niger and São Francisco drainage basins.	90
21.	Discharge/wave power climate of Niger River Delta	91
22.	Discharge/wave power climate of São Francisco River Delta	91

Figure Page

23. Refraction diagram for Niger River Delta 93

24. Refraction diagram for São Francisco River Delta. 94

TABLE

Table Page

1. River Systems Studied 5

INTRODUCTION

A major program of the Coastal Studies Institute for the past 12 years has been a continuing study of deltaic areas. Institute personnel have conducted field investigations of a variety of types of deltas, ranging from tropical, high-tide deltas to arctic, low-tide deltas. These projects have provided some insight into the variability that exists among many parameters from one delta to another. It became apparent that the importance of variability in both process and form was not precisely known because only a small sample had been studied. Furthermore, very little was known about which parameters were important and which were of little value in interpretation of geomorphic, geologic, and hydrologic characteristics of deltas. The field investigator was forced to measure as many variables as possible, often wasting valuable time on meaningless measurements. A rather thorough bibliographic search of published literature revealed that, although a considerable amount of data has been assembled on individual delta areas, little published material is available on comparisons of specific parameters within a variety of delta types. The first attempt at such a comparison was made by Credner (1878), who compiled information known at that time on several world deltas. Obviously many important parameters were not known at the time of that compilation. Following Credner's publication, many articles appeared on specific deltas and comparisons among a few deltas, but no systematic comparisons of a large number of deltas appeared until the publication by Samojlov (1956). This classic was published originally in Russian but later was translated into German. Samojlov's discussion on deltaic processes is accompanied by descriptions of 65 river deltas. Unfortunately, little attempt was made to compare forms and processes between deltas; most of Samojlov's work was descriptive in nature. The most recent attempt to compare parameters within deltas systematically was by Silvester and LaCruz (1970). Their approach differed from previous investigations in that an attempt was made to evaluate and compare parameters within deltas by statistical methods. This initial attempt indicated the feasibility of and the need for a more detailed systematic comparison of parameters between deltas. Silvester and LaCruz (1970, pp. 201-202) adequately stated the need for such a study:

> The importance of deltas in the life of mankind needs no stressing. Civilizations were founded on them and populations have been concentrated on them ever since. Man has required the vegetation that grows in soil for his basic needs. But besides supplying food, deltaic plains provide sources of water and economical means of communication. However, these zones of great human activity suffer some of the greatest natural disasters, in the form of flooding from the river system or of inundation from the sea when storm surges occur.
>
> The economic importance of deltas varies from continent to continent, but as the population of the world increases at the present rapid rate, greater demands will be placed on these food producing areas....

The Coastal Information Program on Deltaic Areas was initiated in 1966 by the

Institute under the auspices of the Office of Naval Research, Geography Programs. In the initial stages of the project, data banks, retrieval systems, statistical comparisons of parameters, and prediction models were envisioned as the major goals. Project personnel began to gather data on world deltas and to discuss with competent scientists computer techniques and retrieval systems. Within a short time the initial goals seemed to fade as problems at a much lower level became apparent.

During the data collection, for example, the following obstacles were encountered: (1) data were unequally distributed within various deltaic areas; (2) tabulated data included both qualitative and quantitative assessments; (3) the quality and standardization of work from one investigator to another varied considerably; and (4) terminology and word definition varied drastically from paper to paper. This latter point was especially difficult to overcome; the fact that in many cases terms were undefined and measurement techniques were not described precluded comparison of data from different sources.

A new evaluation of the project was made and the aims were redefined: to develop a framework for organization and management of information in deltaic areas so that it would ultimately be possible to predict both processes and conditions for areas in which field data were lacking. To accomplish this goal it seemed necessary to examine the entire river system rather than to concentrate solely on the delta. Numerous component parts of a river, shown diagrammatically in Figure 1, affect the physical setting of the delta. The major processes acting within these areas should exert some control over the type of delta which has formed in any geographic area. Water and sediment that will eventually reach the delta and influence its formation are derived mainly from the drainage basin. The alluvial valley acts as a conduit for transport of the sediment-water mixture from the drainage basin to the delta. However, processes such as trading of sediment by channel migration and evaporation of water modify the type and amount of material reaching the delta. Processes active in the receiving basin also influence the formation of the delta. Varying wave energy and littoral drift conditions produce different delta configurations. Thus, the delta cannot be isolated and studied alone; the entire river system must be considered.

The framework shown in Figure 1 can be utilized in the tabulation of a variety of parameters for each component of the river system. A major task lay in determining which parameters should be measured and how they were to be defined; without rigid definitions comparisons between river systems would be impossible. Field experience suggested some parameters; the literature search indicated numerous others. Important parameters were listed and defined; this list and the definitions are discussed in the following section of the report.

Systematic tabulation and management of the data required an organizational framework. Figure 2 illustrates a simplified version of the hierarchically arranged flow chart. The framework contains four levels; each successively lower level subdivides some aspect of the one above. Level I requires a single entry, the river system. The five major components of the river system form the next lower level, number II. All entries in lower levels are related to one of these components. Beneath each of the components are several "data categories," which form level III. Seven categories are listed in Figure 2, but the number need not be restricted. Others, such as economic, cultural, agricultural, and engineering, may be added, depending on the nature of the investigation. Level IV, the parameter level, is the first where recorded data are inserted into the system. Any number of parameters can be specified beneath each of the data categories. The use of such hierarchical arrangement simplifies the data-gathering process and is a necessity when retrieval

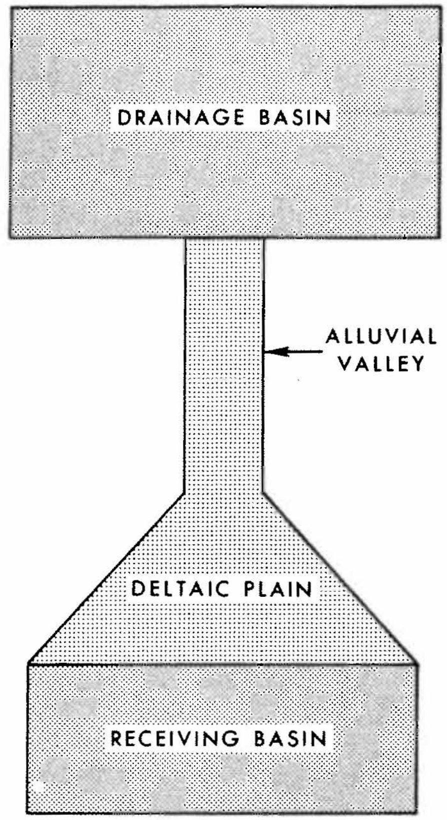

Figure 1. Major components of river systems.

of individual as well as multiple parameters is needed for comparative purposes.

The Coastal Information Program comprises four phases: (a) data structuring and definition; (b) data acquisition and generation; (c) data comparison; and (d) prediction. The first phase of the project has been completed and is the subject of this report. The second phase, data acquisition and generation, is in the final stages, and some examples will be included in this report. The deltas being analyzed are listed in Table 1. The third and fourth phases will encompass the comparisons within and between river systems and will be published in the near future.

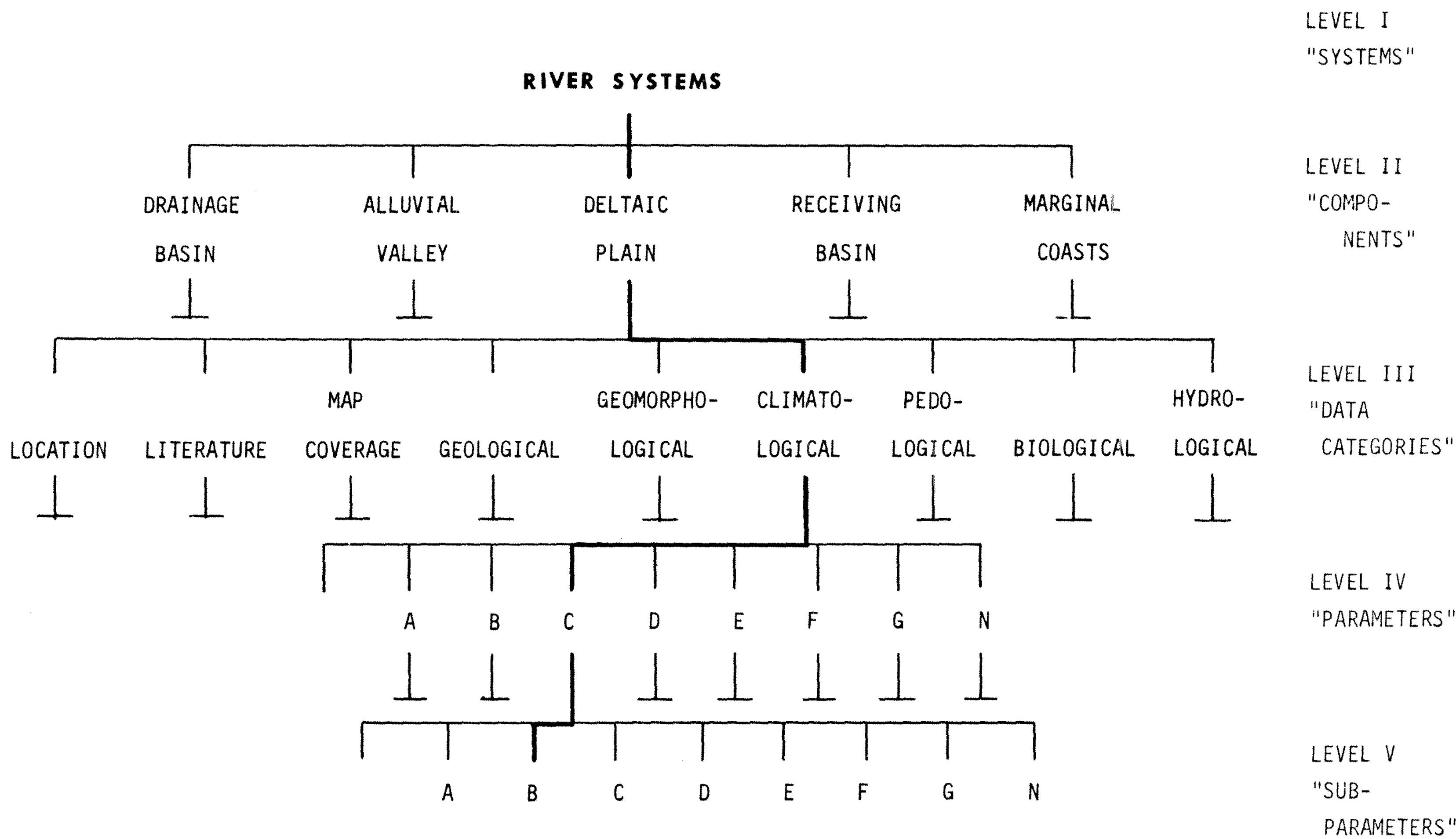

Figure 2. Simplified structure diagram for organizing the data tabulated for each river system.

Table 1

River Systems Studied

River	Country	Latitude
Amur	Russia	53° 00' N
Amur Darya	Russia	43° 30' N
Burdekin *	Australia	19° 30' S
Chao Phyra *	Thailand	13° 30' N
Colville *	USA	70° 30' N
Congo	Rep. Congo	6° 00' S
Danube *	Romania	45° 00' N
Don	Russia	47° 10' N
Dvina	Russia	64° 45' N
Ebro *	Spain	40° 45' N
Fraser	British Columbia	49° 10' N
Ganges-Brahmaputra *	E. Pakistan	22° 30' N
Godavari	India	16° 40' N
Grijalva *	Mexico	18° 30' N
Horton *	Canada	70° 00' N
Hwang Ho	China	37° 45' N
Indigirka	Russia	71° 15' N
Indus *	W. Pakistan	24° 15' N
Irrawaddy	Burma	16° 00' N
Kamchatka	Russia	56° 12' N
Kelantan *	Malaysia	6° 10' N
Kistna	India	16° 00' N
Klang *	Malaysia	3° 00' N
Kolyma	Russia	69° 28' N
Kuban	Russia	45° 10' N
Kura	Russia	39° 20' N
Lena	Russia	73° 00' N
Mackenzie *	Canada	69° 30' N
Magdalena	Colombia	11° 00' N
Mahanadi	India	20° 20' N
Mekong	S. Vietnam	9° 30' N
Mississippi *	USA	29° 30' N
Murray	Australia	35° 45' S
Niger	Nigeria	4° 45' N
Nile	Egypt	31° 15' N
Ob	Russia	66° 33' N
Orange	S. Africa	28° 35' S
Orinoco	Venezuela	9° 15' N
Paraná	Argentina	34° 00' S
Pechora	Russia	68° 00' N
Red	N. Vietnam	20° 20' N
Sagavaniktok*	USA	70° 15' N
São Francisco *	Brazil	10° 20' S
Senegal	Senegal	16° 00' N
Shatt el Arab	Iraq	30° 10' N
Syr Darya	Russia	46° 00' N
Tana	Kenya	2° 30' S
Terek	Russia	43° 35' N
Ural	Russia	47° 00' N
Vistula	Poland	54° 00' N
Volga	Russia	46° 10' N
Yangtze-Kiang	China	31° 40' N
Yenisey	Russia	70° 30' N
Yukon	USA	63° 00' N
Zambezi	Mozambique	18° 30' S

*River deltas in which Institute personnel have made scientific visits.

DEFINITION OF PARAMETERS

Prerequisite to any systematic compilation of data for comparative purposes is the formulation of rigid definitions and methodology for each parameter to be tabulated. The parameters listed below are tabulated for each river system; they are arranged hierarchically by engineering connotation. This listing follows the structure indicated in a simplified manner in Figure 2. Computer routines referred to in the following discussion may be found in the appendices.

Definitions and Methodology

1.0.0.0 RIVER SYSTEM

The river system encompasses the entire drainage network, the dispersal system, and the receiving basin. Four component parts comprise this system: the drainage basin, the alluvial valley, the deltaic plain, and the receiving basin (Fig. 1).

1.1.0.0 Drainage Basin

The drainage basin is the land area contained within the drainage divides; the perimeter generally corresponds with a line connecting the highest points of topography. For each river system the perimeter of the basin is outlined, following the definition given above, on 1:1,000,000-scale maps. The lower (downstream) limit of the drainage basin is considered to be the point where the basin perimeter narrows significantly and tributaries leading into the main channel drain an area less than 1 percent of the total basin area.

1.1.1.0 Location

The following parameters deal with the geographic location and political subdivisions of the drainage basin.

1.1.1.1 Continent: The name of the continent in which the drainage basin is located.

1.1.1.2 Countries: All political subdivisions in which the basin is contained.

1.1.1.3 Coordinates: The latitude of the northern- and southernmost extremities and the longitudes of the easternmost and westernmost extremities of the basin perimeter.

1.1.2.0 Geological

Four geological parameters of the drainage basin are determined.

1.1.2.1 Tectonic stability: This parameter is intended to indicate the major tectonism active within the basin proper and is classified into the following categories:

a. Continental platforms - areas of little present tectonic movement; absence of earthquake epicenters and volcanic activity; subsidence and uplift, if occurring, are on very gentle arches or depressions.

b. Orogenic zones - areas of active tectonic movement and great mobility; high occurrence of earthquake epicenters or volcanic activity.

c. Geosynclinal zones - areas characterized by a predominance of subsidence or depressions in the earth's crust.

1.1.2.2 Types of rocks: The approximate percentages of three rock types--igneous, metamorphic, and sedimentary--are obtained from geologic maps.

1.1.2.3 Geologic age: A list of the major time systems of rocks found in the basin is compiled from geologic maps of the continents.

1.1.2.4 Geologic structure: This parameter indicates generally the structure of the rocks comprising the basin and is divided into five classes.

a. Horizontal strata

b. Monoclinal dipping strata

c. Anticlinal-synclinal structure

d. Strongly folded-faulted structure

e. Fault graben structure

1.1.3.0 Geomorphological

The following 14 parameters all deal with geomorphic properties of the drainage basin. Most have been calculated from measurements taken from 1:1,000,000-scale maps of the entire basin.

1.1.3.1 Area: A Calma Model 303 digitizer is used to obtain x-y coordinates at intervals of 0.01 inch around the basin perimeter. A Fortran program for the IBM 360-65 computer is used to calculate the area of the basin in square miles from the digitized data. Testing of several techniques proved this particular one most accurate and reliable.

1.1.3.2 Basin perimeter: The length of the basin perimeter is calculated, in miles, from the x-y coordinates obtained from the digitized data by the formulae

$$\Delta P_i = \sqrt{\Delta x^2 + \Delta y^2} \qquad (1)$$

$$P_i = \Sigma \Delta P_i \qquad (2)$$

$$P = \Sigma_i \; P_i \tag{3}$$

This calculation is performed by the same computer program used to obtain basin area.

1.1.3.3 Length of major river channel: The length of the main channel, in miles, is computed from the digitized x-y coordinates of the main channel by the following formulae:

$$\Delta \; L_i = \sqrt{\Delta x^2 + \Delta y^2} \tag{1}$$

$$L_i = \Sigma \; \Delta L_i \tag{2}$$

$$L = \Sigma_i \; L_i \tag{3}$$

1.1.3.4 Long axis of basin: A smooth line approximating the longest axis of the basin is measured in miles.

1.1.3.5 Elevation of basin: Random points are generated within the basin, and elevations at each point are recorded. Topography differs considerably among the basins, and no set number of points can be used to obtain an average elevation. In a basin having very low relief, few points are needed to determine the average elevation; but in a basin having extreme relief, a greater number of points is required to give a meaningful measure of the average elevation. Thus the number of measurements needed within a single basin is dependent on the relief in the basin. The procedure used for each basin is as follows:

a. Ten random points are generated and the mean elevation ($\bar{E}$) and standard deviation (S) are calculated for each.

b. Ten more points are randomly selected and the mean of the total (20 points) and standard deviation are calculated.

c. This procedure is continued until the standard deviation ceases to change significantly as additional points are measured.

Thus the number of points measured in each basin is based on the variability within the basin and not on the size of the basin. In the basins examined to date the number of points needed to satisfy this procedure has ranged from 60 to 320. The average elevation ($\bar{E}$), standard deviation (S), coefficient of variability (CV), maximum elevation (E_{max}), and minimum elevation (E_{min}) are recorded for each basin.

1.1.3.6 Basin relief: A procedure similar to the one described above is utilized to obtain the average relief of the basin. The relief, in feet, in the vicinity of the random point is used for the calculation. The average relief ($\bar{R}$), standard deviation (S), and coefficient of variability (CV) are recorded for each basin.

1.1.3.7 Relief ratios: Two common measures of relief within a basin have been defined by Shumm (1956) and Melton (1957). These ratios are calculated from the formulae given by those authors.

a. Shumm: $R_h = R_{max}/A_b$ where R_{max} is maximum basin relief in feet and A_b is the long axis of the basin, in feet, parallel to the principal drainage line.

b. Melton: $R_{hp} = 100\ H/P$ where H is maximum basin relief in feet and P is basin perimeter in feet. R_{hp} is expressed as a percentage.

1.1.3.8 Area-altitude: Several parameters to be calculated are based on area-altitude relationships. On the 1:1,000,000-scale maps contour classes were selected as follows:

Class No.	Meters	Feet	Class No.	Meters	Feet
1	0-150	0-492	9	2500-3000	8202-9843
2	150-300	492-984	10	3000-3500	9843-11483
3	300-600	984-1969	11	3500-4000	11483-13124
4	600-900	1969-2953	12	4000-5000	13124-16405
5	900-1200	2953-3937	13	5000-6000	16405-19686
6	1200-1500	3937-4921	14	6000-7000	19686-22967
7	1500-2000	4921-6562	15	7000-8000	22967-26248
8	2000-2500	6562-8202			

The classes indicated above were governed by the contour data on the maps. The Calma digitizer is utilized to determine the area within a class, and an entire basin can be analyzed in a relatively short period of time. A program was developed to utilize the digitized data as input for calculating the following parameters:

a. Area-altitude

b. Altimetric frequency

c. Dimensionless area-altitude

d. Absolute volume of basin

e. Hypsometric integral

f. Ratio of hypsometric integral above the sharpest break in slope of hypsometric curve to the total hypsometric integral

The area-altitude is simply the area in square miles at each contour level.

1.1.3.9 Altimetric frequency: The digitized data are used to convert the area within each contour class into a percentage of the total basin area.

1.1.3.10 Dimensionless area-altitude: To facilitate comparison of basins of different sizes and shapes, the area-altitude data are made dimensionless by the following method:

$$Y_j \begin{pmatrix}\text{dimensionless}\\ \text{altitude}\end{pmatrix} = h_j/H$$

where h_j is height of contour above the base contour and H is maximum elevation of basin;

$$X_j \begin{pmatrix}\text{dimensionless}\\ \text{area}\end{pmatrix} = a_j/A$$

where a is total area contained by a contour and A is total area of basin.

1.1.3.11 Absolute volume: The absolute volume in cubic miles of the basin landmass above the base contour is calculated from the digitized data by the formulae

$$V = \sum_j a_j(\Delta h);$$

$$V = \sum_j a_j(\Delta h)_j + [\Delta a_j(\Delta h)_j]/2$$

where a_j is the area of a contour class, $(\Delta h)_j$ is the height difference between contour classes j and j-1, and Δa is the area difference between contours j and j-1.

1.1.3.12 Hypsometric integral: The hypsometric integral is obtained from the digitized data by

$$HI = \sum_j X_j \ (\Delta Y)_j + [(\Delta X)_j \ (\Delta Y)_j]/2$$

where X_j is the dimensionless area of a contour class interval; $(\Delta Y)_j$ is the difference in dimensionless height in the interval j; and ΔXj is the difference in dimensionless area in the interval j (Fig. 3).

1.1.3.13 Ratio HI_a/HI: This is a calculated ratio of the dimensionless volume of the basin above the break in slope of the hypsometric curve to the total dimensionless volume.

1.1.3.14 Drainage density: The drainage density is the length of channels per unit area:

$$D_d = \frac{\Sigma L}{A}$$

where ΣL is the summed length of channels in miles per given area A in square miles.

Drainage densities are measured at the same random points used in the relief analyses. At each point, a given area (400 square miles) is blocked off and the lengths of all streams within this

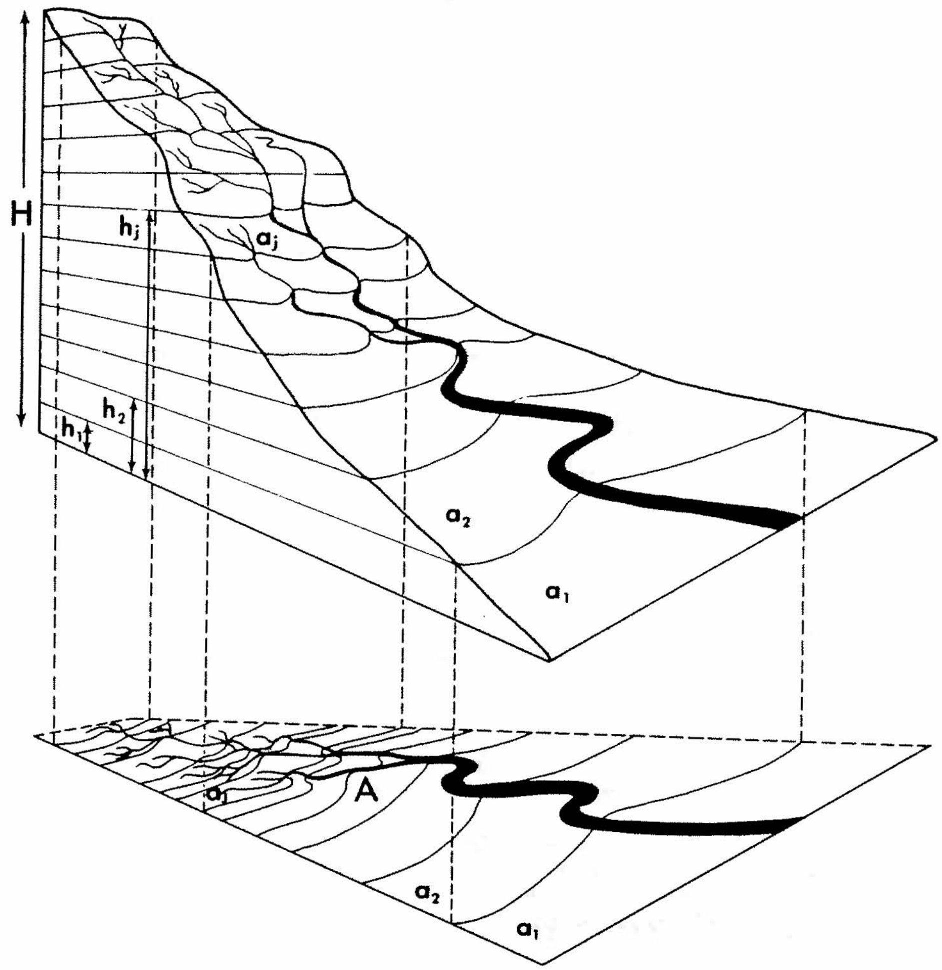

Figure 3. Diagram illustrating definitions of terms used in hypsometric calculations.

area are measured by the Calma digitizer. From the densities at each individual point, the mean and standard deviation are calculated for the basin. Figure 4 shows some typical examples of various drainage densities.

1.1.4.0 Climatological

Meteorological stations within the basin and summary climatic atlases are utilized to determine 11 parameters.

1.1.4.1 Climatic classification: The climate of the basin is classified according to the Koeppen scheme. The climatic type that predominates in the basin is obtained from the atlases and is considered to characterize the basin.

1.1.4.2 Yearly average temperature: The mean annual temperature, in degrees centigrade, is computed from meteorological data collected from stations within the basin.

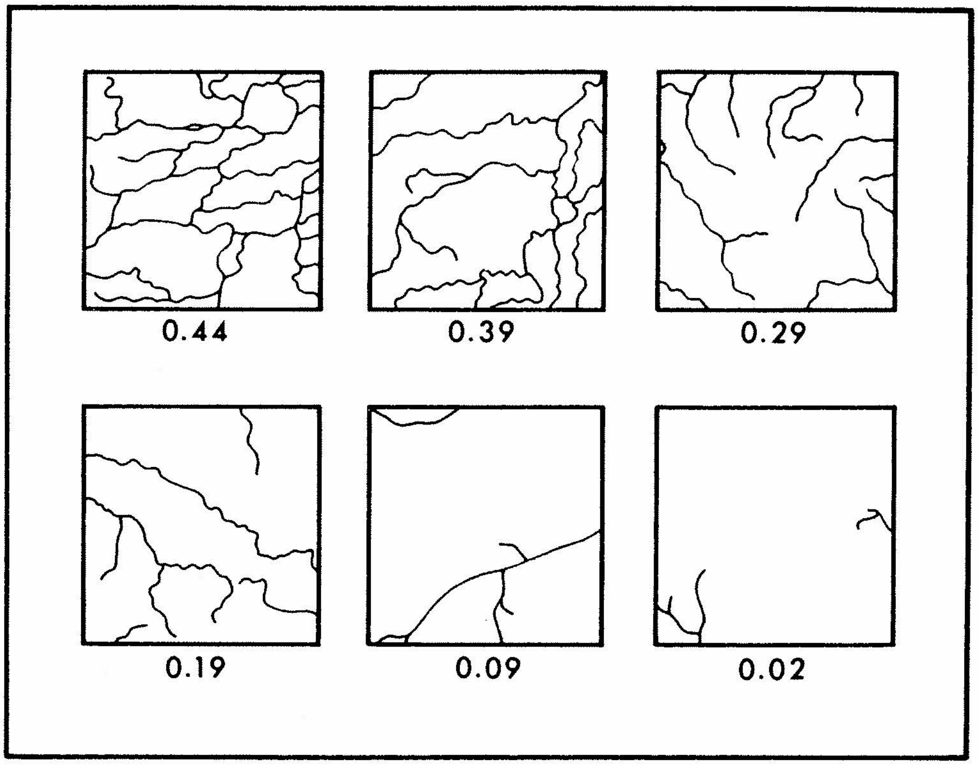

Figure 4. Examples of different drainage densities from 1:1,000,000-scale maps.

1.1.4.3 Mean daily temperatures: Same procedure as above.

1.1.4.4 Mean maximum daily temperature: Bimonthly mean maximum daily temperatures and the standard deviations are computed from data collected at meteorological stations in the basin.

1.1.4.5 Mean minimum daily temperatures: Same procedure as above.

1.1.4.6 Yearly precipitation: The mean annual precipitation, in millimeters, is determined from meteorological records from stations within the basin. The standard deviation, coefficient of variability, and the yearly maximum and minimum are recorded.

1.1.4.7 Mean monthly precipitation: Monthly precipitation data for each station are averaged and the mean, standard deviation, coefficient of variability, and maximum and minimum values are recorded.

1.1.4.8 -
1.1.4.12 Mean monthly water balance: Average monthly potential evapotranspiration, moisture storage, actual evapotranspiration, water deficit, and water surplus for each station are obtained from Thornthwaite Associates publications and the means and standard deviations characteristic of the entire basin are determined.

1.1.4.13 Distribution of annual precipitation: Thirteen rainfall classes have been established as follows:

Class No.	1	2	3	4	5
Rainfall*	0-100	100-200	200-400	400-600	600-800
Class No.	6	7	8	9	10
Rainfall	800-1000	1000-1400	1400-1800	1800-2200	2200-2600
Class No.	11	12	13		
Rainfall	2600-3200	3200-4000	4000-		

*Millimeters

From maps the percentages of the total basin receiving rainfall corresponding to each class are determined.

1.1.4.14 Date of freeze: From published data, the average date of freezing of the river channels in the basin is recorded.

1.1.4.15 Date of thaw: From published data, the average date of breakup of river ice in the channels of the basin is recorded.

1.1.4.16 Duration of freeze: The total number of days during which channels in the basin are frozen is recorded.

1.1.5.0 Pedological

The data on pedological parameters that could be measured in river basins are limited since in most cases only small portions of any one basin are covered adequately by soil surveys. World soil maps (USSR Academy of Sciences, 1964) are used, therefore, to obtain the major soil types found in the drainage basin.

1.1.5.1 Major soil type: The soil types designated on the 1:60,000,000-scale maps are divided into 8 major classes and 93 subclasses, as shown below:

A. Zonal Soils of Plains Territories

1. Arctic
2. Tundra

B. Boreal Soil Formation

1. Turfy coarse-humus and turfy peat (including volcanic) soils of subpolar grassy forests and meadows
2. Gleyey permafrost-taiga and permafrost-taiga illuvial-humus soils of northern taiga and open woodland
3. Permafrost-taiga acid and podzolized soils of the middle taiga
4. Permafrost-taiga pale-yellow soils of the middle taiga
5. Permafrost-taiga residual carbonate soils
6. Gleyey podzolic and podzolic illuvial-humus soils of the northern taiga
7. Podzolic soils and podzols of the middle taiga
8. Turfy podzolic soils of the southern taiga and broadleaf coniferous forests
9. Turfy pale-yellow podzolic soils of broadleaf-coniferous forests

10. Acid nonpodzolized forest soils of broadleaf-coniferous and broadleaf forests
11. Gray forest soils

C. Subboreal Soil Formation

1. Brown forest soils
2. Chernzem-like prairie soils (brunizems)
3. Chernozems of the steppes
4. Chestnut soils of the dry steppes
5. Brown semidesert soils
6. Gray-brown desert soils

D. Subtropical (Warm and Moderately Warm) Soil Formation

1. Yellow-brown soils of broadleaf forests transitional to subtropical forests
2. Yellow soils and red soils of humid subtropical forests
3. Reddish-black soils of subtropical prairies
4. Brown soils of xerophytic subtropical forest and shrub
5. Chernozems of subtropical steppes
6. Gray-brown soils of subtropical shrub steppes
7. Serozems of subtropical semideserts
8. Soils of subtropical deserts

E. Tropical and Equatorial Soil Formation

1. Reddish-yellow lateritic (allitic, ferrallitic, alferritic) soils of permanently humid tropical forests
2. Red lateritic (ferrallitic, alferritic, allitic) soils of seasonally humid tropical forests and tall-grass savannas
3. Brownish-red laterized (alferritized, ferritized) soils of xerophytic tropical forests and shrub
4. Red-brown soils of dry savannas
5. Reddish-brown soils of desertlike savannas
6. Soils of tropical deserts

F. Intrazonal Soils of Plains Territories

1. Bog-permafrost soils
2. Bog-podzolic soils
3. Gray-gleyey forest soils
4. Turf-carbonate soils and grad rendzinas
5. Turf-gleyey soils
6. Peat-bog upland soils
7. Lowland bog soils
8. Brown gleyey and pseudo-podzolic forest soils
9. Chernozem-like gleyey prairie soils
10. Meadow-chernozem soils
11. Meadow-chestnut soils
12. Brown meadow soils
13. Brown rendzinas
14. Gleyey yellow and red soils
15. Brown meadow soils
16. Subtropical meadow chernozems

17. Meadow serozems
18. Red rendzinas and terra rossa
19. Smolnitsa soils and black subtropical soils
20. Takyrs
21. Subtropical bog soils
22. Dark-red lateritic soils on basic rocks
23. Gleyey lateritic soils
24. Brownish-red meadow soils
25. Red-brown meadow soils
26. Black and gray tropical soils
27. Tropical bog soils
28. Salt-marsh soils of mangroves
29. Solod soils
30. Solonets soils
31. Solonchak soils
32. Meadow soils
33. Alluvial soils
34. Irrigated soils

G. Soils of Mountain Territories

1. Arctic mountain soils
2. Mountain tundra and denuded-summit soils
3. Mountain turf-coarse humus and peat soils
4. Mountain permafrost-taiga soils
5. Mountain permafrost-taiga carbonate soils
6. Mountain podzolic soils
7. Mountain gray forest soils
8. Mountain meadow soils
9. Mountain brown forest soils
10. Mountain meadow-steppe soils
11. Mountain chernozems
12. Mountain chestnut soils
13. Mountain brown semidesert soils
14. Highland desert and steppe soils
15. Mountain yellow-brown, yellow, and red soils
16. Mountain brown soils
17. Mountain gray-brown soils
18. Mountain serozems
19. Mountain desert subtropical soils
20. Mountain lateritic soils of permanently humid tropical forests - humus-allitic, ferrallitic, etc.
21. Mountain red soils of seasonally humid tropical forests and tall-grass savannas - ferallitic, ferritic, etc.
22. Mountain brown-red soils of xerophytic tropical forests - ferrallitized, ferritized, etc.
23. Mountain red-brown soils of savannas
24. Mountain desert tropical soils

H. Additional Designations

1. Ferruginous soils and layers (laterites) in tropical soil.
2. Blown and semianchored sands

The major types composing the basin are listed.

1.1.6.0 Biological

Biological parameters, although extremely critical in the drainage basin, are seldom reported. The only consistent data available for the entire basin are with regard to the general type of vegetation cover.

1.1.6.1 Major vegetation types: World vegetation maps (USSR Academy of Sciences, 1964) of small scale (1:60,000,000) are used to divide the vegetation types into 21 major classes and 98 subclasses. The classes and subclasses are listed below:

A. Tundra Vegetation

1. High arctic formations
2. Polar tundra formations

B. Boreal (Taiga) Vegetation

3. North Atlantic (partly tundralike) formations
4. Bering (partly tundralike) formations
5. North European formations
6. Ural-Siberian formations
7. Angara formations
8. North Cordilleran formations
9. Canadian formations

C. Nemoral Vegetation (Broadleaf and Coniferous-Broadleaf)

10. West Atlantic formations
11. Central European formations
12. East European formations
13. North Mediterranean (including Crimean-North Caucasus) formations
14. Euxine and Zagros formations
15. Middle Asian formations
16. Manchurian and North Chinese (subcontinental) formations
17. Far Eastern oceanic formations
18. Cordilleran formations
19. South Canadian formations
20. Appalachian formations

D. Subtropical Shrub Vegetation

21. Mediterranean and Atlantic-Mediterranean formations
22. Asia Minor and West Himalayan formations
23. East Asian formations
24. Chinese southern subtropical formations
25. Californian formations
26. Central American formations
27. South Atlantic-Floridian formations

E. Subtropical Xerophilous Open-Woodland and Upland Vegetation

28. Irano-Afghan formations (including associations of open woodland and ephemeral tall grass)
29. Texas-Mexican formations (including grass-shrub and

cactus-acacia groupings)

F. Steppe Vegetation

30. Black Sea formations
31. Transvolga-Kazakhstan formations
32. Transcaucasian-West Asian formations
33. Mongolian-Chinese formations (including South Siberian and East Transbaykal island steppes)
34. South Tibetan formations
35. East American (Great Plains) formations
36. West American (Prairie Plateau) formations

G. Extratropical Deserts of Northern Hemisphere

37. Saharan-Saudi (subtropical) formations
38. Turanian-Caspian formations
39. West Asian formations
40. Central Asian formations
41. Arizonan-Mexican (subtropical) formations
42. Coloradan formations

H. Cold Highland Deserts (with Cushion Plants)

43. Tibetan formations

I. Highland Vegetation of Tundra and Boreal Types

44. Mountain tundra and subsummit formations
45. Alpine (meadow) and subalpine (meadow, shrub, and woody) formations
46. Quasi-boreal formations in mountains of nemoral zone

J. Humid Evergreen Tropical Forest

47. Guinean-Congolese formations
48. Madagascar formations
49. Bengal-Indochinese formations
50. Malaysian formations
51. Galapagos-Caribbean formations
52. Amazonian formations
53. Brazilian-Atlantic formations
54. Transandean formations

K. Mangrove Vegetation

55. Mangrove formations of various genetic complexes

L. Deciduous and Evergreen Forest of Variably Humid Tropics

56. Nigerian-Congolese formations
57. Indostan-Burmese and Javanese formations
58. Mexican formations
59. South Brazilian formations

M. Tropical Dry (Partly Sclerophyll) Forest, Xerophilous Open Woodland, and Thorny

60. Somali-Yemeni formations
61. Angolan formations
62. Rhodesian-Mozambique and Madagascar formations
63. Indo-Malaysian formations
64. Paraguayan-Argentine formations
65. Tucuman-Bolivian (mountain) formations
66. North Australian formations

N. Tropical Savannas

67. Guinean-Sudanian formations
68. East African and Southwest Arabian formations
69. South African formations
70. Central Madagascar formations
71. South Asian formations
72. Orinoco formations (associated with deserts)
73. Brazilian-Bolivian formations
74. Australian formations

O. Tropical Deserts

75. Saharan-Nubian formations
76. South African formations
77. Somali-Arabian formations
78. South Pacific (Andean) formations
79. East Brazilian formations
80. Central Australian formations

P. Humid Subtropical Forest

81. Uruguayan-Brazilian formations
82. Australian-New Zealand (partly sclerophyll) formations

Q. Subtropical Xerophilous Woody Shrub Vegetation

83. Cape formations
84. Transandean formations
85. South Australian-Tasmanian formations

R. Grassy Savannas and Pampas

86. Southeast African formations
87. Uruguayan-Argentine formations
88. South Australian formations

S. Extratropical Deserts of Southern Hemisphere (monte, mallee scrub, etc.)

89. Karroo-Southern Namib formations
90. Argentine formations
91. Patagonian formations (Patagonian "steppe")
92. South Australian formations

T. Broadleaf and Coniferous-Broadleaf Subantarctic Forest (Subantarctic Nemoral Vegetation)

93. Tasmanian-New Zealand (mainly beech) formations
94. Andean (broadleaf and coniferous-broadleaf) formations
95. Chilean (xerophilous woodland and shrub) formations

U. Grassy, Mossy, and Lichen-Moss Vegetation of Subantarctic (Subantarctic Tundralike Vegetation)

96. Treeless formations of Tierra del Fuego and Oceania

V. Highland Vegetation

97. Mesophilic woodland formations (in mountains of New Guinea)
98. Semi-xerophilous and cryophilic grass, bush, and shrub formations in the highlands of Tasmania, the Neotropics, and southern extratropical Africa

1.1.7.0 Hydrological

Although data on stream discharge, river stage, and sediment yield are available for many tributaries within selected basins, rarely are the data in such form as to permit comparisons between basins. Therefore only one parameter, discharge, was measured.

1.1.7.1 Average monthly discharge: The average monthly discharge at the station nearest the basin mouth is tabulated in cusecs x 10^3. The United Nations Flood Control Series provides the most reliable data for the tributary streams.

1.2.0.0 Alluvial Valley

The alluvial valley connects the drainage basin with the delta. Within the alluvial valley the river is free to migrate laterally between valley walls. The total drainage area of tributaries leading into the main channel normally accounts for less than 1 percent of the total drainage area of the river system.

1.2.1.0 Location

1.2.1.1 Countries: The countries containing all or part of the alluvial valley.

1.2.2.0 Geological

1.2.2.1 Stability: The same categories listed for the basin (section 1.1.2.1) are tabulated in the alluvial valley.

1.2.2.2 Sediment type: From the literature the dominant type of sediment transported by the stream is tabulated.

1.2.3.0 Geomorphological

Seven parameters are tabulated under this category.

1.2.3.1 Channel type: The type of channel plan is determined from maps. Three types, braided, straight, and meandering, are recognized. They are illustrated in Figure 5, and low-angle oblique aerial photographs of each are presented in Figure 6.

1.2.3.2 Channel width: The width is measured in miles at 10-mile intervals along the channel. The section is normalized to the channel axis, and width is measured from bank to bank. From these data the mean ($\overline{CW}$), standard deviation (S), and coefficient of variability (CV) are calculated. The river stage at the time the map was constructed is extremely critical, but this information is rarely available, and as a result some error is undoubtedly introduced into the measurements, particularly in the case of braided streams.

1.2.3.3 Length of valley: The centerline length, in miles, of the valley, measured from the mouth of the drainage basin to the apex of the delta plain.

1.2.3.4 Length of stream: The length of the channel, from basin mouth to delta apex, is calculated from digitized data.

1.2.3.5 Ratio LS/LV: This ratio is the length of the stream divided by the length of the valley and indexes the sinuosity of the stream channel occupying the alluvial valley.

1.2.3.6 Type of flood plain: From maps nine major types of fluvial plains can be identified (Figs. 7 and 8).

Type I, river-scarred plain: Segments of abandoned stream courses are evident in the alluvial plain flanking the active channel. In many cases, these abandoned channels are the sites of freshwater cutoff lakes (Fig. 8A) or linear lakes occupying abandoned braided channels.

Type II, interfluvial lake plain: Abundant freshwater lakes dot the alluvial plain; they tend to be irregular or rounded in shape and are normally much wider than the channel system (Fig. 8B).

Type III, swamp plain: HHeavy swamp vegetation occupies the largest part of the alluvial plain. Other common alluvial valley features are not evident.

Type IV, interior deltaic plain: A depression within the alluvial valley causes derangement of the stream channels, resulting in formation of localized swamp and lake features.

Type V, linear lake plain: Linear lakes trending at right or high angles to the main channel and occasionally indenting the valley wall are present (Fig. 8C).

Type VI, salt flat plains: Low depressions containing evaporites and normally devoid of vegetation are numerous on the alluvial plain (Fig. 8D).

Type VII, sand-dune plains: Eolian dune fields occupy broad

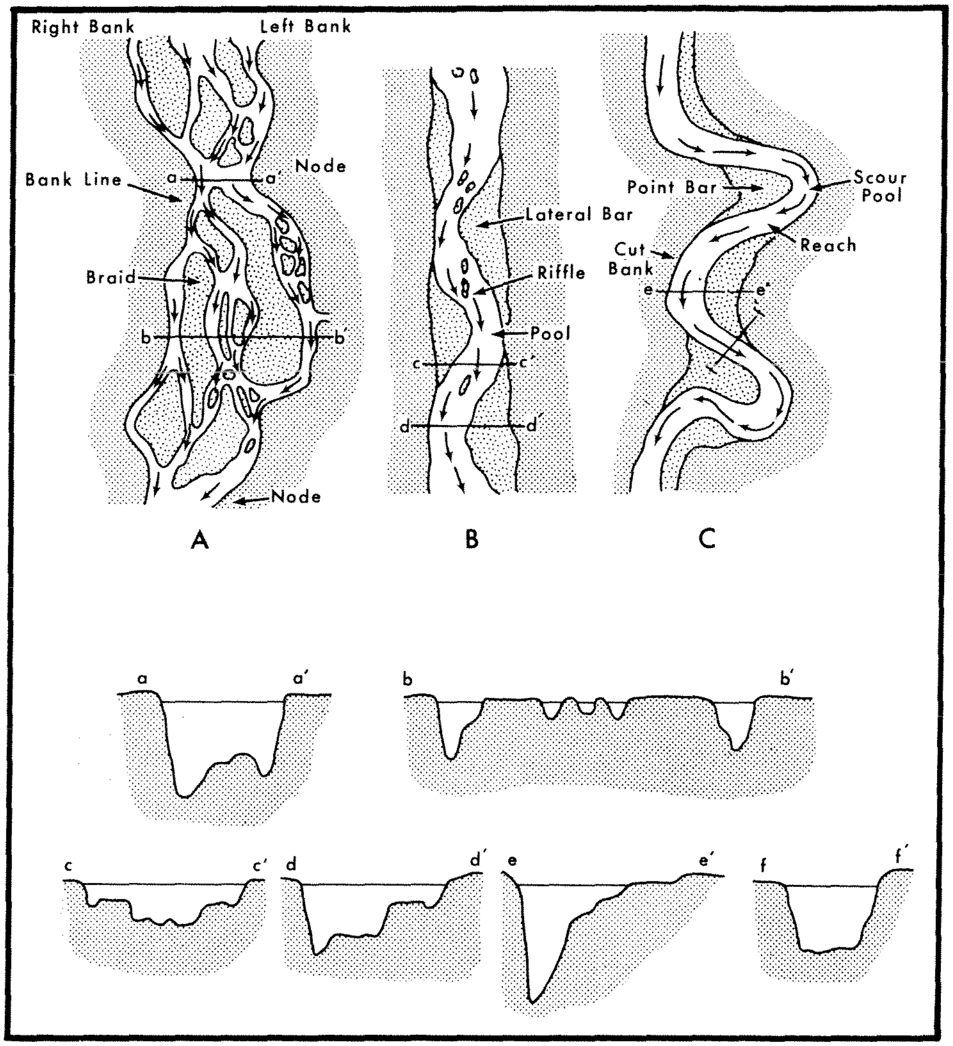

Figure 5. Types of stream channels. A. Braided. B. Straight. C. Meandering.

portions of the alluvial surface. In many cases the dune fields are located near active and abandoned stream channels.

Type VIII, oriented dune swamp plains: Large dune ridges, separated by broad swamps, are aligned with the river channel (Fig. 8E).

Type IX, cultivated plains: The greater fraction of the alluvial plain has been cultivated (Fig. 8F).

1.2.3.7 Number of tributaries: The number of tributaries entering the main stream channel on the right and left banks.

1.2.4.0 Climatological

1.2.4.1 Climatic classification: The dominant climate in the valley is classified according to the Koeppen scheme.

A. Meandering channel of Colville River in Alaska.

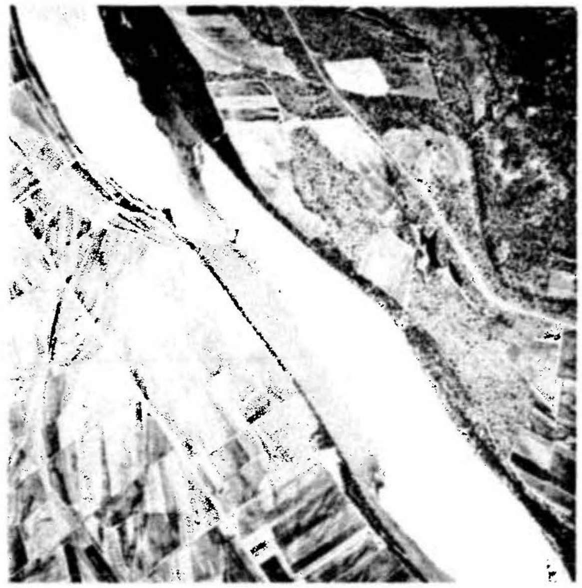

B. Straight channel of Burdekin River in Australia.

C. Braided channel of Ganges-Brahmaputra River in East Pakistan.

Figure 6. Aerial photographs of the three major channel types.

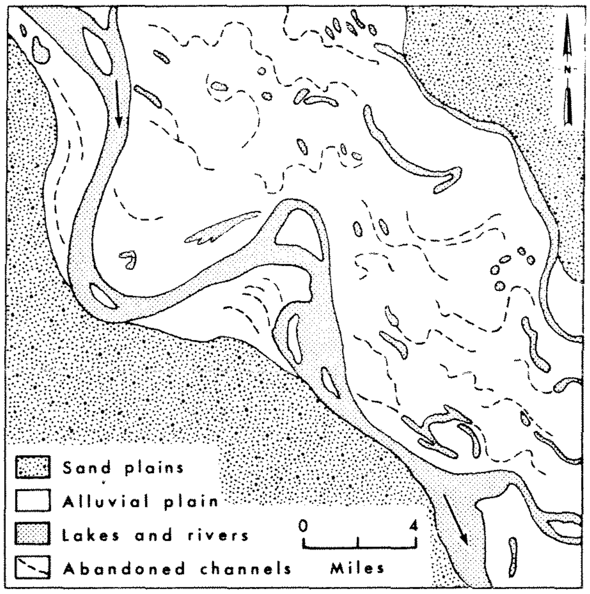

A. River-scarred plain - Volga River, USSR.

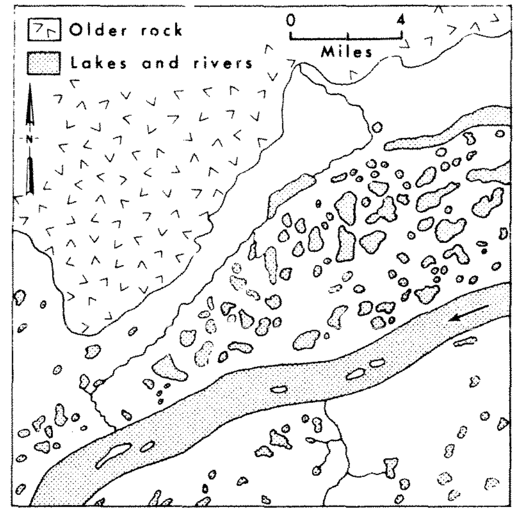

B. Interfluvial lake plain - Mackenzie River, Canada.

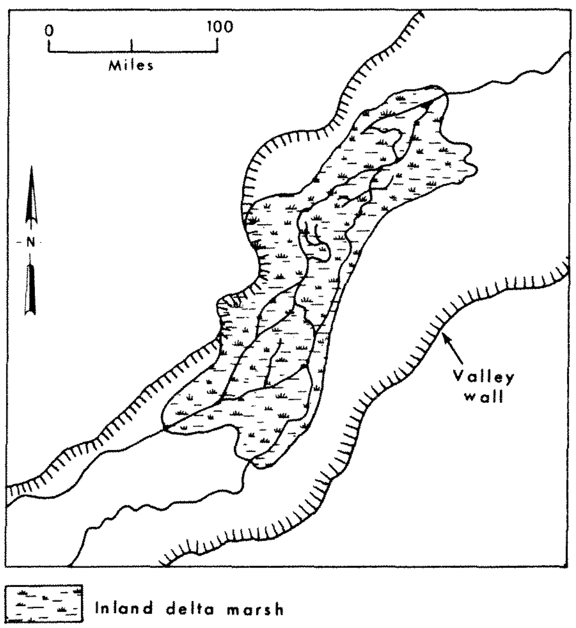

C. Interior delta plain - Niger River, Nigeria.

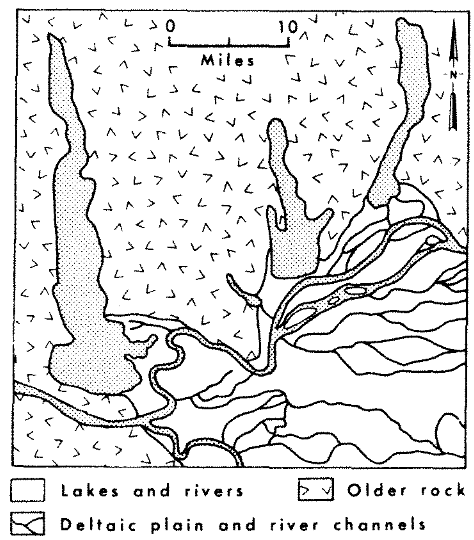

D. Linear lake plain - Danube River, Romania.

Figure 7. Types of landforms in alluvial valleys.

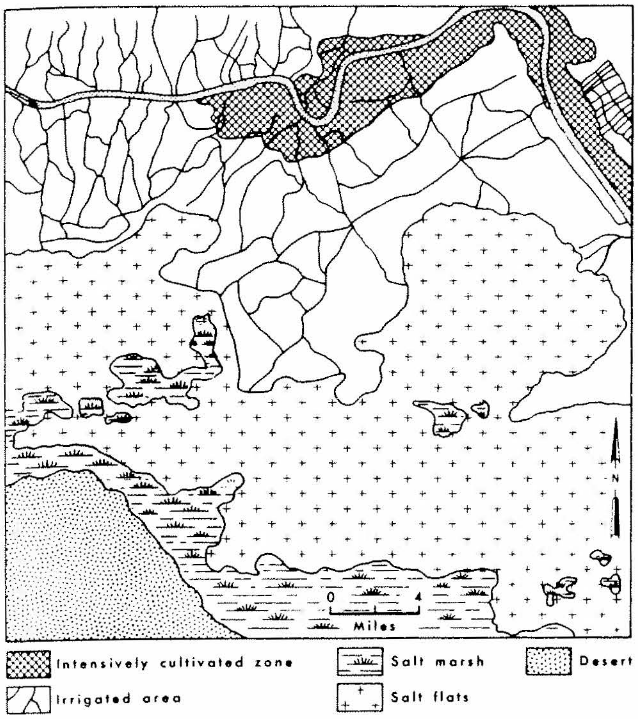

E. Salt flat plains - Shatt al Arab, Iran and Iraq.

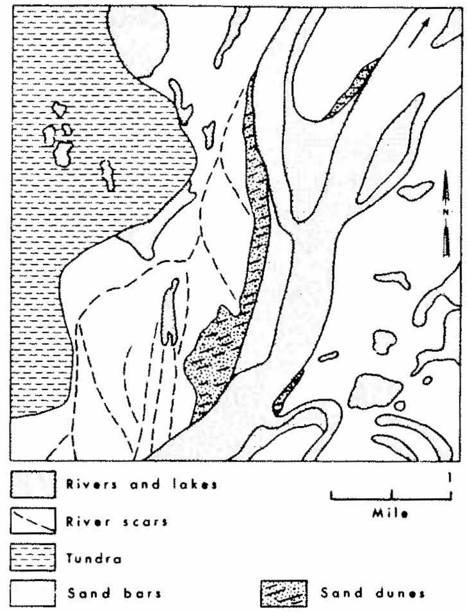

F. Sand-dune plain - Colville River, Alaska, USA.

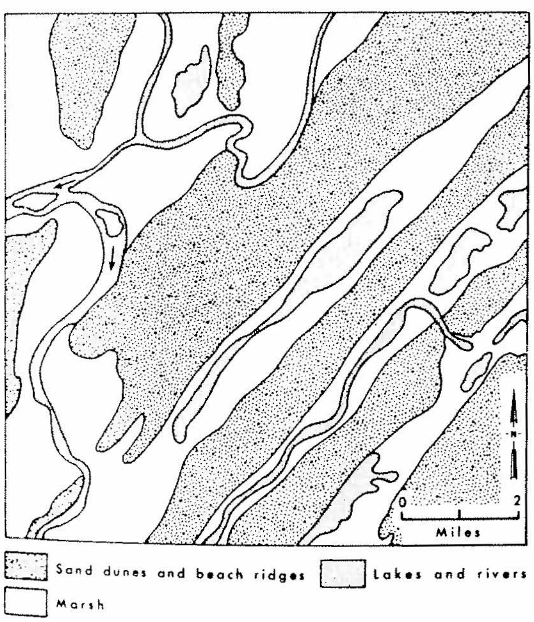

G. Oriented dune-swamp plain - Senegal River, Senegal.

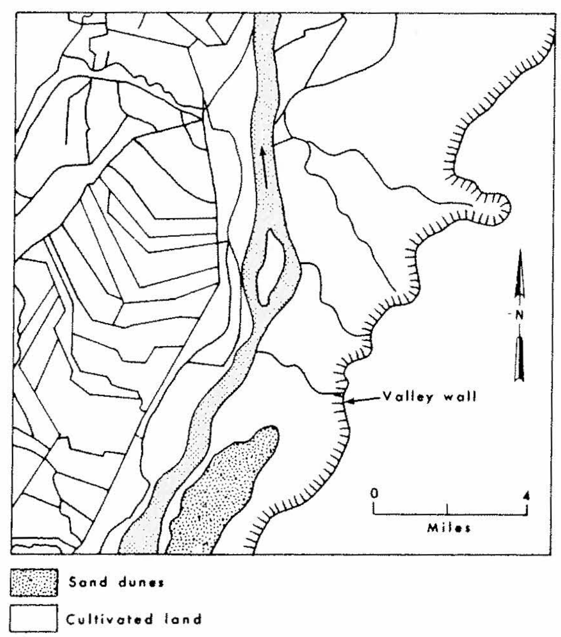

H. Cultivated plains - Nile River, UAR.

A. River-scarred plain - Anderson River, Canada.

B. Interfluvial lake plain - Mackenzie River, Canada.

C. Linear lake plain - Mackenzie River, Canada.

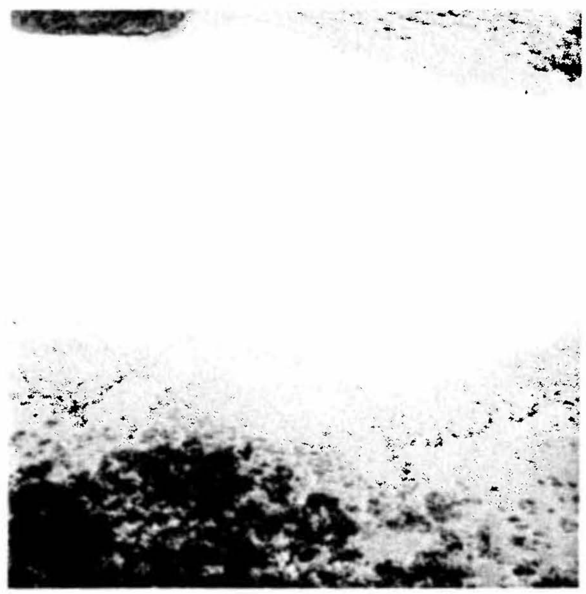

D. Salt flat plains - Burdekin River, Australia.

Figure 8. Aerial photographs of alluvial valley landforms.

E. Oriented dune-swamp plain - Senegal River, Senegal.

F. Cultivated plain - Ganges-Brahmaputra River, East Pakistan.

1.2.4.2 Yearly rainfall: The total yearly rainfall, in millimeters, is taken from published literature or meteorological atlases.

1.2.4.3 Average yearly temperature: The average yearly temperature, in degrees centigrade, is obtained from published literature.

1.2.4.4- 1.2.4.5 Monthly moisture deficit and surplus: Mean values of the water balance parameters, moisture deficit and surplus, are recorded as in 1.1.4.11 and 1.1.4.12.

1.2.5.0 Pedological

1.2.5.1 Major soil type: See 1.1.5.1.

1.2.6.0 Biological

1.2.6.1 Major vegetation type: See section 1.1.6.1.

1.2.7.0 Hydrological

Nine parameters dealing with hydrologic characteristics within the alluvial valley are calculated.

1.2.7.1- 1.2.7.2 Monthly and yearly discharge: Discharge data in graphic form are digitized, and a Fortran IV program is used to calculate monthly mean ($D_{a\ell}$), variance, standard deviation, and coefficient of variability as well as yearly statistics. Figure 9 illustrates three common discharge curves.

1.2.7.3- 1.2.7.4 Maximum and minimum discharge: The maximum and minimum discharge during the year, in cusecs, and the date of occurrence are recorded.

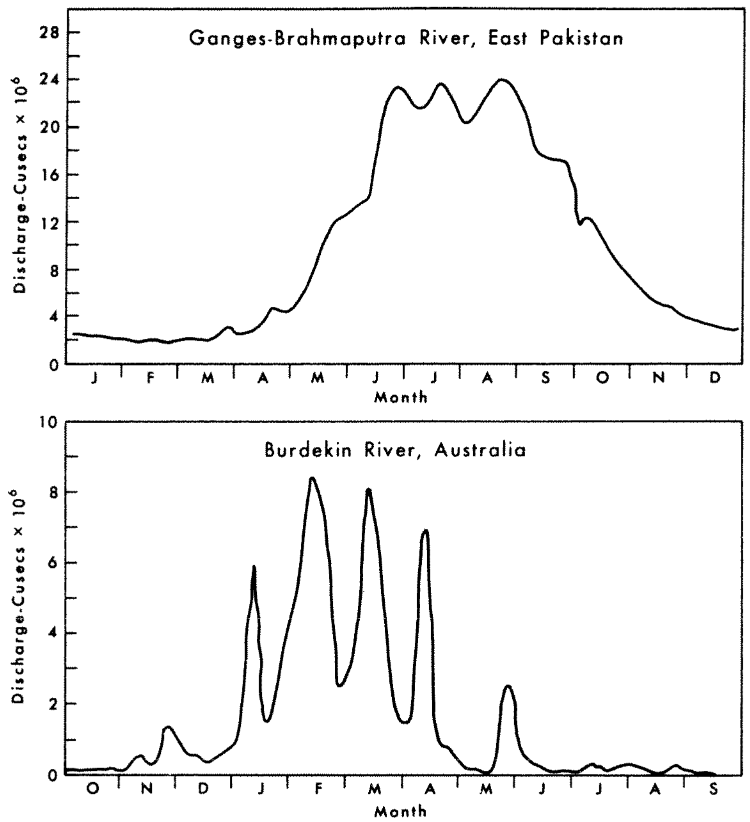

Figure 9. Examples of common types of discharge curves.

1.2.7.5 Flood peakedness: Flood peakedness K_f is calculated from

$$K_f = \frac{T_\ell}{T_g}$$

where T_ℓ is the number of days during which discharge is less than the mean and T_g is the number of days during which discharge exceeds the mean.

1.2.7.6-1.2.7.7 High- and low-water period: Respectively, the months during which discharge is greater than and less than the mean discharge.

1.2.7.8 Monthly rate of rise and fall: The average change in water surface elevation in feet per day is calculated by

$$\frac{1}{n} \sum_{i=1}^{n} \Delta H$$

where ΔH is the daily change in river stage and n is the number of days in the month.

1.2.7.9 Yearly sediment discharge: These data are obtained from published information and reduced to total yearly sediment discharge in cubic feet.

1.3.0.0 <u>Deltaic Plain</u>

The deltaic plain is that portion of a river system in which the sediment-water load is distributed and deposited rather than supplied, traded, or carried in transit. The apex of the deltaic plain is the point at which the main stream channel branches into multiple distributaries. The plain is characterized by interaction between riverine and marine processes, with marine processes becoming more dominant in the seaward direction. The seaward limit of the deltaic plain is, for the purposes of this study, set at the 40-foot-depth contour. Normally this is the first sharp break in slope around the periphery of the subaqueous bulge. The lateral limits of the plain extend to the area which has formed by processes other than deltaic progradation. In many deltas, these lateral limits are well defined by features associated with active or abandoned streams. Six components of the deltaic plain can be recognized (Fig. 10): the subaerial, the subaqueous, the upper, the lower, the active, and the abandoned. The subaerial deltaic plain is that part which is exposed to subaerial conditions during part or all of the year; the subaqueous portion lies primarily beneath the water surface but may be partially exposed during extremely low tides. The upper deltaic plain forms the apex of the delta, and its surface lies above the effective level of tidal influence, where processes are predominantly riverine in nature. The lower deltaic plain is within the realm of effective tidal action. The active portion of the subaerial deltaic plain is the area where the morphology is primarily the function of currently active deposition by the river, whereas the abandoned portion reflects relict deposition by formerly active streams.

1.3.1.0 Location

1.3.1.1 Countries: The countries in which part or all of the deltaic plain is located.

1.3.1.2 Receiving body of water: The body of water into which the river debouches.

1.3.2.0 Geological

1.3.2.1 Stability: The geologic stability of the deltaic plain is obtained from tectonic maps and is classified as in section 1.1.2.1.

1.3.3.0 Geomorphology

1.3.3.1-1.3.3.7 Area of components of deltaic plain: The boundaries enclosing each of the components are digitized and input to a Fortran IV computer program (Appendix 1) to obtain the area in square miles.

1.3.3.8 Ratio AUDP/ALDP: The ratio of the area of the upper deltaic plain, as computed in 1.3.3.4, to the area of the lower deltaic plain, as computed in 1.3.3.3.

1.3.3.9 Ratio $AS_{ae}/DP/AS_{aq}DP$: The ratio is computed as above.

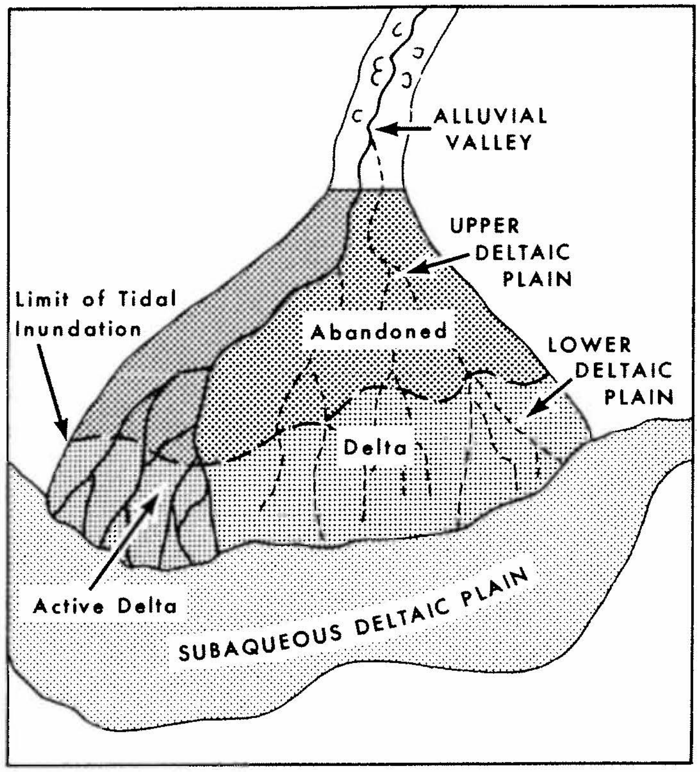

Figure 10. Components of deltaic plain.

1.3.3.10 Ratio AA_bDP/AA_cDP: The ratio is computed as in 1.3.3.8.

1.3.3.11 Length of long axis of delta: The straight-line length (L), in miles, of the long axis from the delta apex to the seawardmost extremity of the subaerial delta.

1.3.3.12 Maximum width of delta: The straight-line distance (W) in miles connecting the lateral extremities of the delta.

1.3.3.13 Length of delta shoreline: The length of the shoreline (LS), in miles, is calculated from digitized data.

1.3.3.14 Ratio L/W of deltaic plain: The ratio of 1.3.3.11 to 1.3.3.12.

1.3.3.15 Ratio LS/W: The ratio of 1.3.3.13 to 1.3.3.12.

1.3.3.16 Distributary index: A series of ten evenly spaced concentric arcs, the first at the delta apex and the tenth located at the shoreline and intersecting all lower distributaries, is constructed (Fig. 11). In index A, the number of distributaries that intersect each arc is tabulated. In index B, the number of channel crossings along that arc, whether by a single channel or multiple channels, is tabulated.

1.3.3.17 Number of bifurcations: The number of times each distributary

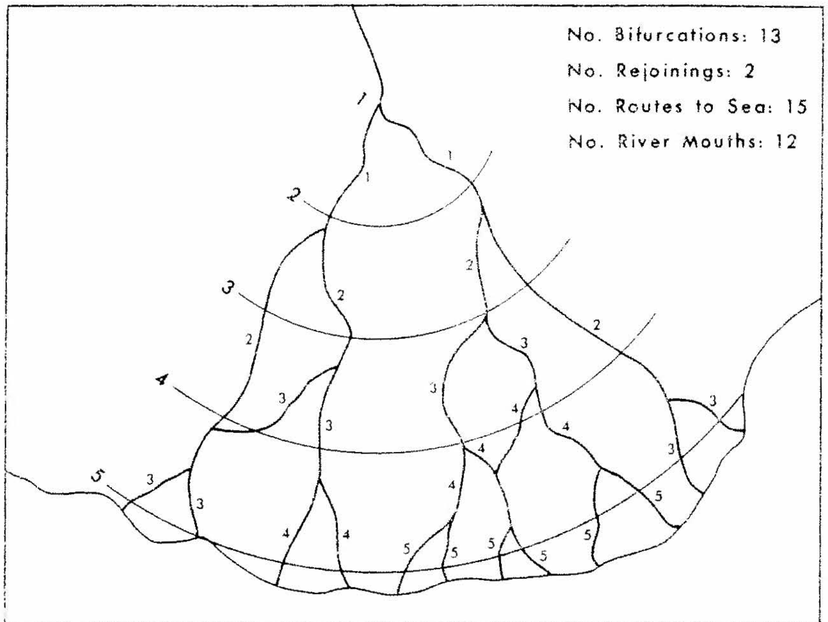

Arc No.	No. Distributaries	Order No.	No. Distributaries	Length
1	1	1	2	2.2
2	2	2	4	6.3
3	4	3	8	8.2
4	7	4	6	4.8
5	12	4	6	4.1

Figure 11. Diagram illustrating distributary index.

splits into two or more channels is counted and the total number of bifurcations in the delta is tabulated (Fig. 11).

1.3.3.18 Number of rejoinings: The number of times any two channels rejoin in a downstream direction (Fig. 11).

1.3.3.19 Number of routes to the sea: The total number of possible routes a water parcel could follow from the apex of the delta to the sea.

1.3.3.20 Distributary density: The total length of all distributaries in the subaerial deltaic plain is calculated from digitized data. This length is divided by the total area of the subaerial deltaic plain and a density figure is derived.

1.3.3.21 Interdistributary types: The landforms that occupy the area between the channels are subdivided into 11 types. Figure 12 shows these types as they exist in various deltas, and Figure 13 gives aerial views of some types. Type A has numerous enclosed or semienclosed lakes or bays occupying the interdistributary regions. The area of open water exceeds the area of vegetated cover. Type B is very similar, but the water bodies are open to the sea and the distributaries prograde into the receiving body

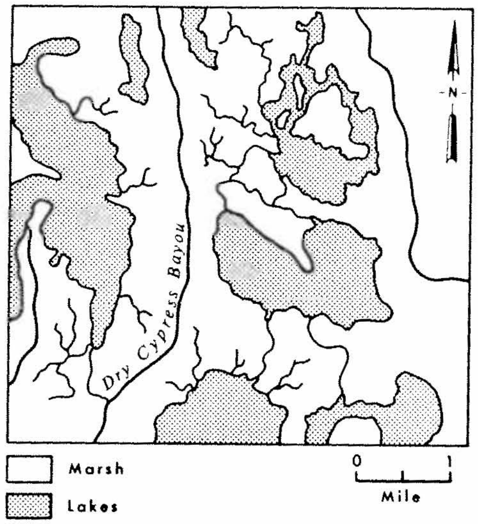

A. Enclosed bays - Mississippi River, USA.

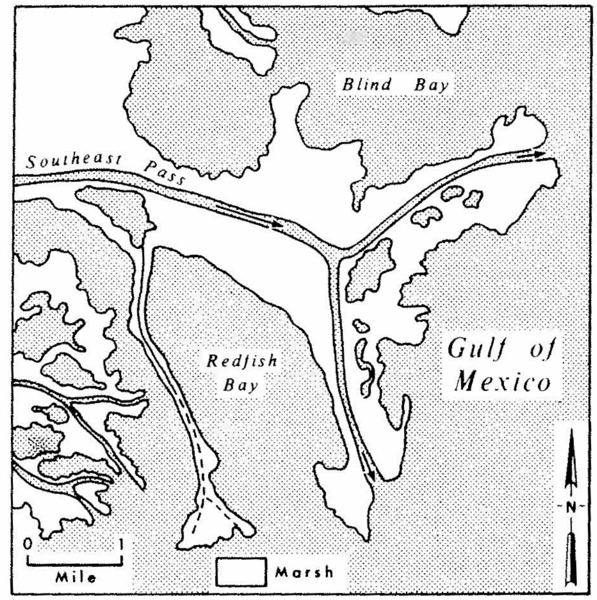

B. Open bays - Mississippi River, USA.

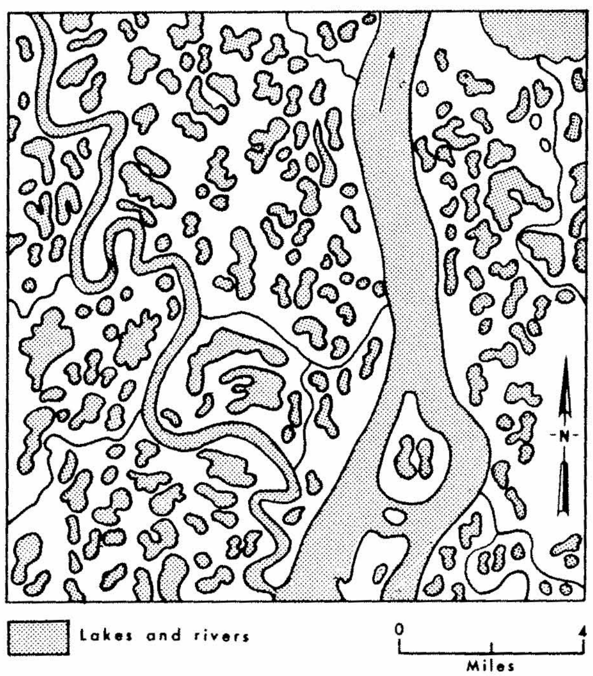

C. Interdistributary lakes - Mackenzie River, Canada.

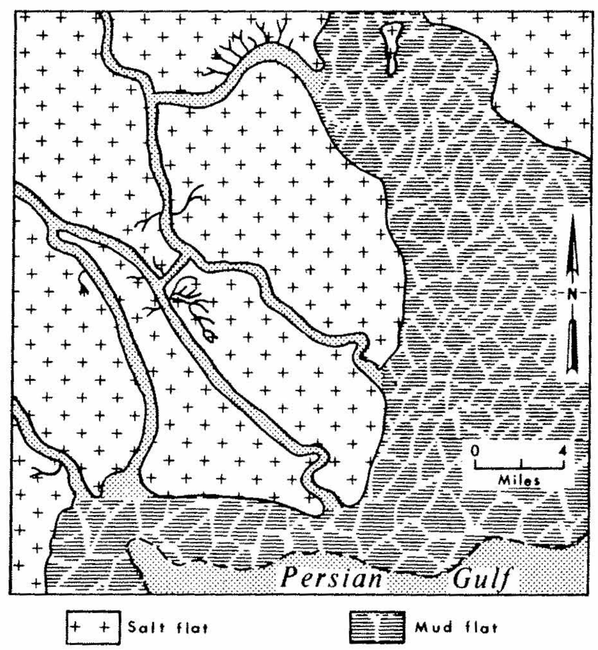

D. Evaporite flats - Shatt al Arab, Iran.

Figure 12. Examples of interdistributary landform types.

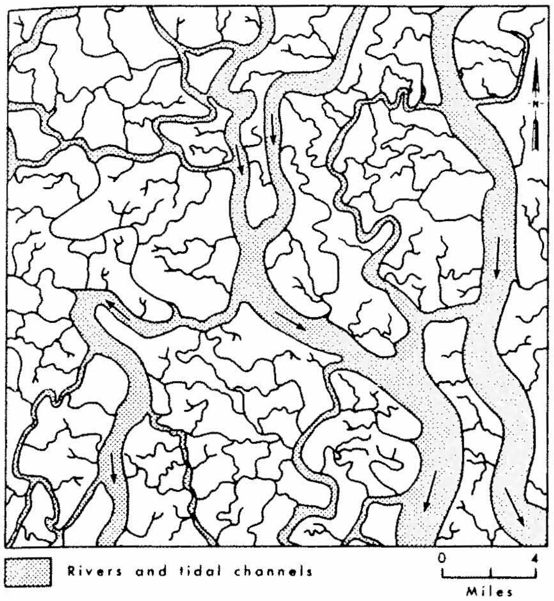

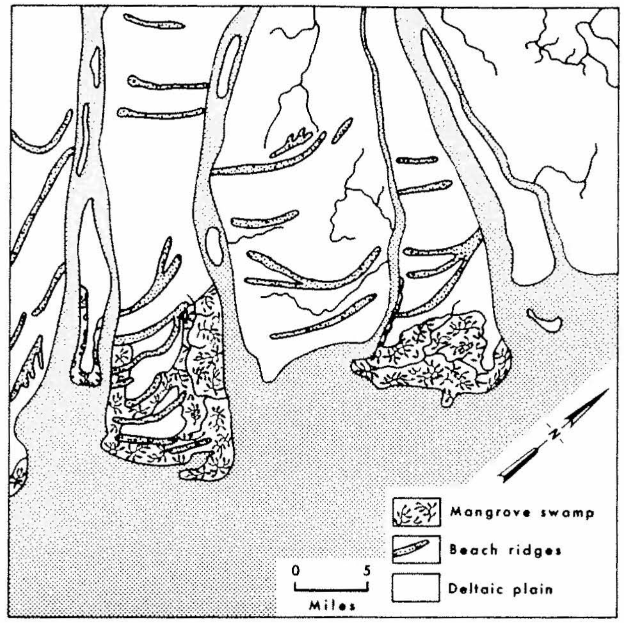

E. Tidal channels - Ganges-Brahmaputra River, East Pakistan.

F. Beach-dune ridge and swale complex - Mekong River, South Vietnam.

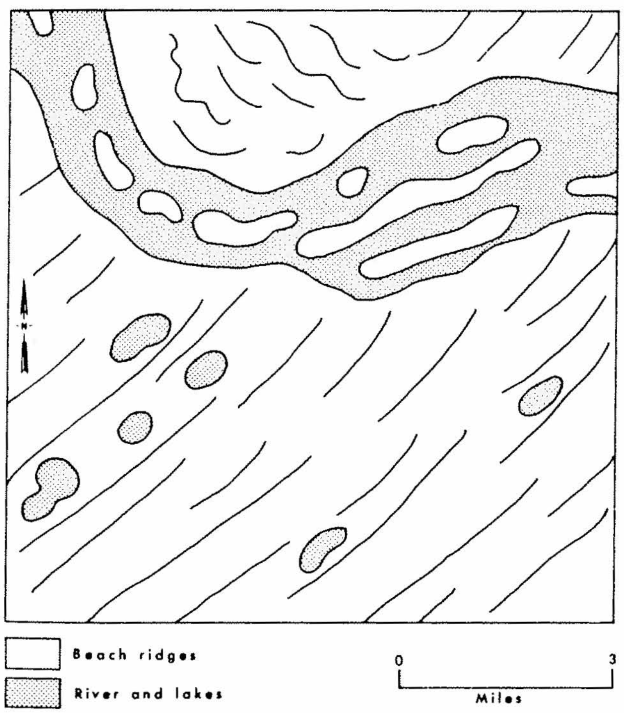

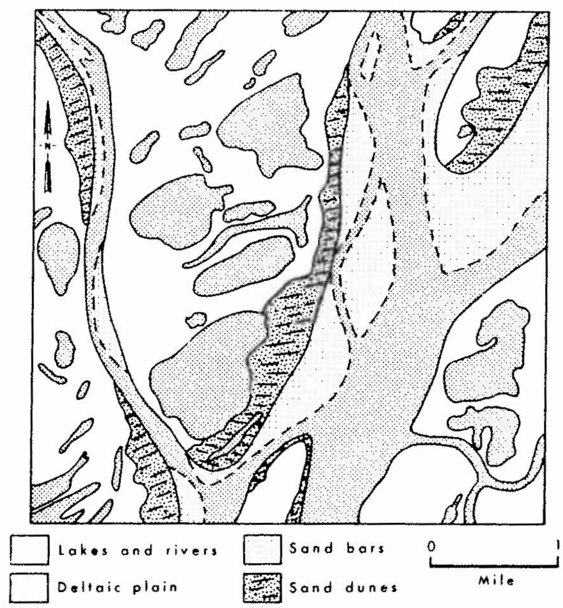

G. Beach ridge plain - São Francisco, Brazil.

H. Eolian dunes - Colville River, Alaska.

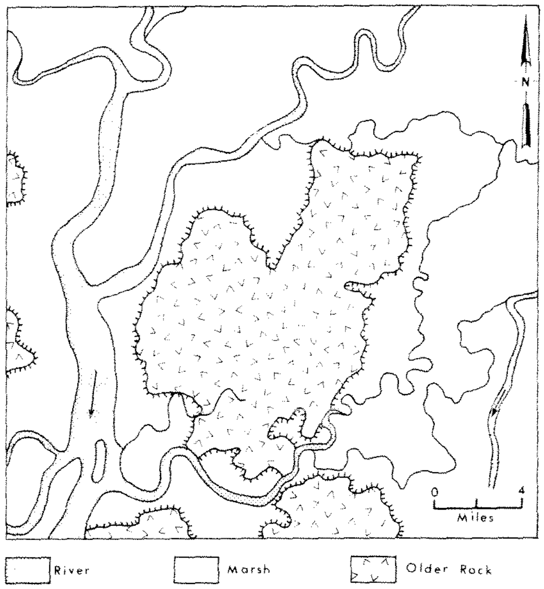

I. Interdistributary highs - Irrawaddy River, Burma.

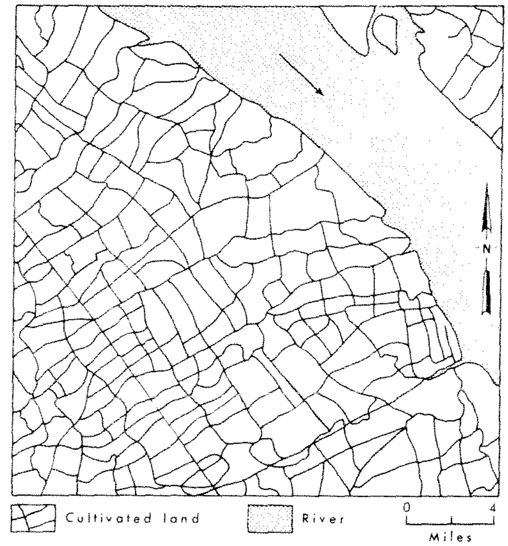

J. Cultivated plain - Yangtze, China.

of water. In type C, a large portion of the interdistributary area is occupied by lakes with few interconnections. In type D evaporite flats and unvegetated regions are the most common features. Tidal channels are often quite numerous, cutting across the flats. Type E is characterized by the presence of innumerable tidal channels dissecting a heavily vegetated area between the distributaries. Although a variety of tidal channel patterns can be recognized, they are not differentiated in this study. Type F consists typically of a heavily vegetated area containing few open water bodies. The type of vegetation varies considerably, ranging from broad freshwater swamps and reed marshes to mangrove swamps. However, data regarding the exact vegetation type normally is lacking. Type G contains beach-dune ridge complexes separated by broad, heavily vegetated swales that are often the site of small lakes or tidal channels. The swales are generally broader than the ridges. Type H displays nearly continuous beach ridge development between the distributaries. Type I is similar to H, but actively migrating dune fields are the most characteristic feature. Type J shows structural highs or outcropping older rock surfaces between the distributaries. Type K results from man's activity and is characterized by intensive cultivation between distributaries.

1.3.3.22 Exposure of delta coast: The exposure of the delta shoreline is classified as either protected or open. The protected class includes those delta shorelines that contain extensive barrier islands, rock outcrops, reefs, and similar features offshore that protect the major portion of the delta shoreline. If the shoreline is unobstructed, the exposure is simply termed open.

1.3.3.23 Number of active river mouths: The number of river mouths found along the delta shoreline.

A. Enclosed bays - Mississippi River, USA.

B. Evaporite flats - Burdekin River, Australia.

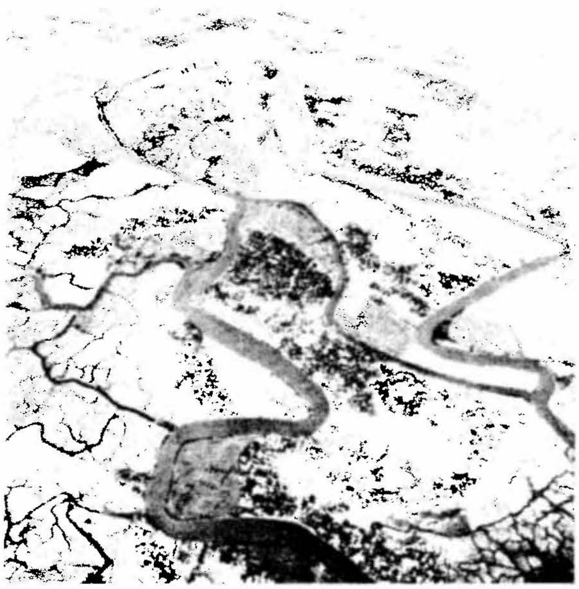

C. Tidal channels - Ganges-Brahmaputra River, East Pakistan.

D. Beach-dune ridge and swale - Burdekin River, Australia.

Figure 13. Aerial photographs of interdistributary types.

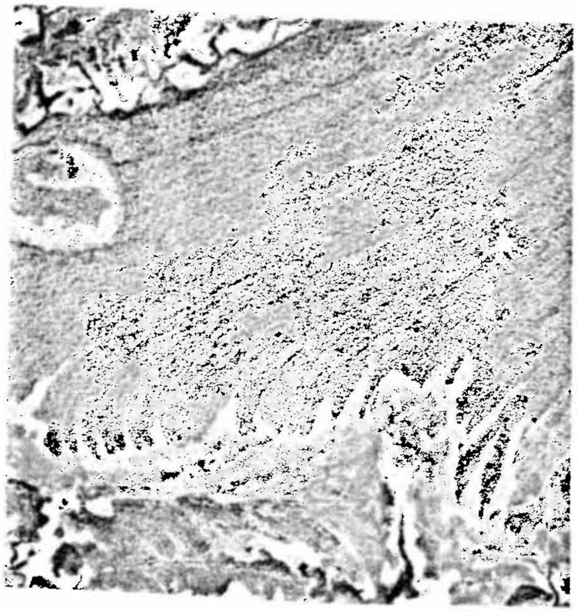

E. Beach ridge plain, Burdekin River, Australia.

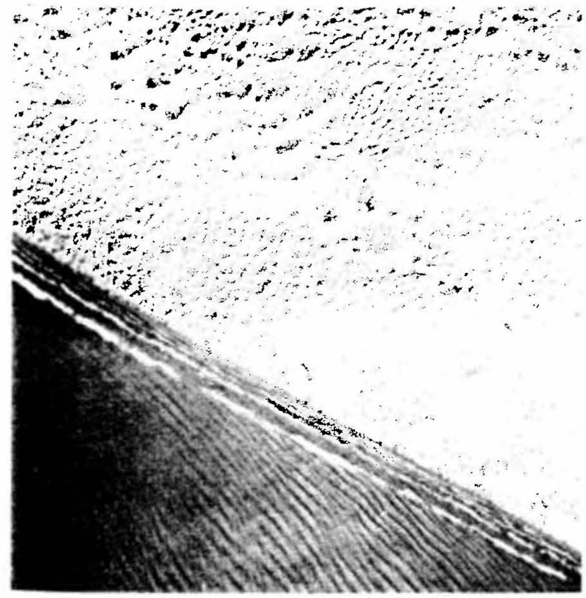

F. Eolian dune plain - São Francisco River, Brazil.

1.3.3.24 Type of river mouths: Four basic river mouth shapes can be distinguished and are illustrated diagrammatically in Figure 14 and by aerial photographs in Figure 15. Type 1 shows relatively straight confining banks (the upstream width is approximately the same as the downstream width) all the way to the sea. Type 2 has a funnel-shaped plan view, and the seaward end is wider than the upstream portion. Type 3 is characterized by constriction at the coast and generally is wider upstream than at the seaward end. Type 4 is the impounded or deflected type where seaward flow is inhibited or diverted by a barrier formation. Each of the four types may or may not protrude seaward. Islands within river mouths may be present or absent. In order to decide objectively whether a single river mouth or two river mouths exist when an island is present, the following criterion is used: If the channel width at the upstream end of the island is greater than the longest axis of the island, a single river mouth is indicated. If the channel width is less than the longest axis of the island, the island is regarded as having separated the flow into two channels.

1.3.3.25-1.3.3.26 Width of river mouths: The width in miles of each river mouth is recorded. The width is measured at the seawardmost part of the channel where it is still confined by well-defined subaerial banks. The mean, standard deviation, and coefficient of variability of river mouth widths are determined.

1.3.3.27-1.3.3.28 Depth of river mouths: The maximum depth, in feet, is recorded from hydrographic charts for each river mouth. The mean, standard deviation, and coefficient of variability are determined for each depth at the river mouths.

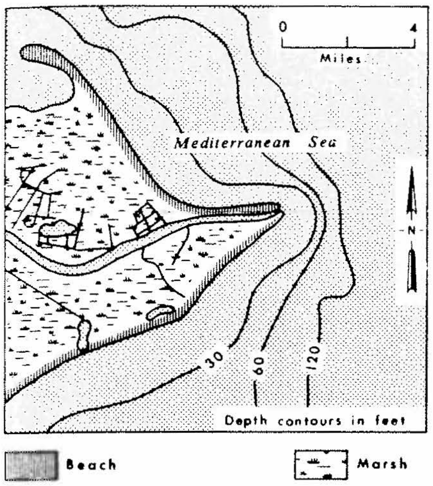

A. Straight, protruding - Ebro River, Spain.

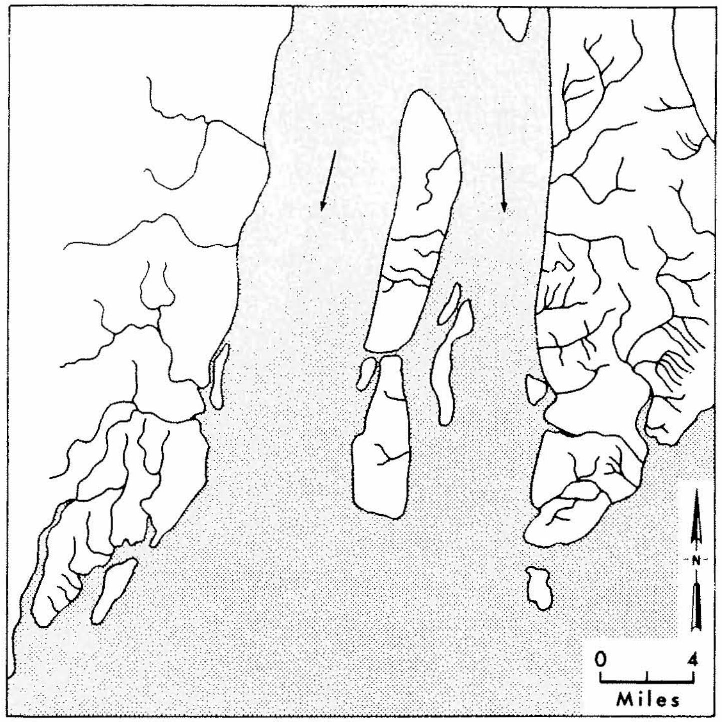

B. Straight, indented - Ganges-Brahmaputra, East Pakistan.

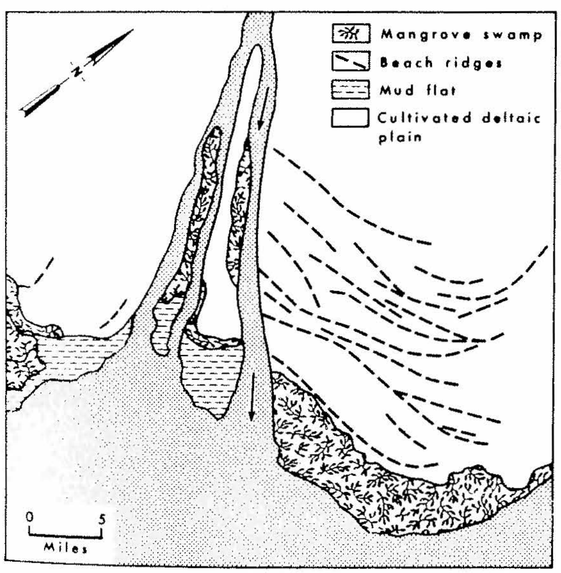

C. Funnel-shaped, indented - Mekong River, South Vietnam.

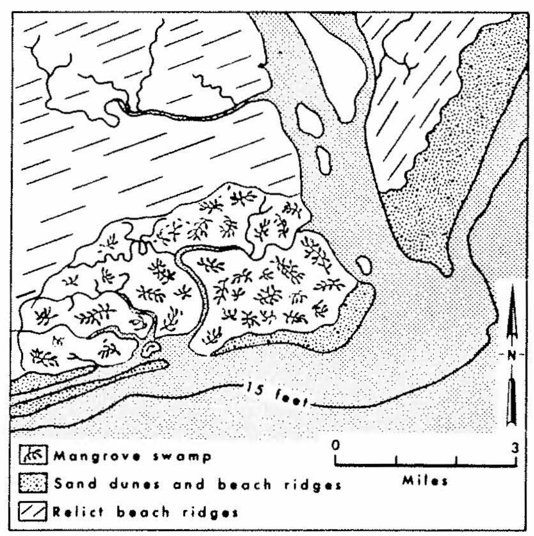

D. Constricted, protruding - São Francisco River, Brazil.

Figure 14. Examples of river mouth types.

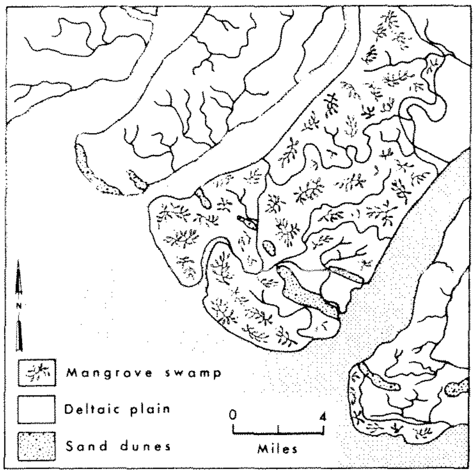

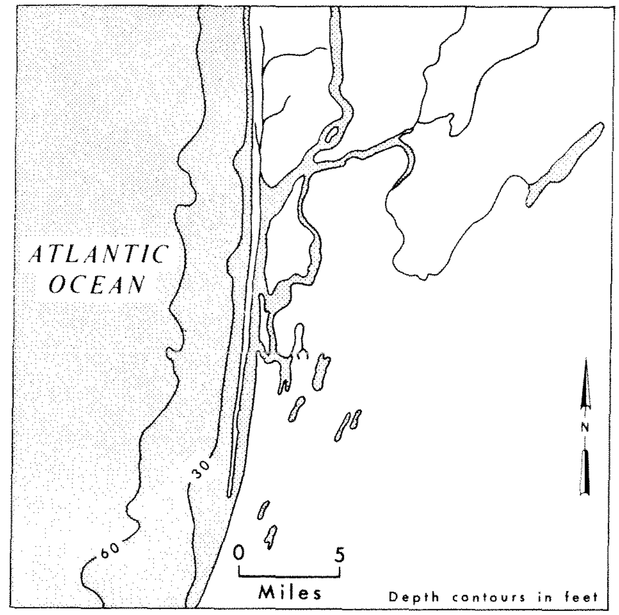

E. Constricted, indented - Irrawaddy River, Burma.

F. Deflected - Senegal River, Senegal.

1.3.3.29- 1.3.3.30 Depth-width ratios of river mouths: The depth-width ratio for each mouth is calculated from the above data obtained for width and depth. The mean, standard deviation, and coefficient of variability are also calculated.

1.3.3.31 Topography of bar: Four major types of bars can be defined. These are illustrated diagrammatically in Figure 16. Type 1 is simply a smooth, flat bulge seaward of the river mouth. Type 2 consists of a lunate-shaped bulge or bar seaward of the river mouth. Type 3 consists of a triangular shoal or middle ground which separates two deeper channels. Type 4 is characterized by subaqueous levees flanking a straight channel directly seaward of the mouth. Each of the four types may or may not be scarred by radial gullies and may or may not be accompanied by the presence of linear tidal ridges.

1.3.3.32 Area of bar: The areas in square miles contained by the peripheral contours of each river mouth bar are computed from digitized data.

1.3.3.33 Distance to edge of bar: The dimensionless distances (in river mouth widths) from each river mouth to the distal edge of each river mouth bar are measured and tabulated.

1.3.3.34 Area of bulge: The deltaic bulge is defined as the portion of the deltaic plain which protrudes seaward beyond the general trend of the flanking coastline. In this study the bulge is considered to be bounded landward by a line x connecting the lateral limits of the protrusion and seaward by the 40-foot-depth contour (Fig. 17). The area in square miles contained by the boundaries of the bulge is computed from digitized data.

A. Straight - Burdekin River, Australia.

B. Funnel-shaped, Ganges-Brahmaputra River, East Pakistan.

C. Constricted - Ganges River, East Pakistan.

D. Deflected - Jequitinhonha River, Brazil.

Figure 15. Aerial photographs illustrating four river mouth types.

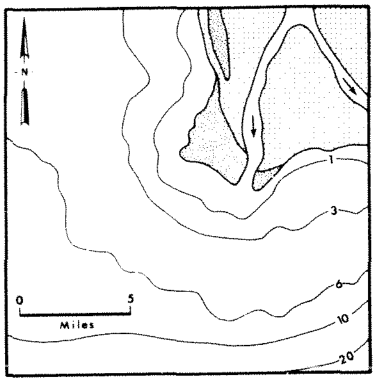

A. Radial.

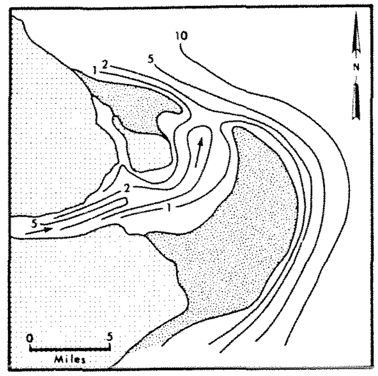

B. Lunate bar.

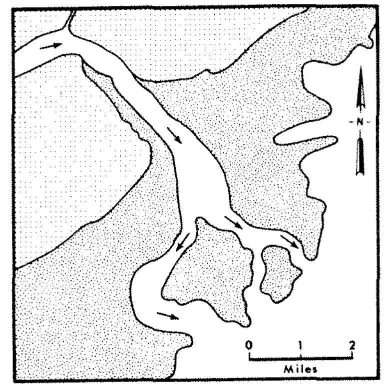

C. Middle-ground bar.

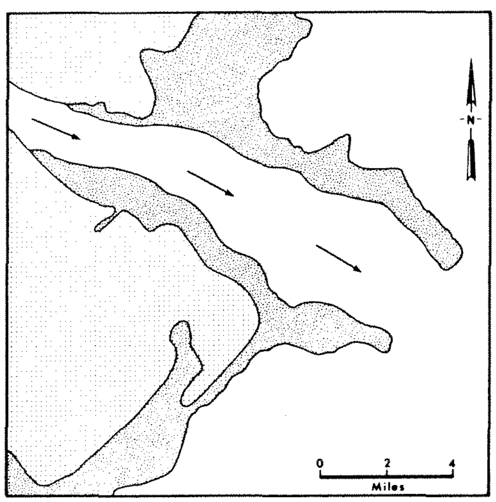

D. Subaqueous jettied.

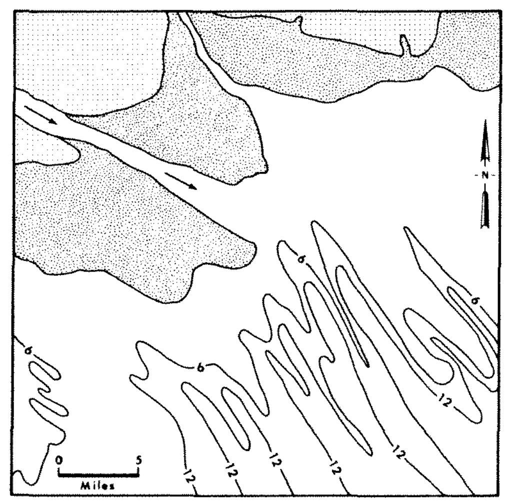

E. Tidal ridge and swale.

Figure 16. River mouth bar types.

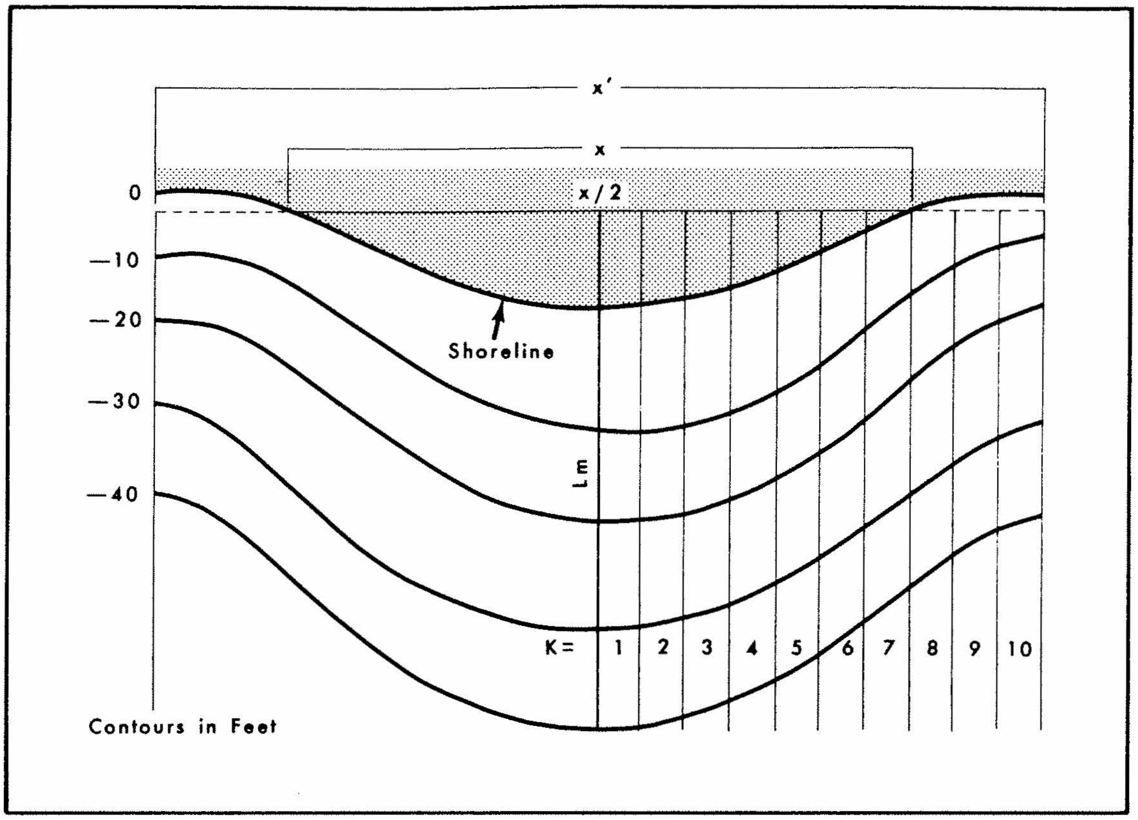

Figure 17. Diagram defining parameters used in deltaic bulge morphometry.

1.3.3.35 Volume of bulge: The total volume of the bulge V_{Bt} in cubic miles is computed from

$$V_{Bt} = \sum_j [A_j + ([\Delta A]_j/2)] (\Delta Z)_j$$

where j refers to the contour, A_j is the area in square miles contained by the contour j, $[\Delta A]_j$ is the difference in area between consecutive contours or $[\Delta A]_j = A_{j-1} - A_j$, and $(\Delta Z)_j$ is the contour interval between contours j and j-1 in miles.

1.3.3.36 Ratio A_R/A_L of bulge: The line x connecting the lateral limits of the bulge (section 1.3.3.35) and the portion of the 40-foot-depth contour constituting the seaward limit of the bulge (Fig. 17) are bisected and a straight line is constructed so as to connect the two midpoints. The bulge is thereby divided into two segments designated right or left, depending on the position of the segment relative to the downstream flow within the distributaries. The total area of each segment is determined by the same technique as described in section 1.3.3.35, and a ratio is obtained by dividing the area of the right segment by that of the left segment.

1.3.3.37 Ratio V_R/V_L of bulge: The volumes of each segment are computed by the same procedure as followed for the entire bulge (section 1.3.3.36), and the ratio of the volume of the right side to the volume of the left side is calculated.

1.3.3.38 Subaerial area of bulge: The area in square miles contained by the line x connecting the lateral limits of the bulge and the 0-foot-depth contour (shoreline) is calculated from digitized data.

1.3.3.39 Subaerial volume of bulge: The volume V_{Bo} in cubic miles of the subaerial portion of the bulge is simply computed from

$$V_{Bo} = A_o \cdot 40$$

where A_o is the area of the subaerial portion of the bulge and the constant 40 refers to the vertical distance between the 0- and 40-foot-depth contours.

1.3.3.40 Subaqueous area of bulge: The area in square miles of the portion of the bulge between the 0-foot-depth contour (shoreline) and 40-foot-depth contour is calculated from digitized data.

1.3.3.41 Subaqueous volume of bulge: The volume V_{Bs} in cubic miles of the portion of the bulge between the shoreline and the 40-foot-depth contour is computed from

$$V_{Bs} = \sum_j (A_j - A_o) \ (\Delta Z)_j$$

where ΔZ is the contour interval and A_j is the area contained by contour j.

1.3.3.42 Ratio V_{Bo}/V_{Bs}: The ratio of the volume of the subaerial portion of the bulge to the volume of the subaqueous portion is computed from the results of 1.3.3.39 and 1.3.3.41.

1.3.3.43 Subaqueous hypsometric integral of bulge: The dimensionless hypsometric integral HI_s of the subaqueous portion of the bulge is computed from

$$HI_s = \sum_j [(A - A_o)/(A_{max} - A_o)] \ [\Delta(Z/Z_{max})]_j + (\Delta[(A - A_o)/(A_{max} - A_o)]_j \cdot [\Delta(Z/Z_{max})]_j)/2$$

where A_{max} is the area and Z_{max} is the depth of the basal (50-foot-depth) contour.

1.3.3.44- Distribution parameter for bulge volume (right and left sides):
1.3.3.45 Each side of the deltaic bulge is divided into ten segments

(designated by the subscript k, where k = 1-10) by a series of equally spaced lines parallel to the central dividing line or axis of the bulge (Fig. 17). The cumulative bulge volume at each interval k is computed from

$$V_k = \sum_{k=1}^{k} [\sum_j A_j (\Delta Z)_j]_k.$$

The dimensionless cumulative volume at each interval k is then computed from

$$V_{Dk} = V_k/V$$

where V is the total volume of the particular side of the bulge (i.e., V_R or V_L). Values of V_{Dk} are then plotted graphically against the dimensionless linear distance from the central axis (i.e., against k/10). From the graph the continuous dimensionless distance β corresponding to the V_{Dk} value of 0.5 may be obtained. The value of β serves as the distribution parameter.

1.3.3.46 Mean bulge volume distribution parameter: The values of 1.3.3.44 and 1.3.3.45 are summed and divided by 2 to obtain the mean for the entire bulge.

1.3.3.47 Offshore slope: The average slopes in feet per mile from each of the 20 equally spaced points along the shoreline to each of the contours are determined by dividing the depth in feet corresponding to each contour by the respective distance. The means, variances, standard deviations, maxima, and minima are tabulated.

1.3.4.0 Climatological

1.3.4.1-1.3.4.8 Climatological information is obtained as in section 1.1.4.0, and climatic classification, average yearly temperature, mean monthly temperature, total yearly precipitation, mean monthly precipitation, dates of freeze, dates of thaw, and duration of freeze are determined and tabulated following the procedures described in sections 1.1.4.1, 1.1.4.2, 1.1.4.3, 1.1.4.6, 1.1.4.7, 1.1.4.14, 1.1.4.15, and 1.1.4.16, respectively.

1.3.5.0 Pedological

See 1.1.5.0.

1.3.5.1 Major soil type: The major soil type is classified according to the scheme listed in 1.1.5.1.

1.3.6.0 Biological

See 1.1.6.0.

1.3.6.1 Major vegetation type: The classification presented in section

1.1.6.1 is followed.

1.3.7.0 Hydrological

More complete and detailed sets of hydrological data are available for the delta regions than for the other physiographic divisions. It is therefore possible to consider more aspects of the hydrologic regime.

1.3.7.1 Monthly discharge: From published discharge records the mean, variance, standard deviation, and coefficient of variability of the discharge (in cusecs x 10^3) are computed and tabulated for each month of the year.

1.3.7.2 Average yearly discharge: From the same sets of data as used in 1.3.7.1 the mean, variance, standard deviation, and coefficient of variability of the discharge in cusecs x 10^3 for the entire year are determined.

1.3.7.3 Maximum discharge: The maximum discharge in cusecs x 10^3 occurring during the year and the date of occurrence.

1.3.7.4 Minimum discharge: The minimum discharge in cusecs x 10^3 occurring during the year and the date of occurrence.

1.3.7.5 Flood peakedness: See 1.2.7.5.

1.3.7.6 High-water period: See 1.2.7.6.

1.3.7.7 Low-water period: See 1.2.7.7.

1.3.7.8 Yearly sediment load: Where data are available the yearly sediment load in tons per year reaching the receiving basin is recorded.

1.3.7.9 Discharge efficiency index: The monthly discharge per foot of river mouth width, obtained by dividing the discharge in cusecs by the total width of all outlets combined, is divided by the wave power per foot of shoreline (see section 1.4.7.3) for the corresponding month. The values are tabulated for each month.

1.3.7.10 Annual summary of the discharge efficiency index: From the values tabulated in 1.3.7.9 the annual mean, standard deviation, and coefficient of variability are computed.

1.4.0.0 <u>Receiving Basin</u>

1.4.1.0 Location

The geographical coordinates of the latitudinal and longitudinal limits of the basin are recorded.

1.4.1.1 Body of water: The name of the major body of water into which the river system debouches.

1.4.2.0 Geological

Very little information that is relevant to the present study is available generally on the geology of most of the receiving basins.

1.4.2.1 Shelf structure: Where information is available from geological maps or published reports, the general geological structure of the continental shelf in the vicinity of the delta or river mouths is classified according to the five categories listed in section 1.1.2.4.

1.4.3.0 Geomorphological

Six general geomorphological characteristics are determined from hydrographic charts.

1.4.3.1 Longest fetch: The maximum distance over which ocean waves are able to travel along an unobstructed course to the coast.

1.4.3.2 Direction of longest fetch: The compass octant (i.e., N, NE, E, etc.) from which unrefracted waves of the longest fetch reach the coast.

1.4.3.3 Directions of fetch greater than 200 miles: All compass octants from which unrefracted waves with fetch lengths of 200 miles or more are able to reach the coast.

1.4.3.4 Average width of continental shelf: The average distance in miles from the shoreline to the break in slope at the seaward edge of the continental shelf (in the vicinity of the deltaic plain).

1.4.3.5 Slope of continental shelf: The mean, variance, standard deviation, coefficient of variability, maximum and minimum of the ratio of the depth in feet at the edge of the continental shelf to the width of the continental shelf in miles are recorded.

1.4.3.6 Topography of shelf: The topography of the continental shelf is classified as regular or irregular.

1.4.4.0 Climatological

Eleven parameters are determined, primarily from marine atlases.

1.4.4.1 Wind frequency (Beaufort 3-12): The percentage frequencies of all winds with Beaufort force greater than 3 from each quadrant (i.e., offshore, onshore, alongshore to left, and alongshore to right) are recorded for each month and for the entire year.

1.4.4.2-1.4.4.6 Vector frequencies for all winds with Beaufort force greater than 3: For winds with Beaufort force 2-3; Beaufort force 4-5; Beaufort force 6-7; and Beaufort force 8-12. All winds are assigned to either the onshore or the offshore hemisphere. For each hemisphere, winds are resolved vectorially into a (parallel to the shoreline) and b (normal to the shoreline) components. The component a is obtained from

$$a = \sum_{i=1}^{n} l_i \cos \theta_i;$$

and the component b from

$$b = \sum_{i=1}^{n} l_i \sin \theta_i$$

where l is the percentage frequency (vector length) and θ is the angle toward which the winds blow in a regular rectangular coordinate system with the coastline trend as the x axis. The subscript i refers to the azimuth (or octant). The components a and b are computed and tabulated for both the onshore and the offshore hemispheres for each month and for the year. The process is repeated for each Beaufort class listed above.

1.4.4.7 Yearly vector strength and direction: The length and angle of the annual vector resultant for all onshore winds are computed by weighting the vector frequencies of the onshore a and b components of each Beaufort class by the median force of that class (i.e., for Beaufort class 2-3 the weighting factor is 2.5, etc.). The length L of the onshore resultant is computed from

$$L = \left[\left(\sum_{B=1}^{n} a_B m_B \right)^2 + \left(\sum_{B=1}^{n} b_B m_B \right)^2 \right]^{-2}$$

and the angle θ of the resultant is computed from

$$\theta = \tan^{-1} \left[\left(\sum_{B=1}^{n} b_B m_B \right) / \left(\sum_{B=1}^{n} a_B m_B \right) \right]$$

where the subscript B refers to the Beaufort class and m is the median force of the class.

1.4.4.8 Storm systems: The average annual frequency of severe storms is recorded.

1.4.4.9-1.4.4.11 Date of freeze, date of thaw, and duration of freeze: See 1.1.4.9, 1.1.4.10, and 1.1.4.11.

1.4.5.0 Pedological

No data available.

1.4.6.0 Biological

The presence or absence of coral reefs is recorded.

1.4.7.0 Hydrological

Data on the oceanographic regime of the receiving basin are obtained from marine climatic atlases, pilot charts, sea and swell data charts, tide tables, and by hindcasting techniques.

1.4.7.1 Vector strength and direction of swell: Frequencies of swell from each direction (onshore) for each month are obtained from sea and swell charts. The resultant vector strengths L_s for each month are then computed from

$$L_s = \left[\left(\sum_{i=1}^{n} l_i \cos \theta_i \right)^2 + \left(\sum_{i=1}^{n} l_i \sin \theta_i \right)^2 \right]^{-2}$$

where l is the frequency and θ is the angle (toward which the swell propagates) of swell from each octant, where the subscript i designates the octant. The resultant angle θ_s is computed from

$$\theta_s = \tan^{-1} \left[\left(\sum_{i=1}^{n} l_i \sin \theta_i \right) / \left(\sum_{i=1}^{n} l_i \cos \theta_i \right) \right] .$$

Values of L_s and θ_s are tabulated for each month.

1.4.7.2 Vector strength and direction of seas: Frequencies and directions of seas are obtained from sea and swell charts and resultant strengths and angles are computed and tabulated as in 1.4.7.1.

1.4.7.3 Weighted wave power (30-foot contour): Wave height, period, and direction of incidence in deep water are determined from wind data by hindcasting procedures (Sverdrup-Munk-Bretschneider technique). Wave characteristics so obtained are input, together with taped digitized data on the offshore contours, to a Fortran IV computer program for computing the changes in wave characteristics caused by refraction, shoaling, and frictional attenuation. (The calculations performed by this program are discussed in Appendix 2.) Along each wave ray (orthogonal), wave power P_o in foot pounds per second is computed at specified intervals from $P_o = \gamma H^2 c_g$ 8 where γ is the unit weight of seawater, H is the wave height in feet, and c_g is the group velocity. The value of P_o at the 30-foot contour on each ray is weighted by the relative frequency of the particular set of deep-water wave characteristics. The total weighted wave power P_o' for each wave ray is given by

$$P_o' = \left(\sum_{j=1}^{n} w_j P_{oj} \right) F/100$$

where the subscript j refers to the given set of wave characteristics (i.e., the particular combination of deep-water height, period, and angle), w is the relative frequency, and F = 1-t where t is the fraction of time seas were calm. The mean, variance, standard deviation, and coefficient of variability are calculated for each month.

1.4.7.4 Annual summary of wave power: From 1.4.7.3 the annual mean, standard deviation, and coefficient of variability are computed. In addition, correlation coefficients (r) and significance levels relating mean annual power to distance alongshore from the central axis of the bulge for the right and left sides are calculated.

1.4.7.5 Weighted wave power (shore): The weighted wave power nearest the 0-foot-depth contour is calculated as in 1.4.7.3 for each month.

1.4.7.6 Annual summary of shore wave power: The statistics listed in 1.4.7.4 are calculated.

1.4.7.7 Weighted longshore power: The longshore power at the shore is computed from

$$P_\ell = P_o \sin \alpha \cos \alpha$$

where α is the angle between the wave ray and the normal to the bottom contour. Weighted longshore power P_ℓ is calculated from

$$P_\ell = \left(\sum_{j=1}^{n} w_j \, P_{\ell j} \right) F/100.$$

1.4.7.8 Annual summary of longshore power: The statistics listed in section 1.4.7.4 are computed and recorded.

1.4.7.9 Weighted power gradient: The rate of increase or decrease in wave power between any two adjacent orthogonals at the shoreline is given by

$$\frac{\Delta P_o}{\Delta x} = \frac{P_{o_{q-1}} - P_{o_q}}{\Delta x}$$

where the subscript q denotes the orthogonal and Δx is the linear distance in miles between orthogonal q-1 and q. The weighted power gradient $(\Delta P_o/\Delta x)/w$ is calculated from

$$\left(\frac{\Delta P_o}{\Delta x}\right)' = \sum_{j=1}^{n} \left[w_j \left(\frac{\Delta P_o}{\Delta x}\right)_j \right] F/100.$$

The value of $(\Delta P_o/\Delta x)$ is determined for each alongshore interval.

1.4.7.10 Annual summary of power gradient: The statistics listed in 1.4.7.4 are calculated.

1.4.7.11 Weighted longshore power gradient: The weighted longshore power gradient $(\Delta P_l/\Delta x)'$ at the shore is determined and analyzed following the procedure described in section 1.4.7.5.

1.4.7.12 Annual summary of longshore power gradient: The statistics listed in 1.4.7.4 are calculated.

1.4.7.13 Type of tide: The tidal regime of the receiving basin is classified according to three main types:

1. Diurnal--one high and one low tide per 24-hour period.

2. Semidiurnal--two highs and two lows occurring within a period

of approximately 24 hours.

3. Mixed--two highs and two lows occurring in a 24-hour period but having a pronounced diurnal inequality, with the result that there is generally one higher high water, one lower high water, one higher low water, and one lower low water per day.

1.4.7.14 Monthly maximum and minimum tide range: The maximum and minimum differences between high and low water in feet are tabulated for each month. These values are obtained primarily from published tide tables.

1.4.7.15 Average tidal range: The annual mean tidal range in feet is recorded.

1.4.7.16 Salinity: The average salinity of the ambient seawater expressed in parts per thousand total dissolved salts is recorded for January and July.

1.4.7.17 Water temperature: The average water temperature in degrees centigrade, as obtained from marine climatic atlases, is recorded for the months of January and July.

1.4.7.18 Water density: The average density of ambient seawater is recorded for the months of January and July.

1.4.7.19 Offshore currents: The direction (set) and velocity in feet per second of the coastal currents in the general vicinity of the delta front are obtained from pilot charts and tabulated for each month.

SIGNIFICANCE OF PROCESS AND MORPHOLOGIC PARAMETERS

A multitude of complex natural systems and subsystems combine to yield the unique suite of environments and configurations characteristic of the earth's surface. Few of these are more internally interdependent than the large river systems. Climatic, geologic, geomorphic, hydrologic, and biologic events which take place in drainage basins hundreds of miles from the coast eventually manifest themselves in modified form in the river delta and in the receiving basin into which the river debouches. Some of these factors and their interactions are illustrated diagrammatically in Figure 18. As the fluids and sediments derived from the drainage basin are transported to the sea, processes active in the alluvial valley and delta play major roles in the modification of the system, as do the oceanographic and climatic regimes of the receiving basin. No component of the system is causally isolated.

The parameters measured in the Coastal Information Program were selected on the basis of causal connections, the existences of which were indicated by experience and by published literature. The purpose of this discussion is to outline the possible significance of these parameters. Determination of their true significance must await the completion of the project, after data from many river systems have been quantitatively correlated and analyzed.

The Drainage Basin

The drainage basin is the "cradle" of the river system inasmuch as it supplies water and sediment to the remainder of the system. The amount of water received by the basin is primarily a function of climate and basin area; but the amounts of water and sediment which ultimately leave the basin as streamflow, as well as the spatial patterns and temporal distributions taken by the discharging substances, are highly dependent upon the geology, geomorphology, vegetative cover, and pedology of the basin.

GEOLOGY

It is the geological setting that Davis (1909) referred to as "structure," the first category of his famous trio of geomorphological factors, structure, process, and stage. In Davis' words, "Structure is the foundation of all geographical classifications in which the trio of controls is recognized....[It] is a pertinent element of geographical study when, as nearly always, it influences form...." (Davis, 1909, pp. 249 and 253). Following the design set by Gilbert (1877, pp. 99-150), and on the basis of considerable field work, Hack (1960) has evolved the hypothesis that erosional topography depends primarily upon "a balance between the processes of erosion and the resistance of the rocks as they are uplifted or tilted by diastrophism" (Hack, 1960, p. 86).

Investigations by Shumm (1954) disclosed that basin relief ratios and sediment losses increase as lithologic resistance decreases. This would indicate that for any given basin area the volume of sediment reaching the delta during any time interval should be inversely proportional to the resistance of basin rocks.

Various other studies on the relationships between lithology and morphology have been carried out. Morisawa (1959) found that resistant beds usually result in increased basin area and stream gradient and concluded that lithological con-

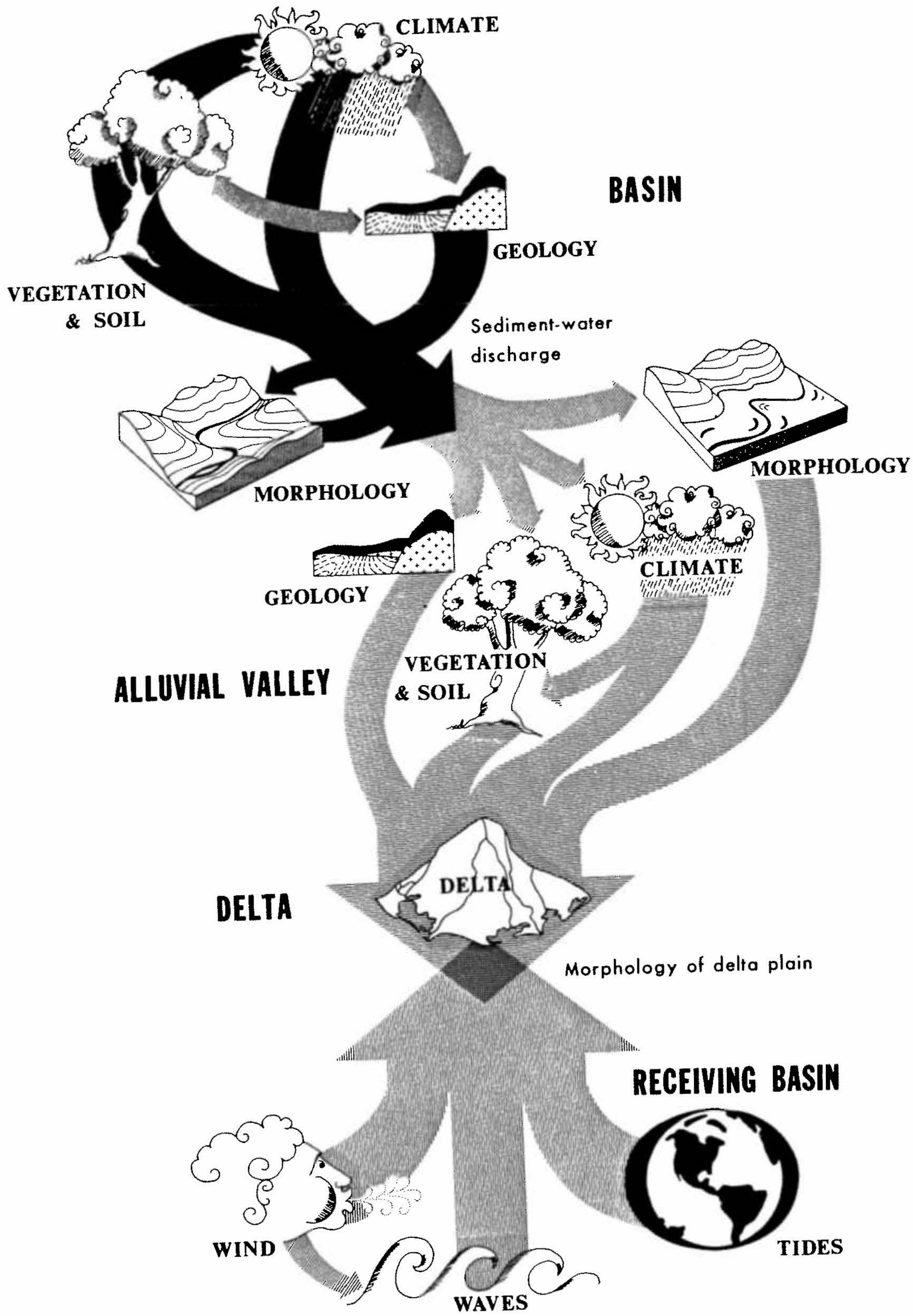

Figure 18. Diagrammatic representation of some parameter interactions in a river system.

trasts usually produce overall morphological differences. Yatsu (1966) has provided the most detailed treatment currently available on the processes of rock control as they influence geomorphology.

Geological structure and tectonic stability within the basin are also fundamental in determining the initial form and relief and should thereby influence the ability of runoff to transport detritus. For example, basins located in orogenic zones or in areas of strong folding or faulting can be expected to possess greater relief and consequently greater potential energy (owing to gravity) than will basins in areas of more subtle geologic activity.

GEOMORPHOLOGY

The surface morphology of the drainage basin, in addition to reflecting the climatic, geologic, biologic, and hydrologic processes, significantly influences the water-sediment output which eventually reaches the sea.

The total volume of water received by a drainage basin over any given time interval is dependent upon the amount of precipitation and the total catchment area. Basin area is therefore a fundamental determinant of water and sediment discharge.

There have been numerous investigations relating the area of low-order basins to various drainage and morphometric characteristics (Horton, 1945; Melton, 1957; Morisawa, 1959; Leopold et al., 1964; Chorley, 1957). Less work has been carried out on the significance of the area of high-order basins, particularly of the world's major river basins. Leopold et al. (1964) found a reasonably good correlation between total basin area and total stream length of 34 major river systems. Hack (1957) obtained the regression equation

$$L = 1.4 \, A_b^{0.6}$$

relating stream length L to basin area A_b. Morisawa (1959) has described relationships between basin area and stream length, stream gradient, relief ratio, and basin circularity. Potter (1953) has included basin area along with three other factors in a regression equation predicting discharge.

To the writers' knowledge there have been no consequential studies quantitatively evaluating the influence of basin area on sediment yield. However, it is expected that a significant correlation will emerge when other salient factors are taken into account.

Basin perimeter is being measured in this study primarily for use in combination with other parameters. For example, it is anticipated that the ratio of basin perimeter to basin area may be correlative with average relief. Basin elevation is a factor of considerable moment inasmuch as it controls the climate of the basin and partially determines overall stream gradients and consequent energy.

Shumm (1954) has demonstrated the existence of a strong relationship between basin relief and the amount of sediment lost from the basin. As a dimensionless index of basin relief, Shumm used a relief ratio obtained by dividing the total relief of the basin (the elevation difference between the highest and lowest points) by the length of the longest axis of the basin. In eight small basins in Utah, New Mexico, and Arizona, Shumm observed a consistent increase in sediment loss with increasing relief ratios. It is difficult in the case of Shumm's data, however, to identify the true cause of increased sediment loss inasmuch as both sediment loss and relief ratio increased with decreasing lithologic resistance.

In nature, relief reflects, and in varying degrees controls, such factors as pedological, climatological, and biological regimes, lithology, drainage density, etc., in addition to influencing the sediment yield. It is uncertain, however, what relationships between drainage density and other variables will emerge from the analyses of maximum-order basins. Considering the complex topography and large area of most of the basins examined in this study, it was anticipated that a single relief ratio such as that of Shumm would be a relatively insensitive parameter. Hence, average relief based upon the relief at numerous randomly determined points is used in addition to the relief ratios.

Area-altitude analyses similar to those proposed by Strahler (1952, 1957, 1958) appear to afford meaningful parameters applicable to the study of large basins. Dimensional analysis as applied by Strahler to the overall three-dimensional configuration of drainage basins permits objective and reasonably accurate comparisons of basins which vary in absolute size. For reasons of expediency, and in order to satisfy specialized requirements of the present study, the writers have introduced some minor modifications to Strahler's original procedures (section 1.1.3.10-1.1.3.13). To facilitate absolute comparisons, the total volume of the basin is used primarily as an index of three-dimensional size. The hypsometric integral and its significance in the study of large basins merit some discussion.

In Strahler's (1952) analysis, relative elevation Y above the basal contour is expressed as a fraction of the maximum elevation, and relative area X is expressed as a fraction of the total basin area (area of basal contour). The hypsometric integral

$$HI = \int_{0}^{100\%} X \, dY$$

is equivalent to the area beneath the curve, obtained by plotting Y as ordinate against X as abscissa. Values of HI always lie somewhere between 1 and 0. A basin consisting of a flat-topped plateau with shear vertical sides would have HI = 1. HI values greater than 0.5 indicate that elevations greater than one-half the maximum elevation occupy more than 50 percent of the basin area; HI < 0.5 indicates the predominance of elevations less than the median.

Strahler reasoned that where lithology was homogeneous high HI values would characterize basins in an inequilibrium (young) stage of development, values near 0.5 would be indicative of the equilibrium (mature) stage, and low values would indicate the "monadnock" phase. This interpretation probably has justification for the case of the small, low-order basins with which Strahler was concerned. However, the cyclic scheme cannot validly be applied to large basins where lithologic and tectonic heterogeneity are the rule rather than the exception. In the case of the large basins, the hypsometric integral provides a valuable index for distinguishing between basins with varying proportions of highlands and lowlands. The shape of the hypsometric curve itself reflects the relative frequencies of varying dimensionless hillslopes (Y/X).

Hypsometric curves constructed for the basins examined so far in this study have exhibited pronounced breaks in slope separating areas of high relative elevation from those of low relative elevation. In a rough fashion, these breaks in slope appear to separate components of high relief and presumably of active erosion from the graded or aggrading portions where relief and hillslopes are minimal. The ratio of the integral lying beneath the portion of the hypsometric curve above the break in slope (high relief portion) to the total hypsometric integral may indicate the fraction of the basin primarily responsible for sediment supply.

The relationships between drainage density (and its inverse, the constant of channel maintenance) and climatic and other morphologic factors in small basins have been the subject of numerous studies (Horton, 1945; Chorley, 1957; Melton, 1957; Shumm, 1956; Strahler, 1957; Leopold et al., 1964). These studies have shown that drainage density (or total length of streams per unit area) increases with increasing runoff. Runoff is, of course, dependent upon numerous factors, including amount of precipitation, precipitation intensity, temperature, vegetation, infiltration capacity of the soil, ground slope, etc. For any given basin area and lithologic resistance, drainage density and discharge at the basin mouth may be expected to be roughly proportional. Owing to the small scale of the maps used in the present study, lower order streams are necessarily neglected, and drainage densities can be expected to be lower than would be the case if larger scale maps were used. However, since the same map scale is used for all basins, drainage density contrasts between basins should remain proportional.

CLIMATE

In all probability the same processes are active to a greater or lesser extent in all basins. However, it would be difficult to deny that the relative intensities of these processes differ considerably from one basin to another. Climate, more than any other single factor, likely determines these variations in process intensity.

The basic concept summarized in the above paragraph constitutes the foundation of the theory of climatic geomorphology and morphogenetic regions as propounded in France, for example, by Tricart and Cailleux (1965) and in the United States by Peltier (1950). Tricart and Cailleux (1965) conclude that, in general, climate influences morphology through its control over vegetation and soils. Peltier (1950) maintains that different climatic provinces are characterized by varying relative intensities of chemical and mechanical weathering, pluvial erosion, mass movement, and wind action.

For the most part, the durations of climates during the Quaternary era have been too short to permit the establishment of "climax" morphological suites. Within the zones of moderate climate, geomorphological differences are usually more likely to reflect differences in lithology and tectonics than differences in climate; however, many morphological contrasts between such extremes as humid tropics, deserts, and arctic regions are undeniably climatic products to a significant degree. Even where climatic differences are less dramatic, the morphology may be expected to differ correspondingly, provided lithology and structure are similar. Chorley (1957) studied basins in three different areas of similar gross lithology, structure, and stage of dissection but significantly different values of the climate/vegetation index (as derived from the Thornthwaite PE index). He found that total stream length, basin area, and drainage density all varied significantly with the climate/vegetation index.

More important to the study of river systems is the basic association between climate and streamflow. Runoff is, of course, a function of precipitation; however, the relationship is far from straightforward. The volume of water which will be available as runoff is, in a broad sense, dependent upon the difference between the actual precipitation and the potential evapotranspiration or the amount of moisture required by the landscape in order to cope with evaporation and to provide the vegetative cover with required water. In turn, potential evapotranspiration and runoff are to a large extent functions of precipitation and temperature, their distribution, and their intensity. Hence, if climate is to be meaningfully related to morphology and hydrology, it is necessary to tabulate monthly precipitation and temperature means, maxima, and minima as well as corresponding potential evapotranspiration, water deficit, and water surplus (runoff) values. Basins in high latitudes are subject to freezing at least part of the year. In such cases knowledge of the dates of freeze and thaw and the average duration of freeze is essential to an understanding of the hydrology.

PEDOLOGY AND VEGETATION

Runoff, sediment loss (supply to the main stream), erosion, and slope processes are highly dependent upon the soils and vegetation in the basin. Soils are important, both as indices of climatic and geomorphic processes and as controlling agents which influence runoff, sediment loss, vegetation, and morphological development. Surface runoff is inversely related to the infiltration capacity of the soil, which in turn is a function of soil texture. Highly cohesive soils are less erodible than are less cohesive ones (e.g., Leopold et al., 1964, pp. 38-39). Mass movement is dependent to a large degree upon soil shear strength.

The role of vegetation is even more direct. The effects of vegetation on binding and stabilizing the soil and thereby reducing sediment loss are well established. Equally important to the hydrology of the river system and ultimately to the growth and development of the delta is the reduction in water surplus as a result of transpiration by plants within the basin. Langbein and Shumm (1958) found that where the mean annual temperature was about 50°F sediment yield attained a maximum for mean precipitation values of 10 to 14 inches. Sediment yield decreased sharply on both sides of the maximum. The decrease in sediment yield with increasing precipitation was attributed to increasing vegetative cover and soil stabilization.

HYDROLOGY

The hydrology of the streams within the basin is a major product of the factors just discussed and is of paramount importance to the remainder of the river system. Unfortunately, available hydrologic data from stations within most of the basins studied are severely inadequate. As a result, only the average monthly discharges (in cusecs) at the station nearest the basin mouth are tabulated. More detailed records are available for stations within the alluvial valley, and analyses are correspondingly more meaningful. The significance of hydrologic factors will be treated in the hydrology section of the discussion on the alluvial valley.

The Alluvial Valley

An important difference exists between the drainage basin and the alluvial valley. The drainage basin functions as supplier of water and sediment. Net streamflow is directed out of the basin; water input is entirely from precipitation. Sediment which leaves the basin at its mouth is never replaced except through continued deterioration of basin rocks; the system is essentially "closed" at its upper limit. The alluvial valley, on the other hand, is a more or less balanced system, "open" at both ends, in which the river flows over and through its own deposits. Typically, there is neither net accumulation nor net erosion of sediment. Addition of water by precipitation is negligible in comparison to the amount which enters the valley at its upper end. From their investigations of river flood plains, Wolman and Leopold (1957, p. 106) concluded that "the volume of material deposited tends to be about equal to the volume eroded. Material eroded from the drainage basin is only temporarily stored in the flood plain." Russell (1954,

p. 365) states, "It is misleading and incorrect to regard one phase of the regimen of a river, say the rising stage, as a time of erosion, and another, say the falling stage, as a time of deposition. The real fact of the matter is that erosion occurs at times of vigorous flow and whenever it is active, deposition is also occurring, and not far away. The more rapid the erosion, the more vigorous the deposition." The alluvial valley serves, then, as a graded conduit through which water and sediment are transported from the drainage basin to the deltaic plain and the sea.

There have been several detailed studies of processes, river activity, and morphology in the alluvial valley. Fisk's (1944) study of the alluvial valley of the Lower Mississippi River, Wolman and Leopold's (1957) flood plain study, Russell's (1954) Alluvial Morphology of Anatolian Rivers, Sundborg's (1956) detailed investigation of the River Klaralven, and Coleman's (1969) Brahmaputra River study are notable examples.

GEOLOGY

In the alluvial valley, as in the drainage basin, local geological conditions play a fundamental role by setting the ambient limitations within which fluvial processes can exert their control. On a broad scale, the courses followed by most alluvial rivers and their flood plains are wholly or partly determined by the underlying geologic structure. Fisk (1944) found that the meander belt of the Mississippi River in its alluvial valley follows directly above the Mississippi Structural Trough, the axis of downwarping in the northern central gulf coastal plain. He also showed that tributary valleys entering the main alluvial valley are aligned parallel to the major faults of the region. According to Russell (1954), tectonic control of the courses of Anatolian rivers is even more distinct than in the case of the Mississippi. Russell (1940) also maintains that regional tilting is responsible for the tendency for river terraces flanking the Lower Mississippi River, as well as those in other parts of the world, to be progressively higher with increasing age.

The nature of the alluvial valley sediments is a determinant of floodplain and river morphology and of the mode of sediment transport. As will be seen shortly, channel type, width, and depth are partially functions of sediment caliber, as are sinuosity and channel stability (e.g., Allen, 1965; Leopold and Wolman, 1957; Shumm, 1960, 1963). Also, the ability of a flow of a given velocity to erode and transport sediments in suspension or as bed load depends to a high degree upon grain size characteristics. Sundborg (1956), for example, has demonstrated that the critical erosion velocities required to initiate sediment transport are at a minimum for sediment sizes in the fine sand range. Increasing frictional resistance with an increase in grain size leads to an increase in the critical erosion velocity, as does the increase in cohesiveness which accompanies decreasing grain size. Important to the eventual dissemination of sediment at the river mouth, as well as to depositional patterns within the alluvial valley, is the tendency for the ratio of suspended load to bed load to increase with increasing relative abundance of silt and clay.

GEOMORPHOLOGY

River and floodplain morphology are important aspects of the river system, both as an intermediate product of the river's activity and inasmuch as they may indirectly yield valuable information with regard to the river's hydraulics, sediment load, and depositional history.

As viewed from the air or from maps and aerial photographs, the most prominent feature in the alluvial valley is usually the river channel itself. There are three commonly recognized channel pattern types: braided, straight, and meandering. There have been copious studies (e.g., Allen, 1965; Russell, 1954; Leopold and Wolman, 1957; Shumm, 1963; Chien, 1961; Sundborg, 1956; Krigstrom, 1962; and Coleman, 1969) on the mechanics and environments of the three stream types, but they are still far from being completely understood. Nevertheless, these studies have established firmly several relationships between channel patterns and various aspects of the depositional environment and have yielded well-founded hypotheses as to the mechanisms of channel development.

Braided channels are those marked by successive divisions and rejoinings of flow around alluvial islands (Coleman, 1969, p. 145) (Fig. 5C). In plan these types of channels are of highly variable but relatively large widths and have poorly defined, nonparallel banks. In profile they are seen to be comparatively shallow and to have numerous channels. They are typically subject to considerable lateral shifting. More detailed descriptions are to be found in Coleman (1969) and Krigstrom (1962). For a given distance braided patterns most commonly occur in reaches or entire river courses where the slope is steep, bed material is relatively coarse (Allen, 1965; Leopold and Wolman, 1957), and sediment yield is high. Often there is considerable variation in the caliber of the bank material along the river course. Where the banks are composed locally of clay or other cohesive material, the channel may narrow and deepen. This phenomenon is described by Coleman (1969) for the Brahmaputra River and by Chien (1961) for the Yellow River. Although Chien (1961) considers the braided pattern of the Yellow River to be associated with channel aggradation, Leopold and Wolman (1957) and Russell (1954) maintain that braiding, as with other channel patterns, occurs with conditions of quasi-equilibrium, where there is neither aggradation nor entrenchment.

With decreasing slope, sediment particle size, or sediment yield, channel patterns shift from braided to straight to meandering. Leopold and Wolman (1957) define as straight those channels with a sinuosity (the ratio of thalweg length to valley length) less than 1.5 and as meandering those channels with a sinuosity greater than 1.5. Both straight and meandering channels are typically undivided, have approximately parallel banks, and, for any given discharge, are deeper than braided channels. Leopold and Wolman (1957) point out that the physiographic differences between straight and meandering channels are primarily in degree. Straight channels are, in fact, sinuous as a result of alternating lateral bars which form adjacent to the straight banks (Fig. 5B; see, for example, Coleman, 1969). The thalweg of such a river usually exhibits successive pools and riffles situated, respectively, opposite to and between the lateral bars.

The meandering channel type (Fig. 5A) encompasses a wide range of sinuosities. Pronounced inflections of the bankline as well as of the thalweg are more strongly evident than in the case of straight channels and occur with more or less consistent frequencies. In latitudinal cross section the profile of a meandering channel at an inflection is more asymmetrical than that of a straight channel. Water depths on the point bar side of a meandering section are generally shallower than those on the lateral bar side of a straight section carrying an equivalent discharge, whereas depths on the cut bank side of the meander are correspondingly deeper (e.g., Fig. 4 of Coleman, 1969). More investigations have been conducted on meandering streams than on either of the other types, yet the details of the meandering process remain elusive. Many scientists, however, regard meandering as a product, at least partially, of helicoidal flow in which surface flow in a meander section has a lateral component directed toward the cut bank side of the channel and bottom flow has a component toward the point bar (Allen, 1965; Leopold and Wolman, 1960).

Although the three channel patterns are most commonly regarded as discrete types, Leopold and Wolman (1957) maintain that they actually constitute phases of a continuum and a single stream may exhibit all three stages within a relatively short distance. The Meander River of Anatolia, from which the term "meandering" was derived, is actually braided, straight, and meandering at different locations along its course (Russell, 1954). Hence, a certain degree of subjective judgment may occasionally be involved in classifying the channel pattern.

For any given discharge, channel widths are usually greatest for braided streams and least for meandering streams, decreasing with increasing sinusoity (Shumm, 1963). It has been adequately demonstrated that, as would be expected, width increases with discharge (Leopold and Maddock, 1953; Leopold and Wolman, 1957; Leopold et al., 1964, pp. 241-248).

The ratio of channel length to valley length gages overall sinuosity of the river in the alluvial valley. Shumm (1963) found from a study of alluvial rivers on the Great Plains that increasing sinuosities were accompanied by decreasing width-depth ratios and increasing percentages of silt-clay fractions. Hence, sinuosity may be used (with caution) as an indirect indicator of sediment caliber where direct sediment data are lacking.

The type of floodplain morphology, as classified in 1.2.3.6 of the definition section, can, when properly interpreted, reveal much as to the depositional history and dynamic environment of the alluvial valley. Floodplain morphology may reflect net aggradation or degradation, tectonic subsidence or uplift, channel stability, climatic regimes, and man's influence. Not all of the form-process relationships are known as yet, and the literature on this subject is sparse. One of the aims of this study is to document these relationships.

CLIMATE

The climate of the drainage basin determines the water-sediment discharge which enters the alluvial valley; however, the climate of the valley itself may considerably affect the amount of discharge which eventually reaches the sea. Although the alluvial valley is usually responsible for the addition of only a small fraction of the total discharge, climatic conditions there occasionally result in substantial discharge reductions. Rivers which arise in humid drainage basins and subsequently flow through arid alluvial valleys, where the water balance is such as to yield a net moisture deficit, are not uncommon. The Nile and the Tigris-Euphrates are prominent examples.

HYDROLOGY

In most cases, hydrological data are more complete for the alluvial valley than for the drainage basin and can usually be used to characterize the hydrologic regime of the system as a whole. Average discharge is an important index of the absolute capacity of a river to deliver sediment to the coast and should be roughly correlative with the overall magnitude of the deltaic mass. However, temporal discharge distributions and variations often exert a greater influence on morphological patterns than do absolute discharge magnitudes and central tendencies. The morphological activity of rivers whose annual flow is concentrated into a relatively small portion of the year is likely to differ considerably from that of a river whose flow is more or less evenly distributed throughout the year. When discharge variations are slight and changes are gradual, the channel will be better able to adjust to an equilibrium configuration. When the discharge coefficient of variability and peakedness index (see 1.2.7.5 of the definition section) are high, the channel often will not have sufficient time to adjust to any given flow and, as a result, may be unstable for much of the year. Such a river may tend to change its course frequently because of the inability of the channel to become established. The flow distribution may also affect the caliber of the sediment load. A river whose total annual discharge is comparatively low but occurs during a short period of intense flooding can have a greater competence to transport coarser material to the coast than one with a higher but more evenly distributed discharge. The effects of discharge and its distribution are not limited to the alluvial valley but are manifest with equal or greater significance in the deltaic plain.

The Deltaic Plain

The materials contributed by the drainage basin and transported through the alluvial valley accumulate at the coast as the deltaic plain. The sediments composing the delta are, in a literal sense, the "gift" of the river system; but the landscape and environment of the delta are products of much more. The delta is a consequence of the conflict between the river and the sea. This fact appears to have been recognized by Homer and is stated explicitly and in detail by Strabo (c. 7 B.C.). Whether the river simply deposits its load as a result of energy dissipation by diffusion with a passive fluid mass or whether, as is often the case, the sea actively strives to mold the alien sediments to its own design, the delta is undeniably the spawn of fluvial-marine reciprocation. The delta morphology in detail reflects the totality of hydrologic regime, sediment load, geologic structure and tectonic stability, climate and vegetation, tides, winds, waves, density contrasts, coastal currents, and the innumerable spatiotemporal interactions of all these factors.

The subdivision of the deltaic plain into subaerial and subaqueous, active and abandoned, and upper and lower provinces, as defined in 1.3.0.0 of the definition list, is based on morphological and process-suite distinctions which are observed in a majority of the world's deltas.

GEOLOGY

A cursory survey of the locations of the world's major deltas reveals that many of them are situated in areas toward which alluviation has been focused by structural troughs. In the environs of the deltaic accumulation, tectonic stability is of paramount importance. Subsidence beneath the weight of accumulating sediments is characteristic of most large deltas. Howe emphasized as early as 1931 the great thicknesses of sedimentary formations beneath the Mississippi Delta, which have resulted from continued subsidence (Howe and Moresi, 1931). Russell (1942) reports slow subsidence as a cause of coastal retreat of the Rhone Delta. Subsidence beneath the Nile Delta is responsible for an extremely thick deltaic mass (Attia, 1954) and apparently for present-day coastline losses of up to 75 feet per year (Said, 1962). Deltaic morphology depends to a considerable degree upon the rate and extent of subsidence. Delta progradation will be more extensive and the delta surface will be more likely to encompass a larger area (for any given sediment supply) when subsidence is slow or negligible. Where subsidence is appreciable, delta margins are usually lowered, forming "delta flank depressions" (Russell, 1940, p. 1228).

GEOMORPHOLOGY

Understanding of delta morphologies and the causes of their variations and distributions in space and time is the primary goal of this study. From this point of view delta configurations are the end result of the other factors; however, the morphology is more than a passive "product"; it profoundly influences the process regime.

There have been numerous studies of the stratigraphy and geology of individual deltas. A few of these have contributed significantly to the scientific appreciation of deltaic processes. Much less attention has been directed toward the present-day morphology of the deltaic surface. Notable among the few geomorphological treatments which have been offered are Russell's studies of the Mississippi (1936) and Rhone (1942) deltas; Welder's (1955, 1959) investigations of Mississippi Delta geomorphic processes; Axelsson's (1967) detailed analytical study of the Laitaure Delta of Sweden; and Allen's (1964, 1965a and b) studies of the Niger Delta.

This investigation is aimed not simply at explaining the landscape of a single delta but at identifying the "common denominators" shared by all deltas and describing the variations of these factors as functions of the process regimes. In order to effect the necessary comparisons and correlations, morphological classifications and parameters must be standardized so as to be applicable to all deltas, regardless of absolute scale.

The areas and ratios of the deltaic components, as well as the length of the delta axis, width of delta, and length of shoreline, are measured primarily to permit comparison of absolute magnitudes and basic geometries. It is anticipated that many of these parameters may reflect the type and degree of riverine and marine influence. Other things being equal, the area of the deltaic plain should be roughly a function of the discharge regime. The area of the lower deltaic plain relative to that of the upper deltaic plain should reflect to some extent the tidal range and the relative significance of marine effects. The width of the delta relative to the length of the delta axis may partially index the confinement of the delta by older surfaces or, more often, the tendency of the sea to cause lateral redistribution of sediments.

Distributary patterns are among the most salient of delta features. There are four primary types of distributary pattern: (1) the continuously bifurcating type in which the distributaries always diverge from one another at more or less the same angle to create a fanlike effect; (2) the internally braided type in which the main stream or individual distributary bifurcates, only to rejoin downstream; (3) the type in which all splitting occurs at a single apex; and (4) the single channel type, in which there is no splitting. These types are seldom discrete; a channel usually grades continuously from one type to another. It is necessary to express the distributary situation in terms of continuous quantities. The indices defined in categories 1.3.3.16 through 1.3.3.21 of the definition list were devised to meet this need.

The factors responsible for observed distributary patterns are as yet undetermined; it is hoped that many of them will be disclosed when analyses are completed. There have been, however, several studies of the processes of channel branching which at least provide some clue as to what relationships may be expected. Leighly (1934) suggested that channel bifurcation is caused by shoaling and bar formation between and parallel to two threads of maximum turbulence (located near the bottom on either side of the channel) and consequent divergence of flow. Axelsson (1967), who has reviewed the problem in some detail, concurs that bar formation is a major cause of channel splitting. The mechanisms of bar formation will be considered later in this discussion. An equally important process leading to the development of multiple channels is crevasse formation. This process has been studied in some detail by Welder (1955, 1959). Crevassing occurs when the natural levee of a channel is breached at some point, creating an outlet for a portion of the discharge, usually at a relatively high angle to the main channel. Vertical scour and bank slumping result in the establishment of the outlet. Shoaling and bar formation within a short distance from the gap often cause further branching and the development of the so-called crevasse splay.

It has been noted by numerous investigators (see, for example, Axelsson, 1967, p. 35) that, as a channel elongates, its gradient and consequently its transporting capacity decrease. This favors aggradation and increases the tendency of the flow to divert to a steeper course. Often the original channel will experience a diminution of flow and will close (Welder, 1959); however, if tidal range is high, tidal currents may contribute to the maintenance of channels, and a complex multichanneled distributary network may be created. Tides may also promote the initial flow diversion by affecting the hydrostatic gradient. Hence distributary patterns probably reflect hydrostatic gradient and tidal regime, as well as numerous other, as yet undetermined, factors.

In most cases, the interdistributary zones comprise the greater fraction of the lower deltaic surface area. The ten interdistributary types defined in the definition list encompass all of the commonly known types of which the writers are aware. There are, no doubt, other types, which may be unique to specific deltas. Certainly there are many cases where two or more types are found in combination.

The interdistributary areas are fundamental in determining the planar configuration of the delta as a whole. It is here in particular that the nonriverine forces play their most effective roles and are most operative in causing a regular or an irregular deltaic plain.

Just as elsewhere in the system, the processes of interdistributary development are highly complex, and it would be incorrect to relate any interdistributary type directly to any single process variable. For purposes of illustration, however, it is permissible to point out certain generalities. For example, it can be stated with some degree of certainty that interdistributary beach ridge plains are indicative of at least moderately high wave energy, whereas a maze of tidal channels or the presence of tidal flats reflects the influence of tide. It has also been demonstrated that interdistributary bays result from rapid compaction or tectonic subsidence (Russell, 1936).

The river mouth is the dynamic dissemination point for sediments which contribute to continued delta progradation. The processes active at the river mouth are responsible for the formation of the subaqueous delta, a prerequisite to further deltaic development. The number of mouths in a delta significantly affects the degree of lateral sediment dispersion and, hence, the relative width of the delta. The river mouth type and geometry and the topography of the river mouth together make up a single unit. The bar is essentially part of the river mouth complex. The form of this complex is a basic determinant of the effluent hydraulics, which, in turn, are responsible for the river mouth and bar topography. Samojlov (1956) has offered a comprehensive treatment of river mouths in general which is supplemented by descriptions of numerous individual river mouths. River mouth processes have also been the object of studies by Bates (1953), Bondar (1963, 1967), Borichansky and Mikhailov (1966), Mikhailov (1966), Axelsson (1967), Takano (1954a and b, 1955), and Wright (1970a).

The most important river mouth processes are those by which the river effluent interacts with the ambient water, resulting in the deconcentration of outflow momentum and consequent loss of transporting ability. Many factors are involved, including initial outflow velocity, density contrasts, tidal regime, winds, waves, and coastal currents. River mouth and bar morphology are functions of the type and degree of these processes and their interactions. Whether or not a river mouth is straight or bell-shaped should depend to a considerable extent upon the rate at which outflow spreads laterally at the mouth. This, in turn, is partially controlled by tendencies for lateral spreading to be inhibited by density contrasts (Wright, 1970a) and promoted by steep hydrostatic gradients (Bates, 1953). The common generalization that bell-shaped river mouths occur where tidal range is high and that straight mouths occur under low tidal range conditions is probably erroneous because bell-shaped mouths are often found in areas with little or no tide and straight mouths frequently occur together with a high tidal range. Tide almost certainly plays an important role by effecting mixing and reducing density gradients and by its influence on hydrostatic gradients (Wright, 1970a). However, it is possible that bottom slopes and water depths at and offshore from the offing are equally important. For example, where a river debouches over a shallow, gently sloping bottom, vertical flow separation and diffusion will be precluded, necessitating greater lateral spreading.

The impounded or deflected river mouth occurs where waves tend to build and maintain barriers or beaches across the river outlet. This type of river mouth appears to develop where the strength of the river outflow is low relative to the wave forces. Such a situation can obtain at the mouth of even a relatively high-discharge river if high-energy waves approaching the coast from deep water are frequent and if offshore slopes are steep enough not to cause appreciable frictional attenuation of the waves. The direction toward which a river mouth is deflected by a sand spit or barrier beach is not necessarily dependent on the direction of longshore drifting, though it may be if there is considerable longshore transport. Perhaps more important is the tendency for the river mouth to be deflected in the direction of decreasing wave energy. Bascom (1954) has noted that the outlets of rivers which debouch on high-wave-energy coasts often seek a position where refraction coefficients and, consequently, wave heights are at a minimum. This may result in river mouths' being deflected in a direction opposite to that of the dominant longshore drift (e.g., Wright, 1970b).

The morphology of the river mouth bar also depends on the effluent spreading patterns, as well as on the geometry, of the outlet. Bates (1953) concluded that the crest of the bar is most commonly situated four channel widths seaward of the mouth. Mikhailov (1966) maintains that the distance from the outlet to the bar crest will vary directly with the outflow velocity. Bar type must be largely a function of the rate of effluent expansion. Bar type 1 (definition list) may reflect appreciable horizontal flow separation and may be characteristic of tide-dominated outlets or of mouths in areas of slight density contrasts. Type 2, the lunate bar, appears to be more typical of river mouths which experience "salt wedge" intrusion or strong density stratification, where lateral spreading of the outflow is inhibited. Type 3 is contingent with the incipient stages of channel bifurcation. Type 4 is closely related to type 2 and appears to occur under a similar set of circumstances.

Frequently river mouth bars are scarred by gullies which radiate from the river mouth (Shepard, 1955). Recent investigations have indicated that these gullies are associated with seaward subaqueous mass movement (F. J. Swaye, personal communication). Another type of linear subaqueous features resulting from tidal currents has been described by Off (1963). These features typically are found at the heads of deep embayments (e.g., Persian Gulf, Bay of Bengal) where tidal flow is restricted to the delta coast.

It has been demonstrated that the river mouth bar is composed primarily of the coarsest sediment fractions transported to the mouth as bed load (Scruton, 1960; Mikhailov, 1966; Fisk et al., 1954; Coleman and Gagliano, 1965). Certainly the high percentage of sand and silt in the bar sediments at the mouths of the Mississippi (Fisk et al., 1954; Henry, 1961; Scruton, 1960; Shepard, 1960) and the abundance of cross laminations among the sedimentary structures of the bars (Coleman and Gagliano, 1965; Coleman et al., 1964) suggest predominantly bed load origin. Hence bar topography is, for the most part, a response to flow and flow deceleration tendencies in the lower layers and may not necessarily be correlative with surface effluent patterns.

The morphometry of the deltaic bulge is intended to describe some gross general tendencies of the delta. The morphometric parameters defined in sections 1.3.3.36 - 1.3.3.49 of the definition list are experimental and may or may not prove meaningful. Admittedly, they are artificial--highly generalized and in some respects arbitrary with regard to boundaries. However, as has already been pointed out, objective comparisons of deltas of various sizes require objective indices. The bulge morphometric parameters are intended primarily to gage quantitatively the relative abilities of the riverine forces to prograde the delta and of the marine forces to redistribute the delta sediments.

Total bulge volume should be approximately proportional to the absolute rate of sediment supply and hence to such factors as basin area, discharge, resistance of basin rocks, etc., but will also depend on subsidence rates, shelf slope, and the strength of ocean waves. The dimensionless hypsometric integral of the subaqueous bulge may prove to be related to the rate of seaward advance of the delta relative to the rate at which waves and tides are able to readjust the subaqueous profile. If this should be the case, a high value for the integral should reflect a rapid supply of sediments and comparative riverine dominance of the nearshore profile of the subaqueous delta.

The obliquity of the approach of dominant waves or the directions of coastal currents is likely to affect the asymmetry or symmetry of the deltaic bulge as indexed by the ratio of the volume on one side of the delta axis to that on the other side. The bulge volume distribution parameter for each side of the axis will vary directly with the relative lateral "spread" of the bulge, which in turn depends appreciably upon the effectiveness of marine forces in disseminating the sediments debouched by the river.

CLIMATE AND VEGETATION

In the delta region climatic factors such as precipitation and water balance parameters are much less important than in the previously discussed provinces. Temperature perhaps plays a more significant role here. Vegetation type and, in the case of high-latitude deltas, dates and durations of freeze and thaw are dependent upon the temperature regime and may on occasion exert a dominating influence on delta morphology. Vegetation not only behaves as a geomorphic process through its stabilizing and binding effects on detrital sediments and by offering a continuous supply of organic material but also serves to disclose the roles of other processes such as tide and salinity regimes.

HYDROLOGY

The roles of the hydrologic regimes, as discussed in connection with the alluvial valley, are equally significant in the deltaic plain region. Discharge tendencies are especially important to the rate and pattern of delta growth. The ability of a river to overcome the sea depends significantly upon the volume and intensity of the outflow. The discharge efficiency index is intended to gage this ability relative to the tendency of the waves to oppose fluvial deposition. The temporal distribution of discharge is no less significant than the absolute discharge magnitude. For example, if discharge peaks coincide with times of greatest wave power, an increased supply of sediment may be more closely balanced by the capacity of the waves to redistribute the material than if discharge and wave power maxima are out of phase.

The Receiving Basin

The sea is every bit as important to the development of a delta as is the river. It receives the sediments brought down to it by the river, but seldom does it do so in a passive manner. Typically, the sea is averse to being displaced by material of alien origin without playing its part in the molding of that material. The various oceanographic processes active near the delta coast are crucial to the shaping of the delta.

GEOLOGY AND GEOMORPHOLOGY

The structure and morphology of the continental shelf profoundly influence the oceanographic forces operative at the delta coast. Shelf width and slope affect the refraction and frictional attenuation of ocean waves as well as the modification of the tidal wave. The same factors also frequently govern the rate and extent to which a delta is able to build seaward. A delta will be more likely to grow farther seaward in a shorter period of time over a broad, gently sloping shelf than over a steep, narrow shelf. The presence or absence of submarine canyons may also affect delta growth. The Congo River, for example, empties its sediment load into a deep submarine canyon and has thus been unable to build a subaerial delta of appreciable size.

CLIMATE

The wind regime, both in the immediate proximity to the delta front and offshore, is of paramount importance. The wind is responsible for transport of sediments over the subaerial delta plain, the generation of wind waves, the generation of coastal currents, and the setup or setdown of the water surface along the coast (i.e., wind tides). The effects of wind on wave propagation are well established. Sets of empirical formulae and graphs (Bretschneider, 1966; Pierson et al., 1967) may be used to compute wave height, period, and direction from wind velocity, duration, fetch length, and direction. The Sverdrup-Munk-Bretschneider wave hindcasting technique (for description see Bretschneider, 1966) is employed in this study to estimate wave characteristics from wind data obtained from climatic atlases.

The resolution of all prevailing winds into vector resultants and components is necessary to the analyses of eolian coastal landforms and littoral wind-generated currents. Bagnold (1941) showed that the effectiveness of the wind in transporting sand is proportional to the cube of the wind velocity above 10 miles per hour. Jennings (1957) found that coastal parabolic dunes on King Island, Tasmania, were oriented with their axes parallel to the vector resultant of the cube of the effective onshore winds.

Determining the relative magnitude of the vector components onshore, offshore, alongshore to the right, and alongshore to the left may make it possible to infer the dominant direction of coastal wind drift currents where direct data are lacking.

HYDROLOGY (PHYSICAL OCEANOGRAPHY)

Generally, no single factor plays a greater role in coastline development than waves. No aspect of coastal morphology has received more attention than the relationship between wave activity and beach profile changes. A review of these studies here would be superfluous. It has been demonstrated that when waves exceed a certain critical steepness the subaerial beach will be eroded and the material will be deposited offshore, flattening the subaqueous profile, while waves of lower steepness will typically cause subaerial accretion. This critical steepness (i.e., wave height/length ratio) has been found by many investigators to be near 0.03 (e.g., Weigel, 1964). Generally, long waves of low height are responsible for subaerial progradation where there is an adequate supply of sediment.

Though considerably less attention has been given to the interrelationships between wave regime and the overall three-dimensional configuration of the coast, it has been shown that shoreline geometries and dominant wave regimes strive to attain mutual adjustment. Lewis (1938) observed that embayed beaches orient so as to parallel the crests of the dominant waves. Later it was noted that the alignment of arcuate beaches is a response to the wave refraction patterns, which in turn are dependent upon the subaqueous topography (Davies, 1958; Jennings, 1955; Wright, 1970b). Recent approaches attempt to explain accumulation forms which are in approximate dynamic equilibrium along coasts with a littoral drift (Zenkovich, 1967; Larras, 1957). Generally, these studies have been based on the premise that alongshore gradients in sediment transport are proportional to longshore variations in the incident angle of the waves resulting from corresponding variations in the degree of wave refraction. Shoreline geometries are assumed to develop in such a way as to minimize or eliminate these gradients by creating a more uniform spatial distribution of forces.

To be thoroughly realistic, explanations must also take into account longshore variations in shoreline energy arising from differing degrees of frictional attenuation of wave energy over varying subaqueous slopes. Depending upon bottom roughness and wave characteristics, wave energy may be substantially dissipated over broad, gently sloping offshore profiles (Bretschneider, 1954; Bretschneider and Reid, 1954). Most wave-regime analyses ignore this effect, even though in many instances it may dominate energy distribution patterns. The amount of frictional attenuation may determine whether waves which reach the shore cause net seaward transport of material or lead to subaerial accretion. The profile of equilibrium must therefore be considered (Zenkovich, 1967, chapters 2 and 4; Johnson and Eagleson, 1966; Keulegan and Krumbein, 1949). The problem of interaction and adjustment between the wave regime and topography thus involves both the transverse profile and planar configurations.

The concepts outlined above apply to coastlines where the sediment budget is balanced by redistribution of wave-energy levels. Near the mouths of large rivers, however, this balance is upset by the introduction of sediments from sources "external" to the littoral sediment transport system. Resultant depositional forms are dependent not only upon the magnitude and distribution of wave forces but also upon the ability of the river to supply sediments. Hence delta shapes may range from those which have been produced solely by the debouchment of the river, without significant interference from wave activity (for example, digital prograded distributaries), to those which reflect complete dominance of the waves in distributing sediments and straightening the coastline according to their own design (for example, the "obstructed" or "impounded" delta).

Tide is reflected by river mouth morphology, the occurrence of tidal flats, vegetation, and crevasse formation. The vertical range of the tide determines how far upstream from the mouth tidal influence extends, and hence should affect the relative area of the lower deltaic plain. Similarly, the higher the tidal range, the greater will be the width of the zone which is alternately exposed and inundated by ebb and flood and, consequently, the more extensive are tidal flats likely to be.

It has been established that tide exerts a significant influence on patterns of effluent diffusion, circulation, and the dissemination of sediments where the Mississippi discharges into the Gulf of Mexico (Wright, 1970a). If such influence is observed in an area such as the Mississippi Delta, where tidal range is low (mean = 11 inches), it follows that tide should play an even more important role in areas of greater tidal range. It was pointed out in the discussion of the deltaic plain that tide also affects the distributary pattern and the tendency for flow to be diverted. Investigations have indicated that in South Pass, Mississippi Delta, hydrostatic gradient varies considerably with tidal phase, experiencing reduction and, at low stage, reversal with flooding tide (Wright, 1970a). It is very likely that the resulting inhibition of direct channelized outflow is at least partially responsible for the development of crevasses along the distributaries. These crevasses may serve as outlets for the river water "impounded" by the rising tide. If this is the case, the frequency of crevassing should correlate with tidal range.

Swift tidal currents also accompany high tidal ranges. These currents are often responsible for bottom scour, formation of tidal channels, and the development of tidal deltas. Elongate subaqueous ridges along depositional coasts with high tidal range have been described by Off (1963).

Whether tides are diurnal, semidiurnal, or mixed depends upon geographic locality. Descriptions and explanations of tides in different parts of the world are offered by Defant (1961, vol. 2). The type of tide is just as important as tidal range in determining the potency of the tide as a geomorphic process. For any given tidal range a semidiurnal tide can be expected to generate swifter currents than a diurnal tide since the change in level must take place in approximately half the time.

Individually, salinity and water temperature affect the ecology and vegetation of the delta as well as certain chemical processes such as the flocculation of colloidal sediments. In combination, these factors determine the water density, a parameter of considerable moment with regard to water-mass mixing and circulation in zones adjacent to the delta front. Density contrasts between river water and seawater are responsible for the intrusion of "salt wedges" into distributary channels and for the occurrence of density fronts seaward of the mouth. These phenomena control appreciably the patterns of sediment transport and mixing between river outflow and ambient seawater. Salt wedge intrusion opposes the downstream transport of bed load in the lower reaches of the channel and appears to have a profound effect on deposition and bar formation (e.g., Bates, 1953; Scruton, 1956). The fronts developed by the convergence of water masses of contrasting densities tend to inhibit the horizontal expansion of effluent river water (Wright, 1970a).

The contributions of coastal currents are sufficiently obvious to require only brief mention. These currents affect the net direction of sediment transport and consequently the orientation and symmetry of the delta mass. They also influence the water temperature, salinity, and density, and in the case of large-scale currents they affect the local climate.

APPLICATIONS OF TECHNIQUES TO THE NIGER AND SAO FRANCISCO DEL NORTE RIVER SYSTEMS

Two river systems, the Niger of West Africa and the São Francisco del Norte of Brazil, have been selected to illustrate the application of the procedures and concepts just described. The parameters presented follow the hierarchical arrangement used in the actual analyses.

1.0.0.0 RIVER SYSTEM: São Francisco del Norte

1.1.0.0 <u>Drainage Basin</u>

1.1.1.0 Location

1 Continent: South America

2 Countries: Brazil

3 Coordinates:

North: 7.21°S   South: 20.9°S

East: 36.5°W   West: 47.8°W

1.1.2.0 Geological

1 Tectonic stability: Stable basement platform

2 Type of rocks:

Igneous: 30%   Metamorphic: 20%   Sedimentary: 50%

3 Geologic age: Silurian, Cretaceous, Precambrian

4 Geologic structure: Stable basement platform

1.1.3.0 Geomorphological

1 Area: 232,642 sq. mi.

2 Basin perimeter: 3,561 mi.

3 Stream length: 1,384 mi.

4 Long axis of basin: 1,152 mi.

5 Basin elevation:

$\bar{E}$ = 1,847 ft. S^2 = 371,142   S = 609.2

CV = 0.3298 E_{max} = 5,100 ft. E_{min} = 430 ft.

6 Basin relief:

$\bar{R}$ = 206 ft. S^2 = 44,073   S = 209.9

CV = 1.0191 R_{max} = 963 ft. R_{min} = 32 ft.

7 Relief ratio:

R_h = 0.0008 R_{hp} = 0.0271

8 Area-altitude: x 10^3 sq. mi.

Class	1	2	3	4	5	6	7
Area	232.6	232.4	230.5	190.7	112.0	42.1	6.5

9 Altimetric frequency

Class	1	2	3	4	5	6	7
%	0.1	0.8	17.1	33.8	30.0	15.3	2.8

10 Dimensionless area-altitude

Class	1	2	3	4	5	6	7
DAA	100.0	99.9	99.0	82.0	48.1	18.1	2.8

11 Absolute volume of basin: V = 130,625 cu. mi.

12 Hypsometric integral: HI = 0.45178

13 Ratio HI_a/HI: 0.009

1.0.0.0 RIVER SYSTEM: Niger

1.1.0.0 Drainage Basin
1.1.1.0 Location
1 Continent: Africa
2 Countries: Guinea, Ivory Coast, Mali, Upper Volta, Niger, Nigeria, Dahomey, Cameroon, Chad
3 Coordinates:
North: 17.0°N South: 6.0°N
East: 16.0°E West: 12.0°W

1.1.2.0 Geological
1 Tectonic stability: Stable basement platform
2 Type of rocks:
Igneous: 60% Metamorphic: 0% Sedimentary: 40%
3 Geologic age: Precambrian, Cretaceous
4 Geologic structure: Strongly folded and faulted

1.1.3.0 Geomorphological
1 Area: 439,792 sq. mi.
2 Basin perimeter: 6,294.2 mi.
3 Stream length: 2,772.9 mi.
4 Long axis of basin: 2,154 mi.
5 Basin elevation:
$\bar{E}$ = 1,354 ft. S^2 = 330,397 S = 574.8
CV = 0.4245 E_{max} = 8,202 ft. E_{min} = 426 ft.
6 Basin relief:
$\bar{R}$ = 306 ft. S^2 = 158,708 S = 398.4
CV = 1.3019 R_{max} = 1,969 ft. R_{min} = 16 ft.
7 Relief ratio:
R_h = 0.0007 R_{hp} = 0.0246
8 Area-altitude: x 10^3 sq. mi.

Class	1	2	3	4	5	6	7	8
Area	439.8	421.9	338.2	159.2	28.5	8.0	3.5	1.0

9 Altimetric frequency

Class	1	2	3	4	5	6	7	8
%	4.1	19.0	40.7	29.7	4.7	1.0	0.6	0.2

10 Dimensionless area-altitude:

Class	1	2	3	4	5	6	7	8
DAA	1.00	0.96	0.77	0.36	0.07	0.02	0.008	0.002

11 Absolute volume of basin: V = 144,764.40 cu. mi.
12 Hypsometric integral: HI = 0.21189
13 Ratio HI_a/HI: 0.038

14 Drainage density:

$\bar{D}$ = 0.1939 S^2 = 0.0125 S = 0.1118

CV = 0.5765 D_{max} = 0.4452 D_{min} = 0.0021

1.1.4.0 Climatological

1 Climatic classification: AW

2 Average yearly temperature: 22.1°C

3 Mean daily temperature:

	J	M	M	J	S	N
°C	23.1	23.49	20.88	19.61	22.5	23.5
S^2	2.36	2.27	4.24	3.41	2.76	2.48
S	1.536	1.51	2.06	1.85	1.66	1.57
CV	0.0665	0.0642	0.0986	0.0942	0.0738	0.0670

4 Mean maximum daily temperature:

	J	M	M	J	S	N
°C	28.78	29.89	27.7	26.99	30.2	29.89
S^2	7.10	5.76	6.14	6.26	9.19	7.33
S	2.66	2.4	2.48	2.50	3.03	2.70
CV	0.0926	0.0803	0.0894	0.0927	0.1003	0.0906

5 Mean minimum daily temperature:

	J	M	M	J	S	N
°C	18.38	18.27	14.7	12.39	15.11	17.88
S^2	3.44	3.32	4.85	5.89	5.42	3.42
S	1.85	1.82	2.20	2.42	2.32	1.85
CV	0.1008	0.0997	0.1496	0.1960	0.1541	0.1035

6 Yearly precipitation: mm

$\bar{P}$ = 1,222.76 S^2 = 279,122.02 S = 528.32

CV = 0.4321 P_{max} = 2,841.75 P_{min} = 593.09

7 Mean monthly precipitation: mm

	J	M	M	J	S	N
$\bar{P}_m$	191.26	143.51	43.18	32.51	34.04	163.58
S	124.46	71.12	63.50	55.88	15.24	88.90
CV	0.6507	0.4956	1.4705	1.7188	0.4477	0.5435
$P_{m\ max}$	521.46	394.46	228.01	196.09	69.6	239.52
$P_{m\ min}$	36.7	51.05	7.62	2.03	10.92	23.11

8 Mean monthly potential evapotranspiration (PE): mm

	J	M	M	J	S	N	Year
$\overline{PE}$	114.44	104.64	76.00	59.56	91.52	106.96	1099.52
S	15.514	15.90	23.06	22.98	27.07	20.22	236.06
CV	0.14	0.15	0.30	0.39	0.30	0.19	0.21

9 Mean monthly moisture storage (ST): mm

	J	M	M	J	S	N	Year
$\overline{ST}$	228.56	238.56	203.16	162.88	124.48	192.28	2301.76
S	108.68	100.85	84.32	77.05	75.02	104.69	1104.99
CV	0.48	0.42	0.42	0.47	0.60	0.54	0.48

Niger

14 Drainage density:

$\bar{D} = 0.2017$ $S^2 = 0.0103$ $S = 0.1014$

$CV = 0.5027$ $D_{max} = 0.3870$ $D_{min} = 0.0165$

1.1.4.0 Climatological

1 Climatic classification: AW

2 Average yearly temperature: 27.6°C

3 Mean daily temperature:

	J	M	M	J	S	N
°C	24.99	30.22	30.27	26.6	26.50	27.1
S^2	2.46	1.47	5.32	3.17	2.25	1.69
S	4.57	1.21	2.31	1.78	1.49	1.30
CV	0.0628	0.0401	0.0762	0.0669	0.0566	0.048

4 Mean maximum daily temperature:

	J	M	M	J	S	N
°C	33.72	37.99	36.38	31.49	30.99	35.11
S^2	3.83	2.09	11.70	6.35	1.95	3.46
S	1.95	1.44	3.42	2.52	1.39	1.86
CV	0.058	0.038	0.094	0.080	0.045	0.053

5 Mean minimum daily temperature:

	J	M	M	J	S	N
°C	16.05	21.9	24.22	21.89	21.72	18.39
S^2	4.69	2.37	2.26	1.35	1.42	2.39
S	2.17	1.54	1.50	1.60	1.19	1.54
CV	0.135	0.070	0.062	0.053	0.055	0.084

6 Yearly precipitation: mm

$\bar{P} = 1{,}061.72$ $S^2 = 281{,}812.34$ $S = 530.86$

$CV = 0.500$ $P_{max} = 2{,}669.54$ $P_{min} = 185.42$

7 Mean monthly precipitation: mm

	J	M	M	J	S	N
$\bar{P}_m$	2.79	16.76	93.47	196.60	208.53	18.29
S	5.08	27.94	66.04	73.66	101.60	48.26
CV	1.82	1.67	0.71	0.38	0.49	2.64
$P_{m\ max}$	33.02	149.86	238.76	419.10	485.14	317.5
$P_{m\ min}$	0.00	0.00	1.02	22.10	22.10	1.02

8 Mean monthly potential evapotranspiration (PE): mm

	J	M	M	J	S	N	Year
$\overline{PE}$	94.7	155.0	171.0	138.9	129.1	123.5	1611.3
S	32.4	21.2	25.6	32.3	27.3	20.3	224.0
CV	0.34	0.14	0.00	0.23	0.21	0.16	0.14

9 Mean monthly moisture storage (ST): mm

	J	M	M	J	S	N	Year
$\overline{ST}$	67.5	31.4	36.1	117.7	202.5	130.6	1183.8
S	50.3	28.3	47.9	114.0	118.3	89.6	907.5
CV	0.75	0.90	1.33	0.97	0.58	0.69	0.77

10 Mean monthly actual evapotranspiration (AE): mm

	J	M	M	J	S	N	Year
$\overline{AE}$	105.20	101.16	57.56	34.76	51.68	99.52	893.04
S	13.52	11.64	18.72	11.48	17.87	18.38	130.36
CV	0.13	0.12	0.33	0.33	0.35	0.18	0.15

11 Mean monthly water deficit (D): mm

$\bar{D}$	9.24	3.48	18.44	24.96	39.84	7.44	206.48
S	19.99	12.95	32.28	29.38	39.36	20.72	283.01
CV	2.16	3.72	1.75	1.18	0.99	2.78	1.37

12 Mean monthly water surplus (SW): mm

	J	M	M	J	S	N	Year
$\overline{SW}$	98.96	52.40	2.60	8.28	2.04	28.00	400.92
S	105.31	67.96	13.00	30.44	10.20	57.35	428.28
CV	1.06	1.30	5.00	3.68	5.00	2.05	1.07

13 Distribution of annual precipitation:

Class	1	2	3	4	5	6	7	8	9
%	0.0	0.0	0.1	5.5	14.1	31.7	15.1	25.1	8.4

14 Date of freeze: -
15 Date of thaw: -
16 Duration of freeze: -

1.1.5.0 Pedological
1 Major soil type:
a.: Class E-2 b.: Class E-3 c.: Class E-4

1.1.6.0 Biological
1 Major vegetation type:
a.: Class N-73 b.: Class 0-79 c.: Class J-52

1.1.7.0 Hydrological
1 Average monthly discharge (cusecs x 10^3):

	J	M	M	J	S	N
$\bar{D}_b$	93.0	86.3	50.2	35.1	25.2	73.8

1.2.0.0 Alluvial Valley
1.2.1.0 Location
1 Countries: Brazil

1.2.2.0 Geological
1 Stability: Stable basement platform
2 Dominant type of sediment: Sand

1.2.3.0 Geomorphological
1 Channel type: Braided
2 Channel width:
$\overline{CW}$ = 0.81 mi. $S^2 = 0.14$ S = 0.37 mi.
CV = 0.46 CW_{max} = 1.6 mi. CW_{min} = 0.5 mi.
3 Length of valley (LV): 86.63 mi.
4 Length of stream (LS): 93.28 mi.
5 Ratio LS/LV: 1.1154

Niger

10 Mean monthly actual evapotranspiration (AE): mm

	J	M	M	J	S	N	Year
$\overline{AE}$	29.2	32.5	98.2	122.7	104.5	62.7	890.0
S	21.8	29.5	52.4	28.4	33.2	40.4	326.1
CV	0.75	0.91	0.53	0.23	0.32	0.64	0.37

11 Mean monthly water deficit (D): mm

	J	M	M	J	S	N	Year
$\overline{D}$	65.5	122.4	72.8	16.2	24.6	61.0	721.3
S	25.1	40.0	72.8	38.4	48.9	48.6	438.5
CV	0.38	0.33	1.00	2.37	1.99	0.80	0.61

12 Mean monthly water surplus (SW): mm

	J	M	M	J	S	N	Year
$\overline{SW}$	0.0	0.0	0.0	29.3	64.7	0.0	171.6
S	0.0	0.0	0.0	71.1	86.0	0.0	261.4
CV	-	-	-	2.43	1.33	-	1.52

13 Distribution of annual precipitation:

Class	1	2	3	4	5	6	7	8	9
%	0.0	1.9	12.3	11.6	13.0	17.8	28.2	11.6	3.6

14 Date of freeze: -
15 Date of thaw: -
16 Duration of freeze: -

1.1.5.0 Pedological
1 Major soil type:
a.: Class D-4 b.: Class E-2

1.1.6.0 Biological
1 Major vegetation type:
a.: Class N-67 b. Class N-70

1.1.7.0 Hydrological
1 Average monthly discharge (cusecs x 10^3):

	J	M	M	J	S	N
$\overline{D}_b$	86.5	69.4	44.8	215.8	631.2	308.8

1.2.0.0 Alluvial Valley
1.2.1.0 Location
1 Countries: Nigeria

1.2.2.0 Geological
1 Stability: Stable basement platform
2 Dominant type of sediment: Sand

1.2.3.0 Geomorphological
1 Channel type: braided
2 Channel width:
$\overline{CW}$ = 1.92 mi. $S^2 = 0.73$ S = 0.86
CV = 0.448 CW_{max} = 3.98 mi. CW_{min} = 0.79 mi.
3 Length of valley (LV): 100.99 mi.
4 Length of stream (LS): 103.65 mi.
5 Ratio LS/LV: 1.0263

6 Type of flood plain: River-scarred plain
7 Number of tributaries:
Left bank = 0 Right bank = 0

1.2.4.0 Climatological
1 Climatic classification: AW
2 Yearly rainfall (mm): 698.5
3 Average yearly temperature: 25.9°C
4 Monthly moisture deficit (D): mm

	J	M	M	J	S	N	Year
$\bar{D}$	76.5	49.5	7.0	0	37.5	74.5	481.0
S	50.20	70.00	9.90	0	51.62	58.69	468.10
CV	0.66	1.41	1.41	-	1.38	0.79	0.97

5 Monthly moisture surplus (SW): mm

	J	M	M	J	S	N	Year
$\overline{SW}$	0	0	0	69.5	0	0	125.0
S	0	0	0	98.29	0	0	176.78
CV	-	-	-	1.41	-	-	1.41

1.2.5.0 Pedological
1 Major soil type: F-33

1.2.6.0 Biological
1 Major vegetation type: J-52

1.2.7.0 Hydrological
1 Monthly discharge (x 10^3 cusecs)

	J	M	M	J	S	N
$\bar{D}_{mv}$	153.9	197.9	120.9	74.5	57.4	61.8
S^2	108.3	62.1	334.7	18.9	7.9	197.2
S	10.2	7.9	18.3	4.3	2.8	14.0
CV	0.066	0.040	0.151	0.058	0.049	0.227

2 Average yearly discharge:
$\bar{D}_{yv} = 120.7$ $S^2 = 2,413.9$ S = 49.1 CV = 0.407

3 Maximum discharge (x 10^3 cusecs):
$D_{yv\ max} = 209.1$ Date: March

4 Minimum discharge (x 10^3 cusecs):
$D_{yv\ min} = 41.9$ Date: November

5 Flood peakedness:
$K_f = 1.48$
6 High water period: November-April
7 Low water period: May-October
8 Monthly rate of rise (+) and fall (-) - ft/day (x 10^{-2})

J	M	M	J	S	N
-3.3	+6.6	-18.6	-3.8	-2.4	+13.6

9 Yearly sediment discharge: (x 10^3 cubic feet)
$\overline{SD}$ = No data SD_{max} = No data Date: No data

Niger

6 Type of flood plain: River-scarred plain
7 Number of tributaries:
Left bank = 6 Right bank = 6

1.2.4.0 Climatological
1 Climatic classification: AW
2 Yearly rainfall (mm): 1,651
3 Average yearly temperature: 25°C
4 Monthly moisture deficit (D): mm

	J	M	M	J	S	N	Year
$\bar{D}$	90.5	92.5	7.5	0	0	37.0	431.0
S	21.92	31.82	10.61	0	0	36.77	195.16
CV	0.24	0.34	1.41	-	-	0.99	0.45

5 Monthly moisture surplus (SW): mm

	J	M	M	J	S	N	Year
$\bar{D}$	0	0	0	40.0	104.0	0	246.0
S	0	0	0	56.57	147.08	0	347.90
CV	-	-	-	1.41	1.41	-	1.41

1.2.5.0 Pedological
1 Major soil type: F-33

1.2.6.0 Biological
1 Major vegetation type: K-47

1.2.7.0 Hydrological
1 Monthly discharge (x 10^3 cusecs):

	J	M	M	J	S	N
$\bar{D}_{mv}$	91.0	72.6	64.1	239.2	801.3	560.3
S^2	71.4	3.7	310.1	2322.3	3986.5	36,689.0
S	8.4	1.9	17.6	48.2	63.1	191.5
CV	0.093	0.027	0.275	0.202	0.079	0.342

2 Average yearly discharge:
$\bar{D}_{yv}$ = 384.8 S^2 = 91,216.8 S = 302.0 CV = 0.784
3 Maximum discharge (x 10^3 cusecs):
$D_{yv\ max}$ = 956.1 Date: October
4 Minimum discharge (x 10^3 cusecs):
$D_{yv\ min}$ = 48.2 Date: May
5 Flood peakedness:
K_f = 2.38
6 High water period: August-November
7 Low water period: December-july
8 Monthly rate of rise (+) and fall (-) - ft/day (x 10^{-2})

J	M	M	J	S	N
-7.0	-4.0	+72.0	+64.0	+13.0	-60.0

9 Yearly sediment discharge: (x 10^3 cubic feet)
$\overline{SD}$ = 59,000 SD_{max} = 79,000 Date: October

1.3.0.0 Deltaic Plain
1.3.1.0 Location
1 Countries: Brazil
2 Receiving body of water: Atlantic Ocean

1.3.2.0 Geological
1 Stability: Stable basement platform

1.3.3.0 Geomorphological
1 Area - deltaic plain: 462.23 sq. mi.
2 Area - subaerial deltaic plain: 266.76 sq. mi.
3 Area - lower deltaic plain: 30.20 sq. mi.
4 Area - upper deltaic plain: 236.56 sq. mi.
5 Area - subaqueous deltaic plain: 195.47 sq. mi.
6 Area - active deltaic plain: 79.98 sq. mi.
7 Area - abandoned deltaic plain: 186.78 sq. mi.
8 Ratio - AUDP/ALDP: 7.83
9 Ratio - $AS_{ae}DP/AS_{aq}DP$: 1.36
10 Ratio - AA_bDP/AA_cDP: 2.33
11 Length long axis of delta: 18.20 mi.
12 Maximum width delta (W): 35.0 mi.
13 Length of delta shoreline (LS): 37.9 mi.
14 Ratio L/W of deltaic plain: 0.52
15 Ratio LS/W: 1.08
16 Distributary index "A" and "B":

Arc	1	2	3	4	5	6	7	8	9	10
"A"	1	1	1	1	1	1	1	1	1	1
"B"	1	1	1	1	1	1	1	1	1	1

17 Number of bifurcations: 0
18 Number of rejoinings: 0
19 Number of routes to sea: 1
20 Distributary density: 0.0947
21 Type of interdistributary: Type G - beach ridges and dunes
22 Exposure of delta coast: Open
23 Number of active river mouths: 1
24 Types of river mouth: Constricted
25 Width of river mouths (miles):

#	1
Width	0.87

26 Summary of river mouth widths:
$\overline{W}$ = 0.87 mi.

27 Depth of river mouths (feet)

#	1
Depth	40

28 Summary of river mouth depths:
$\overline{D}$ = 40 ft.

29 Depth-width ratio of river mouths:

#	1
D/W	.01

30 Summary of river mouth D/W ratios:
$\overline{D/W}$ = .01

Niger

1.3.0.0 Deltaic Plain
1.3.1.0 Location
1 Countries: Nigeria
2 Receiving body of water: Atlantic Ocean

1.3.2.0 Geological
1 Stability: Faulted, subsiding

1.3.3.0 Geomorphological
1 Area - deltaic plain: 12,042.26 sq. mi.
2 Area - subaerial deltaic plain: 10,779.03 sq. mi.
3 Area - lower deltaic plain: 5,264.26 sq. mi.
4 Area - upper deltaic plain: 5,514.77 sq. mi.
5 Area - subaqueous deltaic plain: 1,263.23 sq. mi.
6 Area - active deltaic plain: 4,143.68 sq. mi.
7 Area - abandoned deltaic plain: 6,635.35 sq. mi.
8 Ratio - AUDP/ALDP: 1.05
9 Ratio - $AS_{ae}DP/AS_{aq}DP$: 8.53
10 Ratio - AA_bDP/AA_cDP: 1.60
11 Length long axis of delta: 138.07 mi.
12 Maximum width delta (W): 176.26 mi.
13 Length of delta shoreline (LS): 227.80 mi.
14 Ratio L/W of deltaic plain: 0.78
15 Ratio LS/W: 1.29
16 Distributary index "A" and "B"

Arc	1	2	3	4	5	6	7	8	9	10
"A"	1	1	1	1	1	2	5	16	34	11
"B"	1	1	1	1	1	2	7	24	34	11

17 Number of bifurcations: 63
18 Number of rejoinings: 53
19 Number of routes to sea: 135
20 Distributary density: 0.1621
21 Type of interdistributary: Type F - heavily vegetated (mangrove)
22 Exposure of delta coast: Open
23 Number of active river mouths: 11
24 Types of river mouth: Constricted, deflected
25 Width of river mouths (miles):

#	1	2	3	4	5	6	7	8	9	10	11
Width	2.8	0.7	0.4	1.0	0.7	0.7	0.7	0.9	1.1	1.1	1.46

26 Summary of river mouth widths:
$\bar{W} = 1.05$ $S^2 = 0.42$ $S = 0.65$
$CV = 0.62$ $W_{max} = 2.8$ $W_{min} = 0.38$

27 Depth of river mouths (feet):

#	1	2	3	4	5	6	7	8	9	10
Depth	28	6	6	6	6	-	6	12	42	48

28 Summary of river mouth depths:
$\bar{D} = 17.7$ ft. $S^2 = 291.4$ $S = 17.1$
$CV = 0.96$ $D_{max} = 48.0$ $D_{min} = 6.0$

29 Depth-width ratio of river mouths:

#	1	2	3	4	5	6	7	8	9	10
D/W	.0018	.0015	.0029	.0011	.0015	-	.0017	.0024	.0073	.008

30 Summary of river mouth D/W ratios:
$\overline{D/W} = 16.9$ $S^2 = 190.9$ $S = 13.8$
$CV = 0.82$ $D/W_{max} = 42.5$ $D/W_{min} = 6.1$

31 Topography of bar: Type 1, regular
32 Area of bar:

#	1
Sq. mi.	5.6

33 Distance to edge of bar:

#	1
	1.6

34 Area of bulge: 265.9 sq. mi.
35 Volume of bulge: 1.19 cu. mi.
36 Ratio A_R/A_L of bulge: 0.825
37 Ratio V_R/V_L of bulge: 0.740
38 Subaerial area of bulge: 70.46 sq. mi.
39 Subaerial volume of bulge (V_{Bo}): 0.462 cu. mi.
40 Subaqueous area of bulge: 195.5
41 Subaqueous volume of bulge (V_{Bs}): 0.725 cu. mi.
42 Ratio V_{Bo}/V_{Bs}: 0.637
43 Subaqueous hypsometric integral of bulge (HI_s): 0.31
44 Bulge volume distribution parameter, right side (β_R): 0.41
45 Bulge volume distribution parameter, left side (β_L): 0.36
46 Mean volume distribution parameter $(\beta_R + \beta_L)/2$: 0.39
47 Offshore slope: (ft/mile)

	18'	36'	60'	180'	600'
$\overline{S_0}$	18.7	17.2	10.3	12.3	33.5
S	10.4	10.3	2.2	4.2	7.1
CV	0.5578	0.5999	0.2102	0.3389	0.2124
S_0 max	46.1	42.9	13.0	21.7	52.8
S_0 min	9.4	9.2	6.1	9.1	28.5

1.3.4.0 Climatological
1 Climatic classification: AW
2 Average yearly temperature: 25.8°C
3 Mean daily temperature:

	J	M	M	J	S	N
°C	27.0	27.0	26.0	24.0	25.0	26.0

4 Total yearly rainfall (mm): 1,430.0
5 Mean monthly precipitation (mm):

	J	M	M	J	S	N
$\overline{P_d}$	40.0	160.0	240.0	175.0	50.0	20.0

6 Date of freeze: -
7 Date of thaw: -
8 Duration of freeze: -

1.3.5.0 Pedological:
1 Major soil type: F-28

1.3.6.0 Biological
1 Major vegetation type: K-55

Niger

31 Topography of bar: Types 1 and 4, regular

32 Area of bar:

#	1	2	3	4	5	6	7	8	9	10	11
Sq. mi.	73.9	20.0	10.0	3.1	9.1	-	3.8	5.8	22.3	24.5	13.6

33 Distance to edge of bar:

#	1	2	3	4	5	6	7	8	9	10	11
Miles	5.3	3.3	2.17	1.65	2.26	-	1.32	1.41	3.68	4.23	1.56

34 Area of bulge: 6,683.04 sq. mi

35 Volume of bulge: 51.33 cu. mi.

36 Ratio A_R/A_L of bulge: 1.34

37 Ratio V_R/V_L of bulge: 1.39

38 Subaerial area of bulge: 5,511 sq. mi.

39 Subaerial volume of bulge (V_{Bo}): 41.16

40 Subaqueous area of bulge: 1,172

41 Subaqueous volume of bulge (V_{Bs}): 4.2

42 Ratio V_{Bo}/V_{Bs}: 9.8

43 Subaqueous hypsometric integral of bulge (HI_s): 0.36

44 Bulge volume distribution parameter, right side (β_R): 0.34

45 Bulge volume distribution parameter, left side (β_L): 0.31

46 Mean volume distribution parameter $(\beta_R + \beta_L)/2$: 0.33

47 Offshore slope: (ft/mile)

	18'	36'	60'	180'	600'
$\overline{S_0}$	8.1	6.1	5.7	7.7	16.1
S	3.7	1.0	0.7	1.2	2.1
CV	0.462	0.169	0.121	0.152	0.132
S_0 max	15.9	7.6	6.5	9.0	19.0
S_0 min	3.7	4.0	4.5	5.8	12.2

1.3.4.0 Climatological

1 Climatic classification: Af

2 Average yearly temperature: 26.1°C

3 Mean daily temperature:

	J	M	M	J	S	N
°C	26.5	27.5	26.5	25.0	25.0	26.0
S	0.71	0.71	2.12	1.41	1.41	1.41
CV	0.03	0.03	0.08	0.06	0.06	0.05

4 Total yearly rainfall (mm): 5,697.5

5 Mean monthly precipitation (mm):

	J	M	M	J	S	N
$\overline{P}_d$	107.5	247.5	442.5	845.0	827.5	317.5
S	116.7	208.6	265.2	841.5	972.3	357.1
CV	1.085	0.842	0.599	0.995	1.174	1.124

6 Date of freeze: -

7 Date of thaw: -

8 Duration of freeze: -

1.3.5.0 Pedological

1 Major soil type: F-28

1.3.6.0 Biological

1 Major vegetation type: K-55, J-47

1.3.7.0 Hydrological

1 Monthly discharge (x 10^3 cusecs):

	J	M	M	J	S	N
$\overline{D_{md}}$	153.9	197.9	120.9	74.5	57.3	61.8
S	10.2	7.9	18.3	4.3	2.8	14.0
CV	0.07	0.04	0.15	0.06	0.05	0.23

2 Average yearly discharge:
$\overline{D_{yd}}$ = 120.7 S^2 = 2,413.9 S = 49.1 CV = 0.4069

3 Maximum discharge:
$D_{yd\ max}$ = 209.1 Date: March

4 Minimum discharge:
$D_{yd\ min}$ = 41.9 Date: November

5 Flood peakedness:
K_f = 1.35

6 High water period: December-April

7 Low water period: May-November

8 Yearly sediment load: Unavailable

9 Monthly discharge efficiency index:

	J	M	M	J	S	N
Mean	1.1	2.9	1.7	1.0	0.5	0.4

10 Annual summary of discharge efficiency index:
Mean: 1.29 S: 0.93 CV: 0.72

1.4.0.0 Receiving Basin

1.4.1.0 Location

1 Body of water: Atlantic Ocean

1.4.2.0 Geological

1 Shelf structure: Unavailable

1.4.3.0 Geomorphological

1 Longest fetch: Greater than 2,000 miles

2 Direction of longest fetch: Southeast

3 Fetch directions greater than 200 miles: E, SE

4 Average width of continental shelf: 18.5 mi.

5 Slope of continental shelf:
$\overline{S_{c\varepsilon}}$ = 33.5 ft/mi S^2 = 50.5 S = 7.1
CV = 0.2124 $S_{cs\ max}$ = 52.8 $S_{cs\ min}$ = 28.5

6 Topography of shelf: Regular

1.4.4.0 Climatological

1 Wind frequency (Beaufort 3-12):

	J	M	M	J	S	N	Year
Offshore	4.3	4.2	1.4	0.3	1.4	7.4	3.2
Alongshore +	58.8	51.9	37.6	33.7	46.8	62.7	49.4
Alongshore -	-	-	-	-	-	-	-
Onshore	36.9	43.9	61.0	66.0	51.8	29.9	47.4

Niger

1.3.7.0 Hydrological

1 Monthly discharge (x 10^3 cusecs):

	J	M	M	J	S	N
$\overline{D_{md}}$	91.0	72.6	64.1	239.2	801.3	560.3
S	8.4	1.9	17.6	48.2	63.1	191.5
CV	0.093	0.027	0.275	0.202	0.079	0.342

2 Average yearly discharge:

$\overline{D_{yd}}$ = 384.8 S^2 = 91,216.8 S = 302.0 CV = 0.784

3 Maximum discharge:

$D_{yd\ max}$ = 956.1 Date: October

4 Minimum discharge:

$D_{yd\ min}$ = 48.2 Date: May

5 Flood peakedness:

K_f = 2.38

6 High water period: August-November

7 Low water period: December-July

8 Yearly sediment load: 59.0 x 10^6 cu. ft.

9 Monthly discharge efficiency index:

	J	M	M	J	S	N
Mean	3.5	0.9	0.8	1.2	5.4	16.11

10 Annual summary of discharge efficiency index:

Mean: 4.44 S: 4.87 CV: 1.10

1.4.0.0 Receiving Basin

1.4.1.0 Location

1 Body of water: Atlantic Ocean

1.4.2.0 Geological

1 Shelf structure: Unavailable

1.4.3.0 Geomorphological

1 Longest fetch: Greater than 2,000 miles

2 Direction of longest fetch: Southwest

3 Fetch directions greater than 200 miles: SE, E, S

4 Average width of continental shelf: 38.0 mi.

5 Slope of continental shelf:

$\overline{S_{c\varepsilon}}$ = 16.1 ft/mi S^2 = 4.5 S = 2.1

CV = 0.132 $S_{cs\ max}$ = 19.0 $S_{cs\ min}$ = 12.2

6 Topography of shelf: Regular

1.4.4.0 Climatological

1 Wind frequency (Beaufort 3-12):

	J	M	M	J	S	N	Year
Offshore	9	4	5	0	1	6	2
Alongshore +	2	19	25	29	15	21	17
Alongshore -	4	3	0	0	1	2	1
Onshore	85	74	70	71	83	71	80

2 Vector frequency (Beaufort 3-12):

	J	M	M	J	S	N	Year
Offshore	5.3	5.2	1.7	0.3	1.7	9.3	4.00
Alongshore +	72.2	64.4	43.9	40.3	57.7	79.6	60.34
Alongshore -	0	0	0	0	0	0	0
Onshore	45.2	54.4	71.0	78.8	64.0	37.9	58.06

3 Vector frequency (Beaufort 2-3):

	J	M	M	J	S	N	Year
Offshore	3.2	2.7	1.5	0.3	1.0	3.6	2.31
Alongshore +	43.3	44.2	23.2	19.4	33.6	41.9	34.83
Alongshore -	0	0	0	0	0	0	0
Onshore	29.8	39.4	32.8	27.0	34.8	23.1	31.04

4 Vector frequency (Beaufort 4-5):

	J	M	M	J	S	N	Year
Offshore	2.1	1.7	0.2	0	0.7	5.6	1.59
Alongshore +	29.1	18.8	19.1	20.6	23.2	34.9	24. 05
Alongshore -	0	0	0	0	0	0	0
Onshore	16.4	14.5	33.8	43.6	27.6	14.3	24.71

5 Vector frequency (Beaufort 6-7):

	J	M	M	J	S	N	Year
Offshore	0	0	0	0	0	0.2	0.03
Alongshore +	0	0.8	1.5	4.3	1.0	1.8	1.42
Alongshore -	0	0	0	0	0	0	0
Onshore	0	0.6	4.5	8.2	1.6	0.6	2.39

6 Vector frequency (Beaufort 8-12):

	J	M	M	J	S	N	Year
Offshore	0	0	0	0	0	0	0
Alongshore +	0	0	0	0	0	0	0
Alongshore -	0	0	0	0	0	0	0
Onshore	0	0	0	0	0	0	0

7 Storm systems: -
8 Date of freeze: -
9 Date of thaw: -
10 Duration of freeze: -

1.4.5.0 Pedological (no data)

1.4.6.0 Biological (no data)

1.4.7.0 Hydrological
1 Vector strength - direction of swell:

	J	M	M	J	S	N
V.S.	73.1	72.2	73.9	80.5	77.5	76.6
Dir.	144°	131°	107°	108°	116°	141°

Niger

2 Vector frequency (Beaufort 3-12):

	J	M	M	J	S	N	Year
Offshore	4.5	3.3	4.7	0.0	0.7	5.2	2.0
Alongshore +	0.8	17.6	24.1	28.9	16.5	17.4	14.3
Alongshore -	2.3	2.5	0	0	0.7	2.0	0.9
Onshore	42.9	67.6	66.0	75.0	88.8	56.6	64.7

3 Vector frequency (Beaufort 2-3):

	J	M	M	J	S	N	Year
Offshore	4.5	2.5	3.0	0.7	0.7	3.2	1.9
Alongshore +	0.1	14.0	18.3	12.6	12.2	14.6	10.1
Alongshore -	2.3	1.9	0.0	0.0	0.7	2.1	1.2
Onshore	41.1	57.3	56.2	44.3	62.9	48.9	51.7

4 Vector frequency (Beaufort 4-5):

	J	M	M	J	S	N	Year
Offshore	0.0	0.7	0.0	0.7	0.0	1.5	0.2
Alongshore +	0.0	3.6	5.0	15.3	4.6	2.7	4.1
Alongshore -	0.1	0.7	0.0	0.0	0.0	1.3	0.2
Onshore	1.7	10.3	9.8	25.5	19.9	7.7	12.0

5 Vector frequency (Beaufort 6-7):

	J	M	M	J	S	N	Year
Offshore	0.0	0.0	0.0	0.0	0.0	0.0	0.0
Alongshore +	0.0	0.0	0.0	2.8	0.0	0.0	0.2
Alongshore -	0.0	0.0	0.0	0.0	0.0	0.0	0.1
Onshore	0.0	0.0	0.0	5.2	0.0	0.0	0.1

6 Vector frequency (Beaufort 8-12):

	J	M	M	J	S	N	Year
Offshore	0.0	1.7	0.0	0.0	0.0	0.0	0.1
Alongshore +	0.0	0.8	0.0	0.0	0.0	0.0	0.1
Alongshore -	0.0	0.0	0.0	0.0	0.0	0.0	0.0
Onshore	0.0	0.0	0.0	0.0	0.0	0.0	0.0

7 Storm systems: -
8 Date of freeze: -
9 Date of thaw: -
10 Duration of freeze: -

1.4.5.0 Pedological (no data)

1.4.6.0 Biological (no data)

1.4.7.0 Hydrological
1 Vector strength - direction of swell:

	J	M	M	J	S	N
V.S.	84.3	73.9	70.3	88.7	69.9	87.5
Dir.	114°	120°	112°	108°	103°	116°

2 Vector strength - direction of sea:

	J	M	M	J	S	N
V.S.	83.0	78.9	81.7	84.3	81.8	83.4
Dir.	140°	135°	102°	103°	117°	143°

3 Weighted wave power (P_t') - 30' contour:

	J	M	M	J	S	N
$\overline{P_t'}$	470.25	217.60	371.13	613.06	487.90	618.15
S	109.46	70.90	157.74	436.0	175.12	135.1
CV	0.23	0.33	0.43	0.71	0.36	0.22

4 Annual summary for weighted wave power - 30' contour:
Mean: 438.73 S: 138.47 CV: 0.32
r_{right}: Not significant r_{left}: Not significant

5 Weighted wave power (P_t') - shore:

	J	M	M	J	S	N
$\overline{P_t'}$	29.94	14.84	15.52	16.55	24.88	35.16
S	19.02	9.94	11.34	16.23	17.88	23.84
CV	0.64	0.67	0.73	0.98	0.72	0.68

6 Annual summary for weighted wave power - shore:
Mean: 22.43 S: 8.35 CV: 0.37
r_{right}: Not significant r_{left}: Not significant

7 Weighted longshore wave power (P_l'):

	J	M	M	J	S	N
$\overline{P_l'}$	- 9.07	- 5.11	-11.20	-17.36	-13.49	- 8.55
S	23.99	12.82	25.00	37.60	30.39	24.46
CV	- 2.64	- 2.51	- 2.23	- 2.17	- 2.25	- 2.86

8 Annual summary for weighted longshore power:
Mean: -10.20 S: 4.06 CV: -0.40
r_{right}: Not significant r_{left}: Not significant

9 Weighted wave power gradient:

	J	M	M	J	S	N
$\overline{(\frac{\Delta P_o}{\Delta X})'}$	- 1.76	- 4.95	-10.26	-44.41	-10.39	-10.12
S	31.73	30.51	59.81	208.50	66.19	58.25
CV	-18.03	- 6.16	- 5.83	- 4.69	- 6.37	- 5.76

10 Annual summary for weighted wave power gradient:
Mean: -11.80 S: 12.28 CV: -1.04
r_{right} = Not significant r_{left}: Not significant

11 Weighted longshore power gradient:

	J	M	M	J	S	N
$(\frac{\Delta P_l}{\Delta X})'$	- 0.85	- 0.53	1.61	9.26	1.25	0.77
S	12.97	9.78	19.36	53.87	22.24	18.16
CV	-15.26	18.45	12.02	5.82	17.79	23.58

12 Annual summary for weighted longshore power gradient:
Mean: 1.71 S: 2.87 CV: 1.68
r_{right}: Not significant r_{left}: Not significant

13 Type of tide:

Niger

2 Vector strength - direction of sea:

	J	M	M	J	S	N
V.S.	80.7	52.5	70.1	80.4	83.8	83.8
Dir.	116°	123°	102°	112°	112°	116°

3 Weighted wave power (P_t') - 30' contour:

	J	M	M	J	S	N
$\overline{P_t'}$	17.36	83.64	82.79	444.86	198.23	33.76
S	2.22	5.92	5.97	41.90	14.88	2.57
CV	0.13	0.07	0.07	0.09	0.08	0.08

4 Annual summary for weighted wave power - 30' contour:
Mean: 129.01 S: 138.62 CV: 1.07
r_{right}: Not significant r_{left}: Not significant

5 Weighted wave power (P_t') - shore:

	J	M	M	J	S	N
$\overline{P_t'}$	0.43	1.32	1.37	3.23	2.44	0.57
S	0.35	1.00	1.01	2.37	1.89	0.41
CV	0.81	0.76	0.74	0.73	0.77	0.72

6 Annual summary for weighted wave power - shore:
Mean: 1.48 S: 1.00 CV: 0.68
r_{right}: Not significant r_{left}: Not significant

7 Weighted longshore wave power (P_l'):

	J	M	M	J	S	N
$\overline{P_l'}$	0.02	0.13	0.14	0.38	0.23	0.06
S	0.18	0.43	0.47	1.21	0.80	0.19
CV	9.00	3.31	3.36	3.18	3.48	3.17

8 Annual summary for weighted longshore power:
Mean: 0.14 S: 0.15 CV: 1.07
r_{right}: Not significant r_{left}: Not significant

9 Weighted wave power gradient:

	J	M	M	J	S	N
$\overline{(\frac{\Delta P_o}{\Delta X})'}$	0.13	0.32	0.32	0.51	0.56	0.13
S	0.36	1.01	1.09	1.95	1.78	0.44
CV	2.77	3.16	3.41	3.82	3.18	3.38

10 Annual summary for weighted wave power gradient:
Mean: 0.33 S: 0.16 CV: 0.48
r_{right}: Not significant r_{left}: Not significant

11 Weighted longshore power gradient:

	J	M	M	J	S	N
$(\frac{\Delta P_l}{\Delta X})'$	0.01	0.09	0.08	0.13	0.15	0.04
S	0.61	0.29	0.26	0.50	0.49	0.11
CV	61.00	3.22	3.25	3.85	3.27	2.75

12 Annual summary for weighted longshore power gradient:
Mean: 0.08 S: 0.06 CV: 0.75
r_{right}: Not significant r_{left}: Not significant

13 Type of tide: Diurnal

14 Monthly maximum and minimum tide range (ft.):

	J	M	M	J	S	N
Maximum	7.5	8.2	6.5	7.2	8.2	6.5
Minimum	2.8	1.3	2.2	2.5	1.3	2.2

15 Average tidal range: 4.5 ft.

16 Salinity:
January: 37.0 °/oo July: 36.5 °/oo

17 Water temperature:
January: 27°C July: 25°C

18 Water density:
January: 1.0235 July: 1.0242

19 Offshore currents:

	J	A	J	O
Direction	SW	SW	SW	SSW
Speed (knots)	0.5	0.5	0.7	0.7

Niger

14 Monthly maximum and minimum tide range (ft.):

	J	M	M	J	S	N
Maximum	5.4	5.8	5.4	5.4	5.7	5.4
Minimum	1.8	1.5	1.8	1.8	1.1	1.8

15 Average tidal range: 3.6 ft.

16 Salinity:
January: 33 °/₀₀ July: < 32 °/₀₀

17 Water temperature:
January: 24°C July: 29°C

18 Water density:
January: 1.019 July: 1.022

19 Offshore currents:

	J	A	J	O
Direction	SE	E	E	E
Speed (knots)	0.8	1.0	0.9	0.8

The Niger and São Francisco River Systems: A Comparison

The parameters tabulated in the foregoing section indicated the existence of numerous similarities as well as some significant contrasts between the two river systems. Some of the more striking differences and their meaning are discussed below. Identification of differences such as these among a large number of deltas should eventually lead to an appreciation of the most salient process-form interactions and their variability.

BASIN GEOLOGY AND GEOMORPHOLOGY

Figure 19A and B are maps of the Niger and São Francisco drainage basins, respectively. Geologically, both basins are tectonically stable. Lithologies, however, are appreciably different. Whereas the Niger basin is characterized by a predominance of igneous rocks, sedimentary rocks are more abundant in the São Francisco system. Hence, the material composing the São Francisco drainage basin is presumably less resistant, as a whole, than that of the Niger basin.

The basin of the Niger has nearly twice the area of the São Francisco basin and, in proportion, twice the stream length. Though Hack's (1957) empirical equation relating stream length to basin area yields for the two observed basin areas stream lengths in excess of those observed, both predicted and observed values lie within the same general order of magnitude. The discrepancy is probably attributable to the fact that the lowest order segments of the streams are not measurable from the 1:1,000,000-scale maps used in this study.

Relief ratios were found to be slightly but insignificantly higher in the São Francisco basin. Though this trend is in general agreement with Shumm's (1954) observations that relief increases with decreasing lithologic resistance, the differences in relief here are too slight to warrant any assignment of causality.

Hypsometric analyses yielded more contrasting results. The hypsometric curves of the Niger and São Francisco basins are shown graphically in Figures 20A and B. The hypsometric integral of the São Francisco basin is more than twice as large as that of the Niger. This appears to reflect primarily the predominance of high terrace formations along the course of the São Francisco. From the hypsometric curves it can be seen that in the São Francisco basin slopes are gentle and apparently more or less graded to elevations as high as 75 percent of the maximum. Less than 1 percent of the total dimensionless volume lies above the graded portion, and it may be inferred that the greater portion of the basin is either aggradational or in a state of equilibrium. Most of the area of the Niger basin is also characterized by what appear to be graded slopes (Fig. 20A). However, the low gradients reach altitudes of only 36 percent of the maximum elevation, and 3.8 percent of the hypsometric volume (6 percent of the total basin area) is accounted for by steeper, higher altitude portions of the basin. This suggests that, in spite of the slightly higher relief ratios of the São Francisco basin, the Niger basin offers greater potential energy to supply sediment through erosion of the upper portions of the basin.

BASIN CLIMATE AND HYDROLOGY

Climatically, the Niger and São Francisco basins are somewhat similar. Both are situated in the wet-and-dry tropics and experience pronounced seasonality of precipitation and runoff. In the Niger basin moisture surplus is on the average

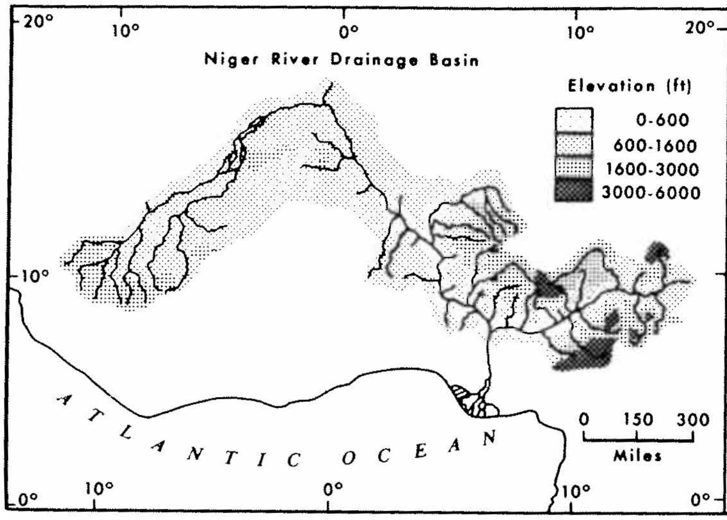

Figure 19A. Niger River drainage basin.

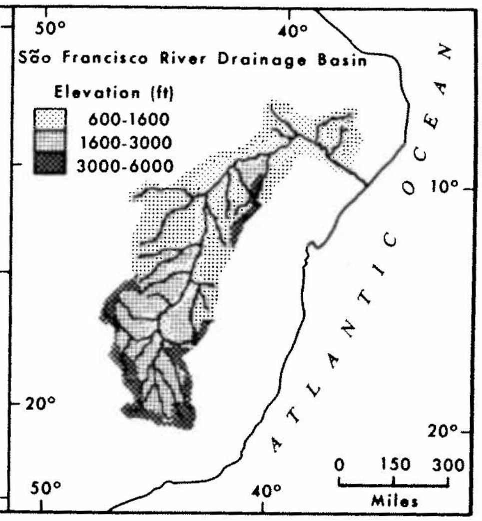

Figure 19B. São Francisco River drainage basin.

nil during the months of November through May; maxima occur in late summer. Correspondingly, discharge is at a minimum in May and at a maximum in October. The São Francisco basin has a generally wetter climate than the Niger in spite of its identical Koeppen classification. Moisture surplus is significant during all months, though the maximum, which occurs in December, is nearly 100 times higher than the minimum in October. Although the São Francisco basin has nearly two and a half times the annual moisture surplus of the Niger, the average annual discharge of the Niger is more than three times greater than that of the São Francisco, probably as a result of its larger basin and more intense runoff.

ALLUVIAL VALLEY CHARACTERISTICS

Both the Niger and São Francisco rivers follow braided courses of low sinuosity through sandy alluvial deposits. The Niger has the highest coefficient of variability for discharge in the alluvial valley, as well as a higher flood peakedness index. This tendency is probably partially responsible for the multiple distributary system of the Niger Delta.

DELTAIC PLAIN MORPHOLOGY AND THE OCEANOGRAPHIC REGIME

Aside from differences in absolute magnitudes, the two river systems exhibited few major contrasts in either the basin or alluvial valley. However, there are striking differences between the two deltas and their respective coastal energy regimes, as indicated by Figures 21 and 22. The Niger deltaic plain is crossed by a complex, multichanneled distributary pattern which disseminates sediments broadly around a symmetrical, arcuate delta shoreline over 200 miles in length. Deltaic progradation across a more or less gently sloping shelf has resulted in a conspicuous seaward bulge with an area which comprises 54 percent of the entire deltaic plain. Along the coastline, distributary mouths are separated by narrow beach-ridge barrier islands. Behind these, the interdistributary areas are occupied by

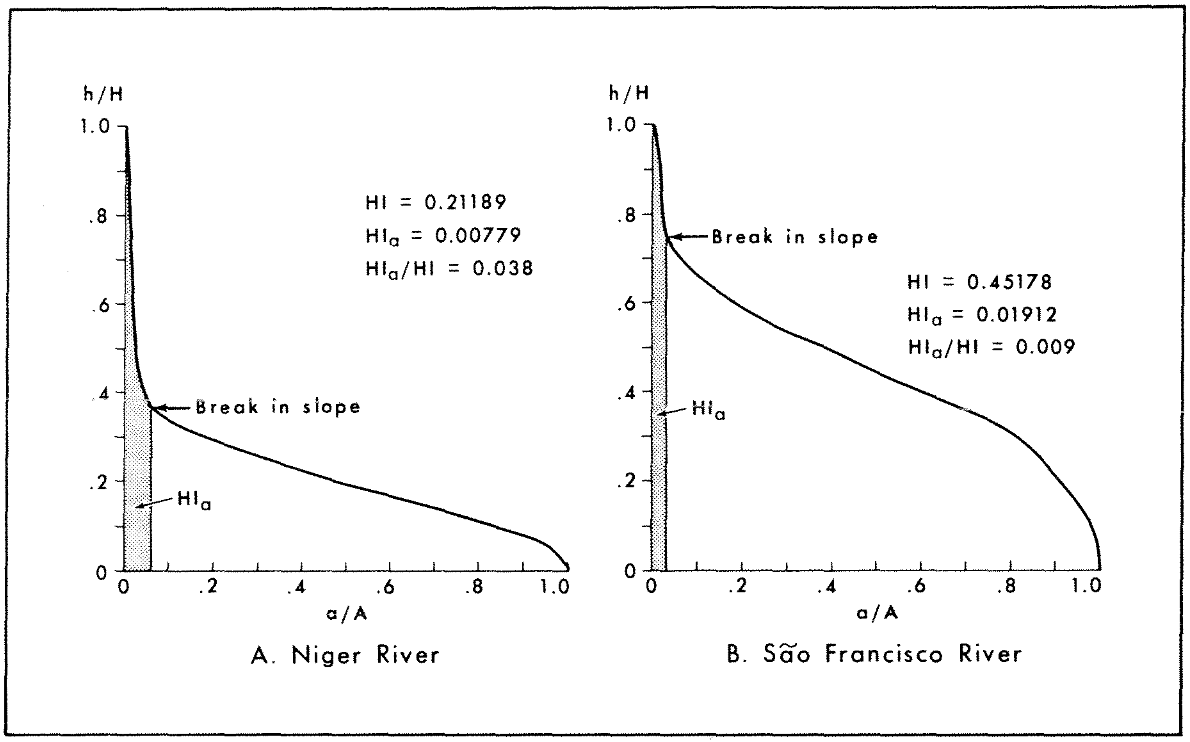

Figure 20. Hypsometric curves for Niger and São Francisco drainage basins.

extensive mangrove swamps.

In contrast, the São Francisco (Fig. 22) follows a single channel all the way to its mouth, where it debouches over a continental shelf more than twice as steep as that fronting the Niger Delta. Although the average annual discharge of the Niger is, at the coast, only a little more than 3 times that of the São Francisco, the former has built a deltaic bulge 25 times as large as those of the latter. The bulge volume distribution index is appreciably higher in the case of the São Francisco, reflecting the more cuspate form of that delta. Broad beach ridge and sand dune plains flank the river mouth on either side, reaching inland to mantle relict Pleistocene terraces.

These salient differences between the two deltas may be correlative with discharge distribution, shelf slope, and the coastal wave power climate. Deep water immediately seaward of the Niger Delta is characterized by moderate wave energy; the most frequent waves arrive from the southwest along orthogonals which are approximately normal to the average trend of the coast and to the apex of the deltaic bulge (Fig. 23). As Figure 21 indicates, wave power at the 30-foot contour exhibits considerable variability throughout the year but varies only slightly between sectors (statistical analysis indicated a nonsignificant correlation with distance alongshore from the delta axis). The diagram also illustrates the appreciable attenuation of power between the 30-foot contour and the shore. A high

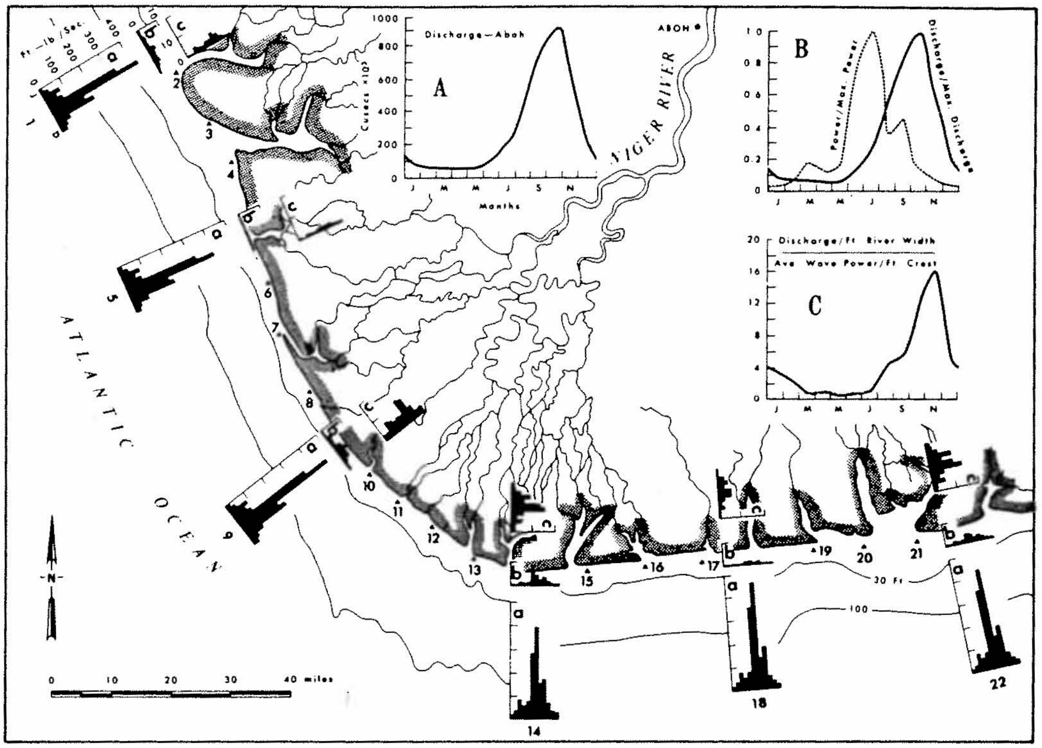

Figure 21. Discharge/wave power climate of Niger River Delta.

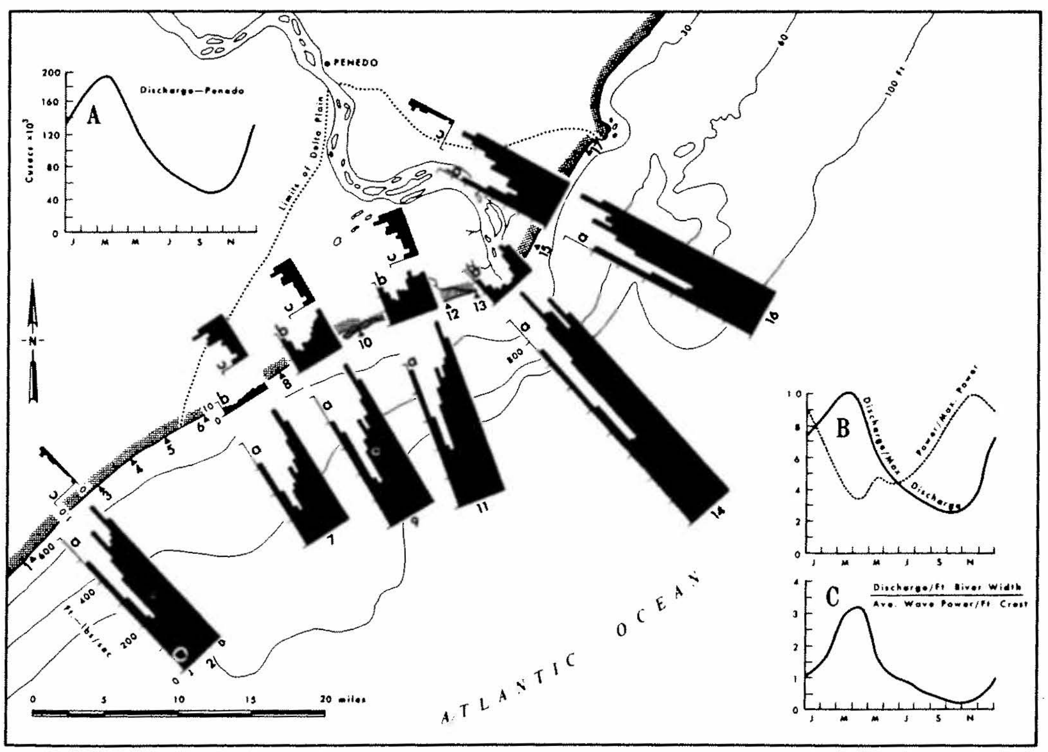

Figure 22. Discharge/wave power climate of São Francisco River Delta.

variance for the power at the shore is explicable in terms of the tendency for power to be highest along stretches of unbroken coast and minimal at the mouths of outlets as a result of associated slope variations. Variation with distance from the axis was again nonsignificant. The divergence of directions of longshore power from the axis presumably contributes to rounding the shoreline and is responsible for the observed directions of river mouth deflection (Fig. 21). Variations of longshore power with lateral position were nonsignificant.

Although discharge and wave power curves are about 3 months out of phase, the difference does not seem sufficient to produce any consequential overall inequilibrium. The river appears to retain its superiority throughout the year, partially by supplying enough sediment during times of high stage to flatten the subaqueous profile and attenuate the wave power. Hence, the discharge efficiency index is relatively high. On the other hand, the lack of net overall power and longshore power gradients, as well as the presence of beach ridges around the delta fringe, indicates that the waves have been able to influence sediment distribution enough to yield a configuration with which they are in harmony.

The São Francisco River debouches along an exposed section of the South Atlantic coast of South America. The offshore slope is steep, and deep-water wave energy is comparatively high; seas and swells arrive primarily from the east and southeast. The coast is so aligned that after refraction the orthogonals of the southeasterly waves are everywhere normal to the shore (Fig. 24A); however, the easterly waves impinge at an angle acute enough (Fig. 24B) to generate appreciable longshore power directed to the southwest (Fig. 22).

In contrast to the Niger Delta, the delta of the São Francisco shows definite effects of wave supremacy. Power levels at the 30-foot contour are considerably higher for the São Francisco; and, owing to the steeper subaqueous slope, there is considerably less frictional reduction in power between the 30-foot contour and the shoreline except at the river mouth, where the slope has been reduced by the development of a river mouth bar. The relationships between power attenuation and bottom slope are clearly evident from Figure 22. The discharge efficiency index is low in comparison to that of the Niger. Dimensionless discharge and wave power distribution curves (Fig. 22, inset B) are in complete opposition. In combination these tendencies have resulted in sediments' being reworked back onshore to straighten the coast and form broad beach ridge plains which flank the river mouth on either side. Only in the proximity of the mouth has the river been able to oppose the waves enough to build a protrusion into the sea. Strong onshore winds acting in combination with the high wave energy have led to the development of large transgressive dunes.

CONCLUSION

The two river systems just described were seen to share many traits in common as well as to exhibit several significant contrasts. Some process variables appeared to exert profound control upon the morphology of the delta; the influences of others were less conspicuous. The true roles of each variable can be ascertained only after many river systems have been analyzed following the procedures described and the results have been statistically compared.

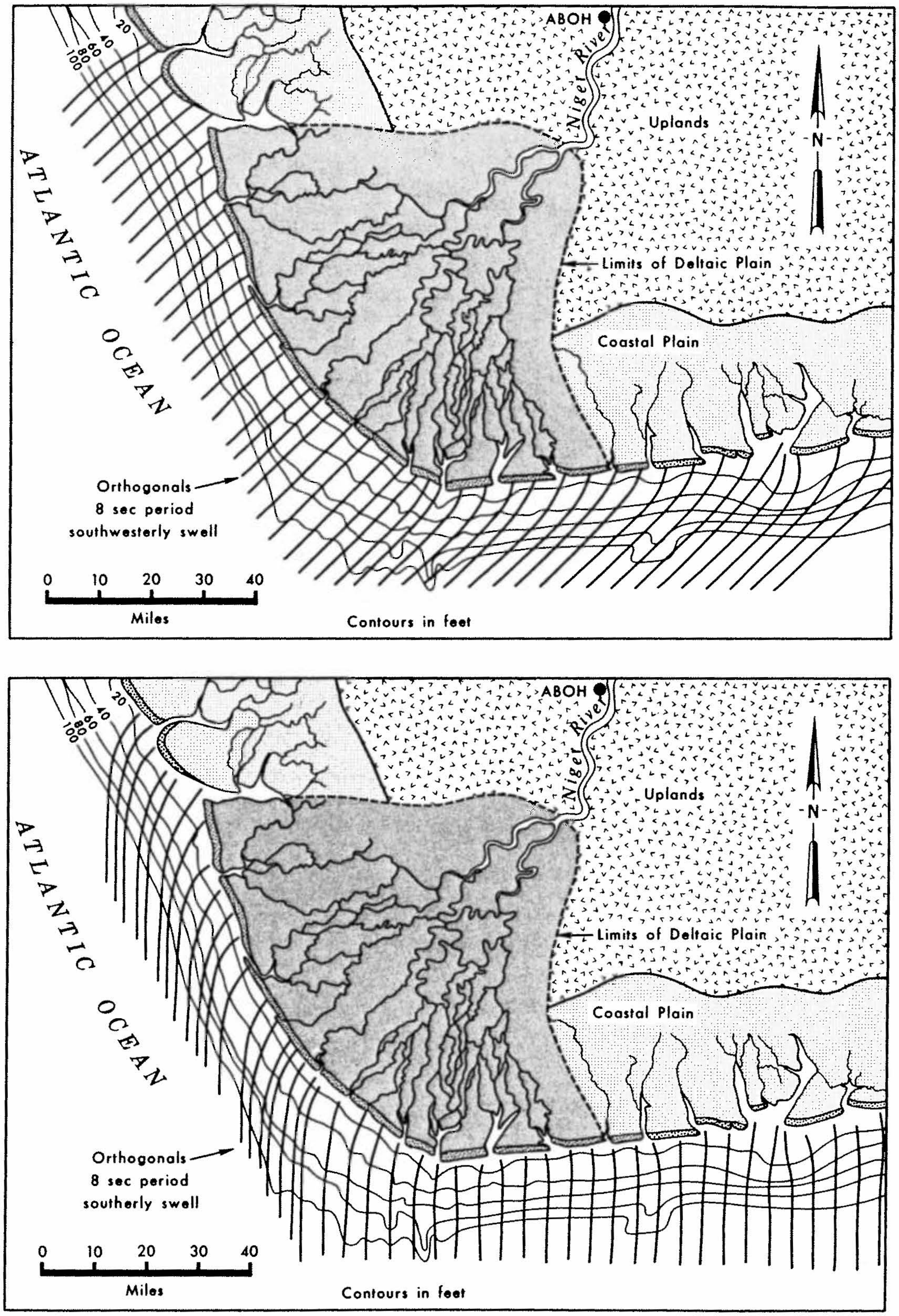

Figure 23. Refraction diagram for Niger River Delta. A. Eight-second southwesterly swell. B. Eight-second southerly swell.

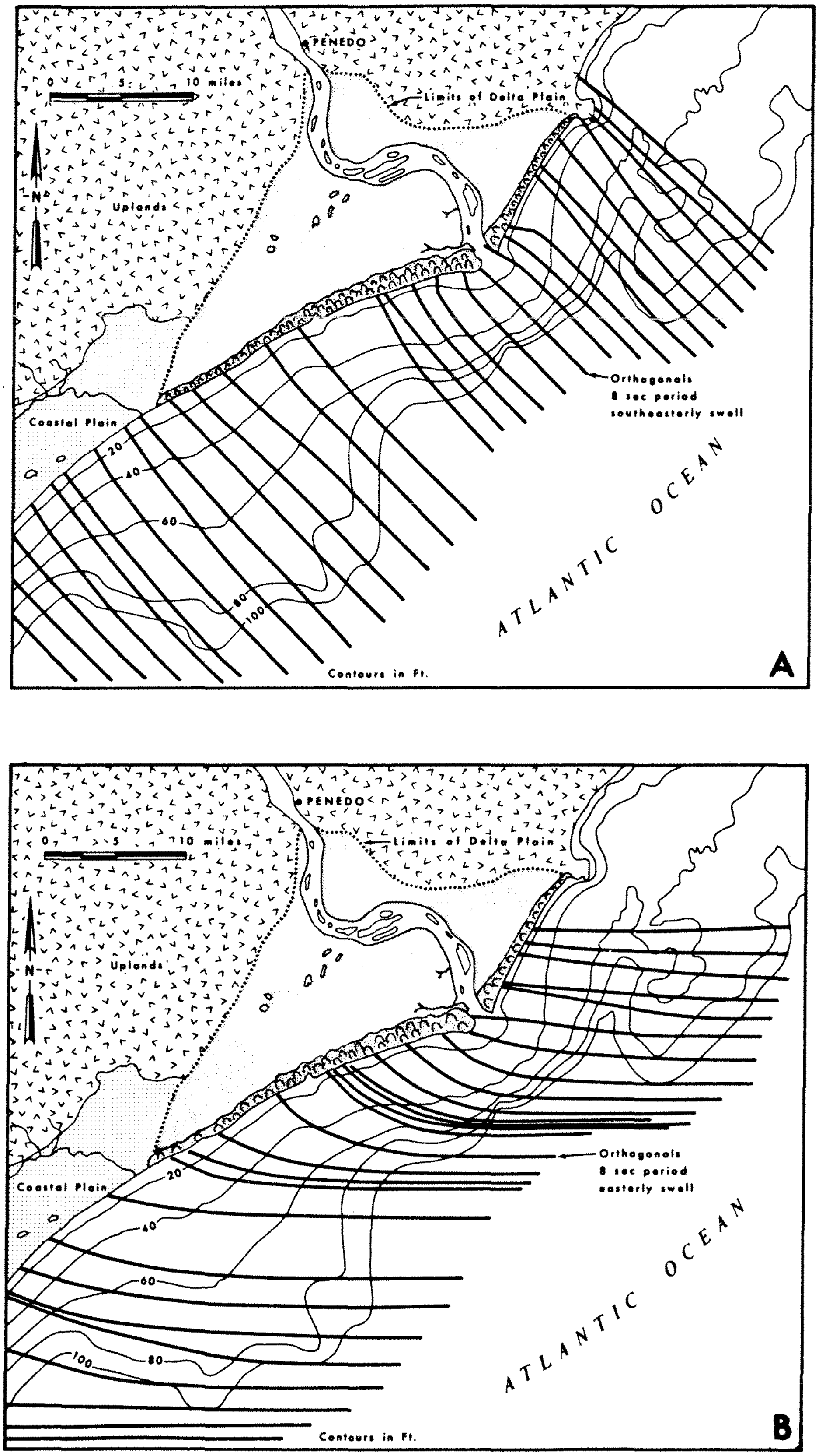

Figure 24. Refraction diagrams for São Francisco River Delta. A. Eight-second southeasterly swell. B. Eight-second easterly swell.

REFERENCES

Allen, J. R. L., 1964, Sedimentation in the modern delta of the River Niger, West Africa. In (Van Straaten, ed.) Deltaic and shallow marine deposits. Amsterdam (Elsevier), pp. 26-34.

______, 1965a, Late Quaternary Niger Delta, and adjacent areas: sedimentary environments and lithofacies. Bull. Am. Assoc. Petrol. Geologists, 49(5):547-600.

______, 1965b, Coastal geomorphology of Eastern Nigeria: beach ridge barrier islands and vegetated tidal flats. Geologie en Mijnbouw, 44:1-21.

Attia, M. I., 1954, Deposits in the Nile Valley and the Delta. Geological Survey of Egypt, Cairo (Government Press).

Axelsson, V., 1967, The Laitaure Delta. Geografiska Annaler, 49A(1).

Bagnold, R. A., 1941, The physics of blown sand and desert dunes. London (Methuen).

Bascom, W., 1954, Control of stream outlets by wave refraction. J. Geol., 62: 600-605.

Bates, C. C., 1953, Rational theory of delta formation. Bull. Am. Assoc. Petrol. Geologists, 37(9):2119-2161.

Bondar, C., 1963, Data concerning marine water penetration into the mouth of the Sulina channel. Studii de Hidraulica, 9(1):293-335 (in Romanian).

______, 1967, Contact of fluvial and sea waters at the Danube River mouths in the Black Sea. Studii de Hidrologie, 19:153-164 (in Romanian).

Borichansky, L. S., and V. N. Mikhailov, 1966, Interaction of river and sea water in the absence of tides. In Scientific problems of the humid tropical zone deltas and their implications. UNESCO, pp. 175-180.

Bretschneider, C. L., 1954, Field investigation of wave energy loss in shallow water ocean waves. U.S. Army Corps of Engineers Beach Erosion Board Tech. Memo., No. 46:1-21.

______, 1966, Wave generation by wind, deep and shallow water. In (Ippen, ed.) Estuary and coastline hydrodynamics. New York (McGraw-Hill), pp. 133-196.

______, and R. O. Reid, 1954, Modification of wave height due to bottom friction, percolation and refraction. U.S. Army Corps of Engineers Beach Erosion Board Tech. Memo. 45, 36 pp.

Chien, N., 1961, The braided stream of the lower Yellow River. Scientia Sincia, 10(6):734-754.

Chorley, R. J., 1957, Illustrating the laws of morphometry. Geol. Mag., 94:140-149.

Coleman, J. M., 1969, Brahmaputra River: channel processes and sedimentation. Sedimentary Geology, 3(2/3):129-239.

______, and S. M. Gagliano, 1965, Sedimentary structures: Mississippi River deltaic plain. In Primary sedimentary structures and their hydrodynamic interpretation. Am. Assoc. Petrol. Geologists Spec. Pub. No. 12.

______, S. M. Gagliano, and J. E. Webb, 1964, Minor sedimentary structures in a prograding distributary. Marine Geology, 1(3):240-258.

Credner, G. R., 1878, Die deltas, ihre morphologie, geographische, verbreitung, und entstehungs bedingungen. Petermanns Geographische Mitheilungen (Erganzungsland) 12(56):1-74.

Davies, J. L., 1958, Wave refraction and the evolution of shoreline curves. Geographical Studies, 5(2):51-52.

Davis, W. M., 1909, The geographical cycle. In (D. W. Johnson, ed.) Geographical Essays. Dover Edition, 1954, 777 pp.

Defant, A., 1961, Physical oceanography. Vol. 2, New York (MacMillan), 598 pp.

Dobson, R. S., 1967, Some applications of a digital computer to hydraulic engineering problems. Dept. Civil Engineering, Stanford Univ., Tech. Rept. 80, 172 pp.

Fisk, H. N., 1944, Geological investigations of the alluvial valley of the lower Mississippi River. Mississippi River Commission, Vicksburg, Miss.

______, E. McFarlan, C. R. Kolb, and L. J. Wilbert, 1954, Sedimentary framework of the modern Mississippi Delta. J. Sediment. Petrol., 24(2).

Gilbert, G. K., 1877, Report on the geology of the Henry Mountains. U.S. Geol. Survey, Rocky Mt. Region.

Hack, J. T., 1957, Studies of longitudinal stream profiles in Virginia and Maryland. U.S. Geol. Survey Prof. Paper 294-B, pp. 45-97.

______, 1960, Interpretation of erosional topography in humid temperate regions. Am. J. Sci., 258A:80-97.

Henry, V. R., 1961, Recent sedimentation and related oceanographic factors in the west Mississippi Delta area. Ph.D. Thesis, Texas A & M, College Station, Texas.

Horton, R. E., 1945, Erosional development of streams and their drainage basins. Bull. Geol. Soc. Am., 56:275-370.

Howe, H. V., and C. K. Moresi, 1931, Geology of Iberia Parish, Louisiana. Louisiana Geological Survey, Geology Bull. 1, 187 pp.

Jennings, J. N., 1955, The influence of wave action on coastal outline in plan. Australian Geographer, 6:36-44.

______, 1957, On the orientation of parabolic dunes. Geographical J., 123:474-480.

Johnson, J. W., and P. S. Eagleson, 1966, Coastal processes. In (Ippen, ed.) Estuary and coastline hydrodynamics. New York (McGraw-Hill), pp. 404-492.

Keulegan, G. H., and W. C. Krumbein, 1949, Stable configuration of bottom slope in a shallow sea and its bearing on geological processes. Trans. Am. Geophys.

30:855-861.

Krigstrom, A., 1962, Geomorphological studies of Sandur plains and their braided rivers of Iceland. Geografiska Annaler, H. 3-4, pp. 328-346.

Langbein, W. B., and S. A. Shumm, 1958, Yield of sediment in relation to mean annual precipitation. Trans. Am. Geophys. Union, 39:1076-1084.

Larras, J., 1957, Plages et cotes de Sable. Paris (Eyrolles), 117 pp.

Leighly, J., 1934, Turbulence and the transport of rock debris. Geographical Review, 24:453-464.

Leopold, L. B., and T. Maddock, 1953, The hydraulic geometry of stream channels and some physiographic implications. U.S. Geol. Surv. Prof. Paper 252, pp. 1-57.

Leopold, L. B., and M. G. Wolman, 1957, River channel patterns: braided, meandering and straight. U.S. Geol. Surv. Prof. Paper 282-B, pp. 39-85.

______, 1960, River meanders. Bull. Geol. Soc. Am., 71:769-794.

Leopold, L. B., M. G. Wolman, and J. P. Miller, 1964, Fluvial processes in geomorphology. San Francisco (W. H. Freeman and Co.), 522 pp.

Lewis, M. V., 1938, The evolution of shoreline curves. Proc. Geological Assoc., 59:107-127.

Melton, M. A., 1957, An analysis of the relations among elements of climate, surface properties and geomorphology. Dept. Geology, Columbia Univ., Tech. Rept. No. 11, 102 pp.

Mikhailov, V. N., 1966, Hydrology and formation of river mouth bars. In Scientific problems of the humid tropical zone deltas and their implications. UNESCO, pp. 59-64.

Morisawa, M. E., 1959, Relation of quantitative geomorphology to stream flow in representative watersheds of the Appalachian Plateau Province. Dept. Geology, Columbia Univ., Tech. Rept. 20.

Off, J., 1963, Rhythmic linear sand bodies caused by tidal currents. Bull. Am. Assoc. Petrol. Geologists, 47(2):324-341.

Peltier, L. C., 1950, The geographic cycle in periglacial regions as it is related to climatic morphology. Annals, Assoc. Am. Geographers, 40(3):214-236.

Pierson, W. J., G. Neumann, and R. W. James, 1967, Practical methods for observing and forecasting ocean waves by means of wave spectra and statistics. U.S. Naval Oceanographic Office H. O. Pub. No. 603, 284 pp.

Potter, W. D., 1953, Rainfall and topographic factors that affect runoff. Trans. Am. Geophys. Union, 34(1):67-73.

Russell, R. J., 1936, Physiography of the lower Mississippi River Delta. In Lower Mississippi Delta: Reports on the geology of Plaquemines and St. Bernard parishes. Louisiana Dept. Conservation, Geological Bull. 8.

______, 1940, Quaternary history of Louisiana. Bull. Geol. Soc. Am., 51:1199-1234.

______, 1942, Geomorphology of the Rhone Delta. Annals, Assoc. Am. Geographers, 32(2):149-254.

______, 1954, Alluvial morphology of Anatolian rivers. Annals, Assoc. Am. Geographers, 44(4):363-391.

Said, R., 1962, The geology of Egypt. Amsterdam (Elsevier).

Samojlov, I. V., 1956, Die Flussmundungen. Germany (Veb Hermann Haack), 647 pp. (translated from the Russian original Ust'ia Rek).

Scruton, P. C., 1956, Oceanography of Mississippi Delta sedimentary environments. Bull. Am. Assoc. Petrol. Geologists, 40(12):2864-2952.

______, 1960, Delta building and the deltaic sequence. In Recent sediments, Northwestern Gulf of Mexico. Am. Assoc. Petrol. Geologists.

Shepard, F. P., 1955, Delta front valleys bordering the Mississippi distributaries. Bull. Geol. Soc. Am., 66(12):1489-1498.

______, 1960, Mississippi Delta: marginal environments, sediments and growth. In Recent sediments, Northwestern Gulf of Mexico. Am. Assoc. Petrol. Geologists.

Shumm, S. A., 1954, Evolution of drainage systems and slopes in badlands at Perth Amboy, New Jersey. Dept. Geology, Columbia Univ., New York, Tech. Rept. No. 8, ONR Contract N6ONR271-30.

______, 1956, Evolution of drainage systems and slopes in badlands at Perth Amboy, New Jersey. Bull. Geol. Soc. Am., 67:597-646.

______, 1960, The shape of alluvial channels in relation to sediment type. U.S. Geol. Surv. Prof. Paper 352-B, pp. 17-30.

______, 1963, Sinuosity of alluvial rivers on the Great Plains. Bull. Geol. Soc. Am., 74(9):1089-1100.

Silvester, R., and C. LaCruz, 1970, Pattern forming processes in deltas. J. Waterways and Harbors Div. Am. Soc. Civil Engrs., 96(WW2):201-217.

Strahler, A. N., 1952, Hypsometric (area-altitude) analysis of erosional topography. Bull. Geol. Soc. Am., 63:1117-1142.

______, 1957, Quantitative analysis of watershed geomorphology. Trans. Am. Geophys. Union, 38(6):913-920.

______, 1958. Dimensional analysis applied to fluvially eroded landforms. Bull. Geol. Soc. Am., 69:279-300.

Sundborg, A., 1956, The river Klaralven, a study of fluvial processes. Geografiska Annaler, 38:127-316.

Takano, K., 1954a, On the velocity distribution off the mouth of a river. J. Oceanographcc Soc. Japan, 10(2):60-64.

_______, 1954b, On the salinity and velocity distributions off the mouth of a river. J. Oceanographic Soc. Japan, 10(3):92-98.

_______, 1955, A complementary note on the diffusion of the seaward flow off the mouth of a river. J. Oceanographic Soc. Japan, 11(4).

Thornthwaite, C. W., Associates, 1962, Average climatic water balance data of the continents. Part I. Africa. Publications in Climatology, XV(2):115-287.

_______, 1963a, Average climatic water balance data of the continents. Part II. Asia (excluding the USSR). Publications in Climatology, XVI(1):5-262.

_______, 1963b, Average climatic water balance data of the continents. Part III. USSR. Publications in Climatology, XVI(2):267-378.

_______, 1964a, Average climatic water balance data of the continents. Part V. Europe. Publications in Climatology, XVII(1):5-299.

_______, 1964b, Average climatic water balance data of the continents. Part VI. North America (except the United States). Publications in Climatology, XVII (2):235-414.

_______, 1964c, Average climatic water balance data of the continents. Part VII. United States. Publications in Climatology, XVII(3):419-615.

_______, 1965, Average climatic water balance data of the continents. Part VIII. South America. Publications in Climatology, XVIII (2):297-433.

Tricart, J., and A. Cailleux, 1965, Introduction a la geomorphologie climatique. Paris (Societe d'edition d'enseignement superieur), 306 pp.

USSR Academy of Sciences, 1964, Physical-geographic atlas of the world. Moscow, 298 pp.

Weigel, R. L., 1964, Oceanographical engineering. New Jersey (Prentice-Hall), 532 pp.

Welder, F. A., 1955, Deltaic processes in Cubits Gap area, Plaquemines Parish, Louisiana. Ph.D. Thesis, Louisiana State Univ., 119 pp., available University Microfilms.

_______, 1959, Processes of deltaic sedimentation in the lower Mississippi River. Louisiana State Univ., Coastal Studies Institute Tech. Rept. No. 12.

Wolman, M. G., and L. B. Leopold, 1957, River flood plains: some observations on their formation. U.S. Geol. Surv. Prof. Paper 282-C, pp. 87-109.

Wright, L. D., 1970a, Circulation, effluent diffusion and sediment transport, mouth of South Pass, Mississippi River Delta. Louisiana State Univ., Coastal Studies Institute Tech. Rept. No. 84.

_______, 1970b, The influence of sediment availability on patterns of beach ridge development in the vicinity of the Shoalhaven River Delta, N.S.W. The Australian Geographer, 11(4):336-348.

Yatsu, E., 1966, Rock control in geomorphology. Tokyo (Sozosha), 135 pp.

Zenkovich, V. P., 1967, Processes of coastal development. New York (John Wiley and Sons), 739 pp.

Appendix 1

FORTRAN IV LISTING FOR MAPCAL PROGRAM

```
C      * - * - * - * - * - * - * - * - * - * - * - * - * - * - * - * - * - * - * - *
C      CALMA TAPE FOR STREAM LENGTH, BASIN AREA, CONTOUR, AND DRAINAGE STUDY.
C      * - * - * - * - * - * - * - * - * - * - * - * - * - * - * - * - * - * - * - *
       DIMENSION CPM(50),CAREA(50),AST(20)
       COMMON/SL/X(126),Y(126),D(251),XO,YO,X1,Y1,CORL,CORA,ACLOSE
      *         ,CLOSE,KLAST,IFIRST
       LOGICAL*1 IFIRST
       REAL*8 SUM,SUMA,DUM
       DATA CON,AST,BLK/'CONT',20*'****',' '/
       SL=0.
       DEN=0.
       BAREA=0.
       BPRMT=0.
       DO1I=1,50
       CPM(I)=0.
     1 CAREA(I)=0.
       IEND=0
       ICONT=0
       JBOLD=0
       IFIRST=.TRUE.
     2 READ(8,END=9)NRC,KK,(D(I),I=1,KK)
       IF (KK.EQ.1) GO TO 2
       IF (NRC.EQ.0.AND.D(1).EQ.CON.AND.JBRCH.EQ.3) GO TO 65
       IF (NRC.EQ.0) GO TO 3
       K2=KK/2
C         BRANCHING TO CALCULATION OF EACH JOB.
       GOTO(10,20,30,40),JBRCH
C
C      READ IN THE MAP AND PARAMETER CONTROLS.
C      ***************************************
C
C         SEQUENCE OF CALCULATION OF THE JOBS HAS NO FIXED ORDER.
C         JOBS MAY BE OMITTED IF SO DESIRED.  HOWEVER, TO START THE CALCULATION
C         'STREAM LENGTH' MUST LEAD THE SEQUENCE.  SINCE 'JOBOLD' IS SET
C         TO 0 AT THE BEGINNING OF CALCULATION.
C         STREAM LENGTH CAN BE OMITTED AT LATER CALCULATIONS.
C
     3 MAP=INTF(D(1))
       JBRN=JBOLD+1
       JBRCH=INTF(D(2))
       JBOLD=JBRCH
       NTRACE=1
       XR=0.
       YR=0.
       X1=0.
       Y1=0.
C         BRANCHING TO PRINT.
       GO TO (4,5,6,7,8),JBRN
C
C         JBRN IS THE (JBOLD+1) OF THE BRANCH JUST FINISHED CALCULATION.
C         STATEMENT 2 READS IN THE TITLE OF THE NEXT JOB, THEN THE PROGRAM
C         PRINTS OUT THE LAST JOB (JBRCH) RESULTS BEFORE GOING TO STATEMENT 4
C         FOR THE PRINTING THE NEXT JOB TITLE.
C         STATEMENT 65 BEGINS THE PRINTING OF EACH SUB-CONTOUR VALUES.
C
C      PRINT THE TITLE OF THE MAP
C      **************************
     4 WRITE(6,300)(D(I),I=1,KK)
       WRITE(6,301)(AST(I),I=1,KK)
   300 FORMAT(////5X,20A4)
   301 FORMAT(5X,20A4)
       CP=0.
       CA=0.
       IFIRST=.TRUE.
       GO TO 2
C
C         IFIRST IS USED TO PICK UP THE FIRST POINT XR,YR IN ANL SUBROUTINE.
C         IT ALSO MEANS THE FIRST PASS OF EACH SUB-CONTOUR JOB.
C
C      PRINT THE STREAM LENGTH.
```

```
C       ************************
  5     WRITE(6,350)MAP,SL
  350   FORMAT (//15X'STREAM LENGTH FOR MAP NO.',I3,' =',E16.7)
        SL=0.
        IF (IEND.EQ.1) STOP
        GO TO 4
C
C       PRINT THE BASIN AREA.
C       *********************
C       BASIN AREA IS ALWAYS CLOSED BY THE FOLLOWING STATEMENT.
  6     BAREA=BAREA+ACLOSE
        WRITE (6,360) BPRMT,MAP,BAREA
        BAREA=0.
        BPRMT=0.
  360   FORMAT (//15X'BASIN PERIMETER =',E16.7,5X'BASIN AREA FOR MAP NO.'
       *           I3,' =',E16.7)
        IF (IEND.EQ.1) STOP
        GO TO 4
C
C       PRINT CONTOUR AREA AND CONTOUR PERIMETER.
C       *****************************************
C          IF IT IS THE FIRST PASS, IT GOES TO STATEMENT 25 AND PRINTS OUT
C          THE CONTOUR NUMBER AND MAP NUMBER AS THE SUB-TITLE OF THE PRESENT
C          CONTOUR JOB.
  65    IF (IFIRST) GO TO 25
C
C          LAST DATA POINT OF A CONTOUR IS FIRST DATA POINT OF THE NEXT CONTOUR.
C          KLAST IS SET IN ANL SUBROUTINE.  IF IT IS 1, IT MEANS THE LAST DATA
C          POINT HAS BEEN ADDED IN ALREADY AND SHOULD BE SUBTRACTED OUT BY 'CORL'.
C          KNT COUNTS THE NUMBER OF SUB-CONTOURS AT EACH CONTOUR ELEVATION.
C
  7     IF (JBRCH.NE.3) GO TO 75
        CPL=0.
        IF (KLAST.EQ.1) CPL=CORL
        CP=CP-CPL
        CA=CA-CORA
  75    KNT=KNT+1
        CA=CA+CLOSE
        CPM(ICONT)=CPM(ICONT)+CP
        CAREA(ICONT)=CAREA(ICONT)+CA
        CPMP=CPM(ICONT)
        CARP=CAREA(ICONT)
        WRITE (6,410) KNT,CP,CA
  410   FORMAT (15XI2,2E19.7)
        CP=0.
        CA=0.
        IF (IEND.EQ.1) GO TO 27
        IF (JBRCH.EQ.3) GO TO 25
C
C          THE FOLLOWING STATEMENT PRINTS OUT THE ACCUMULATED CONTOUR RESULTS
C          AND GOES TO THE NEXT JOB, WHICH MEANS THE CONTOUR JOB IS DONE.
C
        IF (JBRCH.NE.3.AND.JBRN.EQ.4) WRITE (6,450) CPMP,CARP
        GO TO 4
C
C       PRINT DRAINAGE DENSITY.
C       ***********************
  8     DEN=DEN/400.
        WRITE (6,440) MAP,DEN
  440   FORMAT (//15X'MAP ='I3,3X'DRAINAGE DENSITY 400 SQ. MILE AREA ='
       *          E16.7)
        DEN=0.
        IF (IEND.EQ.1) STOP
        GO TO 4
C
C       END OF TAPE.
C       ************
  9     IEND=1
        GO TO (5,6,75,8),JBRCH
C
C       STREAM LENGTH CALCULATION. (JBRCH=1)
C       **************************
```

```
0081     10   CALL ANL(0.,0.,K2,SUM,0,DUM)
0082          SL=SL+SUM
0083          GO TO 2
        C
        C     BASIN AREA AND PERIMETER CALCULATION. (JBRCH=2)
        C     ***********************************
0084     20   IF (NRC.EQ.NTRACE) GO TO 21
0085          NTRACE=NRC
0086          XR=X1
0087          YR=Y1
        C
        C        XR,YR PICK UP THE LAST POINT X1,Y1 OF TRACE 1 AS A REFERENCE
        C        POINT FOR TRACE 2, WHICH IS THE MAP BOUNDARY CALCULATION.
        C
0088     21   CALL ANL (XR,YR,K2,SUM,1,SUMA)
0089          BAREA=BAREA+SUMA
0090          IF (NRC-NRC/2*2.EQ.1) BPRMT=BPRMT+SUM
0091          GO TO 2
        C
        C     PRINT CONTOUR NUMBER.
        C     *********************
0092     25   ICONT=INTF(D(2))
0093          IF (D(3).EQ.BLK) IFIRST=.TRUE.
        C        IFIRST NOW RESETS TO INITIALIZE THE FIRST POINT OF A NEW CONTOUR.
0094          IF (D(3).EQ.BLK) GO TO 2
0095          IF (IFIRST) GO TO 29
        C
        C        STATEMENT 27 PRINTS OUT THE ACCUMULATIVE CONTOUR AREA AND PERIMETER.
        C        THEN, IT WILL EITHER STOP OR PRINT OUT THE NEXT CONTOUR NUMBER AND
        C        MAP NUMBER FOR CONTINUING CALCULATION.
        C
0096     27   WRITE (6,450) CPMP,CARP
0097    450   FORMAT (15X40('-')/17X2E19.7)
0098          IF (IEND.EQ.1) STOP
0099          CP=0.
0100          CA=0.
0101     29   KNT=0
0102          CONT=D(3)
0103          WRITE (6,400) CONT,ICONT,MAP
0104    400   FORMAT (//15X'CONTOUR 'A4,' ASSIGNED AS CONTOUR NO.'I3,
             *        ' FOR MAP NO.'I3/15X,4('---')//20X'CONTOUR PERIMETER',6X,
             *        'CONTOUR AREA'/)
0105          GOTO2
        C
        C     CONTOUR AREA AND PERIMETER CALCULATION.(JBRCH=3)
        C     **************************************
0106     30   CALL ANL (0.,0.,K2,SUM,1,SUMA)
0107          CP=CP+SUM
0108          CA=CA+SUMA
0109          GO TO 2
        C
        C     DRAINAGE CALCULATION.(JBRCH=4)
        C     ********************
0110     40   CALL ANL(0.,0.,K2,SUM,0,DUM)
0111          DEN=DEN+SUM
0112          GO TO 2
0113          END


0001          SUBROUTINE ANL (XR,YR,K2,SUM,L,SUMA)
0002          COMMON/SL/X(126),Y(126),D(251),X0,Y0.X1,Y1.CORL,CORA,ACLOSE
             *          ,CLOSE,KLAST,IFIRST
0003          LOGICAL*1 IFIRST
0004          REAL*8 SUM,XX,YY,ZERO
0005          DATA ZERO/0./
        C     XR, YR ARE THE REFERENCE POINT.  X0,Y0 IS CORRECTED BY XR,YR.
        C     L=1 CALCULATES THE AREA, 6=0 SKIP THE AREA CALCULATION.
        C     X1,Y1 IS THE LAST POINT OF THE LAST CONTOUR (OR, THE SAME AS X0,Y0
        C     POINT, IF IT IS THE FIRST PASS).
0006          KLAST=0
0007          IF (.NOT.IFIRST) GO TO 10
```

```
      XC=D(1)+XR
      YC=D(2)+YR
      X1=XC
      Y1=YC
      IFIRST=.FALSE.
   10 X(1)=X1
      Y(1)=Y1
      DO22I=1,K2
      J=2*I-1
      X(I+1)=D(J)+XR
   20 Y(I+1)=D(J+1)+YR
      IF (L.EQ.0) GO TO 28
      SUMA=0.
      DO25I=1,K2
      XX=X(I+1)-X(I)
      YY=Y(I)+Y(I+1)
   25 SUMA=SUMA+YY*XX/2.D0
C     STREAM LENGTH AND DRAINAGE CALCULATON. TAKE EVERY 10 POINTS.
   28 KP=10
      KF=K2
      KI=K2/KP*KP
      IF (K2.GT.KI) KF=KI+KP
      SUM=0.
      DO 30 I=1,KF,KP
      K=I
      J=I+KP
      IF (J.GT.K2) J=K2
      IF (I.GT.K2) K=I-KP
      XX=X(J)-X(K)
      YY=Y(J)-Y(K)
      IF (XX.EQ.ZERO) SUM=SUM+DABS(YY)
      IF (XX.EQ.ZERO) GO TO 30
      IF (YY.EQ.ZERO) SUM=SUM+DABS(XX)
      IF (YY.EQ.ZERO) GO TO 30
      SUM=SUM+DSQRT(XX*XX+YY*YY)
      IF (J.EQ.K2) KLAST=I
   30 CONTINUE
      X1=X(K2+1)
      Y1=Y(K2+1)
C     CURL AND CORA ARE USED FOR THE LAST POINT CORRECTION FOR CONTOURS.
C     CLOSE IS USED TO CLOSE THE CONTOUR AREA ONLY, ACLOSE IS FOR OTHER AREAS.
      CURL=DSQRT(XX*XX+YY*YY)
      CORA=(Y1+Y(K2))*(X1-X(K2))/2.
      CLOSE=(Y0+Y(K2))*(X0-X(K2))/2.
      ACLOSE=(Y0+Y1)*(X0-X1)/2.
      RETURN
      END
```

```
      FUNCTION INTF(ID)
      DATA IBLK/Z00000040/
      DATA KF/Z000000F0/
      K=1
      INTF=0
      DO 10 I=1,4
      J=5-I
      KD=0
      CALL SPOT (J,ID,4,KD)
      IF (KD.EQ.IBLK) GO TO 10
      INTF=INTF+K*(KD-KF)
      K=K*10
   10 CONTINUE
      RETURN
      END
```

```
      SUBROUTINE SPOT (N,A,M,B)
      LOGICAL*1 XL(4),YL(4)
      EQUIVALENCE (X,XL),(Y,YL)
      X=A
```

```
      Y=B
      YL(M)=XL(N)
      B=Y
      RETURN
      END
```

Sample Output for MAPCAL Program

```
00020001 STREAM LENGTH
*************************

         STREAM LENGTH FOR MAP NO.  2 =    0.3727661E 03


00020002 PERIMETER AREA
*************************

         BASIN PERIMETER =    0.5832476E 03     BASIN AREA FOR MAP NO.  2 =    0.2792772E 05


00020003 CONTOUR
********************


         CONTOUR  100 ASSIGNED AS CONTOUR NO. 11 FOR MAP NO.  2
         ------------

             CONTOUR PERIMETER        CONTOUR AREA

          1        0.3962828E 02       0.2206709E 02
         -----------------------------------------
                   0.3962828E 02       0.2206709E 02

         CONTOUR  800 ASSIGNED AS CONTOUR NO. 12 FOR MAP NO.  2
         ------------

             CONTOUR PERIMETER        CONTOUR AREA

          1        0.7568890E 02       0.1330507E 03
          2        0.2089418E 02       0.1135573E 02
          3        0.1460621E 02       0.8390717E 01
         -----------------------------------------
                   0.1111893E 03       0.1527972E 03


000200040017 DENSITY
*************************

         MAP =  2    DRAINAGE DENSITY 400 SQ. MILE AREA =    0.3563141E 00
```

Appendix 2

WAVE ANALYSIS

In order to make the detailed wave regime analyses described in this report feasible, a FORTRAN IV computer program and data reduction procedures had to be designed. An original computer program by Dobson (1967) was modified by the addition of several subroutines to satisfy the requirements of this study. In its original form, Dobson's routine computed only the effects of ordinary refraction and shoaling on wave direction, celerity, and height over a changing bottom configuration, given deep-water wave characteristics and gridded depth data input in card form.

In the modified version, ungridded depth data are input from magnetic tape on which the x and y coordinates at 0.01-inch intervals along each depth contour are stored, together with the depth value (in feet), by tracing the contours directly from hydrographic charts. A CALMA Model 300 electronic digitizer is used. An interpolation routine in the program then converts these data into gridded form, the grid size being optional and selected on the basis of the intricacy of the bottom. Hindcast deep-water wave period (T) in seconds, height (H) in feet, direction, and initial (deep-water) coordinates of each ray are input in card form.

The change in wave direction, celerity, and length caused by refraction and the change in wave height because of shoaling are computed by Dobson's (1967) original routines. Dobson (1967) has fully described and discussed the calculations, which are based on conventional linear wave theory. Wave theory and the theory of wave refraction may also be found in Weigel (1964). The FORTRAN IV program listing in this appendix may be referred to for the actual calculation procedures.

Wave height, energy, and power depend not only upon the degree of wave refraction and shoaling but also upon the amount of energy expended by frictional interaction between the bottom and the shoaling wave. The equations derived by Bretschneider (1954) and Bretschneider and Reid (1954) are used to compute the dissipation of energy and consequent reduction in wave height caused by bottom friction. At each increment, j, along the ray (the step length is optionally specified) the mean wave height, H_j, is computed as a function of the wave height at the previous interval, H_{j-1}, change in shoaling coefficient, Ks, refraction coefficient, Kr, and frictional attenuation by the following:

$$H_j = Hm_j/([f\ Hm_j^2\ \phi\ (\Delta x)_j/Ks_j\ T^4] + 1)$$

in which $$Hm_j = H_{j-1} + \Omega_j/Z$$

where $$\Omega_j = H_{j-1}\left(\frac{Ks_j}{Ks_{j-1}}\quad \frac{Kr_j}{Kr_{j-1}}\right);$$

f is a constant friction factor, the value of which depends on, among other things, bottom roughness, (Δx) is the linear distance along the ray between points j and j-1, and

$$\phi = \frac{64\pi^3}{3\ g^2} \left[\frac{Ks_j}{\sinh\ 2\pi d/L} \right]^3$$

where g is the acceleration of gravity, d is the water depth, and L is the wave length.

Wave characteristics are determined at each interval. From these the following additional parameters are computed:

Wave steepness, H/L, the ratio of height to length;

Wave energy, E, from

$$E = \gamma\ H^2 L/8$$

where γ is the unit weight of water;

Longshore energy, E_ℓ,

$$E_\ell = E \sin\theta \cos\theta$$

where θ is the angle between the wave orthogonal and the normal to the bottom contour;

Wave power, P,

$$P = \gamma H^2 C_g/8$$

where C_g is the group velocity of the wave train given by

$$C_g = 1/2\ C \left(1 + \frac{4\pi d/L}{\sinh\ 4\pi d/L}\right)$$

where C is the phase velocity;

Longshore wave power, P_ℓ, is given by

$$P_\ell = P \sin\theta \cos\theta.$$

All values are output at each increment along each ray as indicated by the sample output following the program listing. In addition, bottom contours and wave rays are plotted automatically by a CALCOMP plotter. From this output the monthly and annual wave climate parameters (weighted values) are calculated; a Wang 700 programmable calculator is used.

A listing and a sample output of the program just described follow.

FORTRAN IV LISTING FOR WAVE PROGRAM
(Modified after Dobson, 1967)

```
C           MI      = MAX. VALUE FOR I SUBSCRIPT, NOW FIGURED IN PROGRAM
C           MJ      = MAX. VALUE FOR J SUBSCRIPT, NOW FIGURED IN PROGRAM
C          XMAX,YMAX  = DIMENSIONS OF AREA DIGITIZED
C           IGRCON = GRID UNIT IDENTIFER. 1 = FEET. 2 = MILES. 3 = METRES.
C           LIMNPT = MAX. NUMBER OF RAY COMPUTATION POINTS. (I5).
C           NPRINT = FREQUENCY OF PRINTED OUTPUT FOR EACH RAY. (I5).
C           GRID    = NUMBER OF GRID UNITS PER GRID DIVISION. (F10.5)
C                     NOW FIGURED IN PROGRAM
C           DCON    = MULTIPLIER TO CONVERT DEPTH UNITS TO FEET. (F10.5).
C           DELTAS = MINIMUM STEP LENGTH ALONG RAY IN SHALLOW WATER. (F10.
C           GRINC   = STEP LENGTH ALONG RAY IN DEEP WATER. (F10.5).
C           FMT     = FORMAT FOR DEPTH DATA. (EG. (10F8.3)). (2A6).
C            IOPT    = 1,IF PRINT OF DEPTH ARRAY IS WANTED
C                      0,OTHERWISE
C    ...   CONDITIONS FOR MARK II. MI .GE. MJ AND LIMNPT .GE. 500.
          REAL*8 IFEET,IMILES,IMETRE,IGCON
          COMMON    IPT(200),  D(12),E(6),B1,B2,CO,CXY,DCDH,DCON,DELTAS,DRC,
         .DTGR,DXY,GRINC,HO,IGO,JGO,LIMNPT,NPRINT,NPT,PHX,PHY,RCCO,RHS,RK,
         .SIG,SK,TOP,V,WL,WLO,THETA(200),ET(200),EL(200),STEEP(200),CG(200),
         . PL(200),P(200),IDIR(200),WX(200),WY(200),FACTOR,IWRT,DTHETA(200)
          COMMON/COMPLT/XPLT(500),YPLT(500),SCAFAC
          COMMON /NEWH/ SKPREV,RKPREV,HPREV,DS,HNEW,T
          COMMON /RAYNUM/ NORAY
          DIMENSION TITL(18),FMT(18), DATA(1024)
       51 FORMAT(2F10.2,3I5,3F10.5,F5.0,I5)
          COMMON /KOUNT/ DEPCNT
          DIMENSION DEP(10000)
       52 FORMAT(18A4)
       56 FORMAT(I5)
       58 FORMAT(I5, 2F10.2)
       59 FORMAT(3F6.2)
       60 FORMAT(1H1,41HWAVE REFRACTION BY METHOD OF R.S. DOBSON,//51H CIVIL
         .ENGINEERING DEPARTMENT, STANFORD UNIVERSITY.///)
       61 FORMAT(1H1,18A4/8H SET NO.,I3,10H, PERIOD =,F7.2,7H SECS.,,8H RAY
         1NO.,I3,13H, TIME STEP =,F8.4,6HSECS.//1H ,5HPOINT,5X,1HX,8X,1HY,
         2 6X,5HANGLE,5X,5HDEPTH,3X,7HMAX DIF,4X,3HFIT,5X,6HLENGTH,4X,5HSPEE
         3D,5X,6HHEIGHT,5X,2HKR,8X,2HKS,4X,4HNEWH//1H ,I5,3F9.1,28X,3F9.2)
       62 FORMAT(39H0 ALL SETS COMPLETED,  NUMBER OF SETS =,I4)
       63 FORMAT(1H0,5X,21HPROGRAMME PARAMETERS.//25H  GRID LIMITS, ABSCISSA
         . =,I4,12H, ORDINATE =,I4,1H./27H  PRINTED OUTPUT INTERVAL =,I4,8H
         .POINTS./19H  GRID SIZE, UNIT =,F7.3,1X,A6,1H./31H  DEEP WATER INCR
         .EMENTAL STEP =,F7.3,12H GRID UNITS./49H  DEPTH CONVERSION, DEP(I,J
         .) TO FEET, MULTIPLY BY,F6.3)
       64 FORMAT(1H0,45HPROGRAMME STOPPED, MI OR MJ GREATER THAN 100.)
       65 FORMAT(1H0,62HPROGRAMME STOPPED, MI LESS THAN MJ OR LIMNPT GREATER
         . THAN 500.)
          DATA IFEET,IMILES,IMETRE/4HFEET,5HMILES,6HMETRES/
C    ...   READ BASIC DATA
          READ(5,51) XMAX,YMAX,IGRCON,LIMNPT,NPRINT,DCON,DELTAS,GRINC,
         1      DEPMAX,IOPT
          DEPCNT=DEPMAX-10.
          CALL GETDEP (DEP,M,N,GRID,XMAX,YMAX,IOPT)
          IWRT=1
          MI=M
          MJ=N
          RHS = MI
          RHS = RHS-1.5
          TOP = MJ
          TOP = TOP-1.5
          UNIT = GRID
          FACTOR=GRID
```

```
      GO TO (16,17,18), IGRCON
   16 IGCON  = IFEET
      GO TO 19
   17 GRID = GRID*6080.27
      IGCON  = IMILES
      GO TO 19
   18 GRID = GRID*3.281
      IGCON  = IMETRE
   19 CONTINUE
      WRITE(6,60)
      WRITE(6,63) MI,MJ,NPRINT,UNIT,IGCON, GRINC,DCON
      IF (MI .LT. MJ .OR. LIMNPT .GT. 500) GO TO 11
      XMI = MI-1
      YMJ = MJ-1
      SCAFAC = 10./YMJ
      XMI = XMI*SCAFAC
      NOX=AMAX1(11.0, XMI+1.5)
      XMI = XMI+6.
      CALL PLOTS(DATA(1), 1024)
C   ...   READ WAVE DATA
      READ(5,56) NOSETS
      DO 120 NOSET=1,NOSETS
      READ(5,52) TITL
      READ(5,58) NORAYS, T, HO
      DO 130 I=1,NOX
      XPLT(I) = I-1
  130 YPLT(I) = 0.
      CALL SYMBOL(0.21,0.,0.21,TITL,90.,55)
      CALL PLOT(1.,0.,-3)
      XPLT(NOX+1)=0.
      YPLT(NOX+1)=0.
      XPLT(NOX+2)=1.
      YPLT(NOX+2)=1.
      CALL LINE(XPLT,YPLT,NOX,1,-1, 3)
      XPLT(12)=0.
      YPLT(12)=0.
      XPLT(13)=1.
      YPLT(13)=1.
      CALL LINE(YPLT,XPLT,11,1,-1, 3)
      SIG = 6.28318531/T
      CO = 5.1204062*T
      WLO = CO*T
      DRC = WLO*0.6
      DTGR = GRINC/CO
      UNIT = DTGR*GRID
      DO 110 NORAY = 1,NORAYS

      READ(5,59) X1,Y1,A
      Y=Y1/FACTOR
      X=X1/FACTOR
      NPT = 1
      DS=GRINC
      CXY = CO
      WL = WLO
      HPREV=HO
      B1 = 1.
      B2 = 1.
      RK = 1.
      SK = 1.
      RKPREV=1.
      SKPREV=1.
      A1=450.-A
      IF (A1.GT.360.) A1=A1-360.
      WRITE(6,61) TITL,NOSET,T,NORAY,UNIT,NPT,X1,Y1,A1,WLO,CO,HO
      XPLT(1) = X*SCAFAC
      YPLT(1) = Y*SCAFAC
      CALL RAYCON(X,Y,A,DEP,M,N)
      NPT = NPT-1
      RAYNO = NORAY
      XRAYNO = XPLT(1)-0.1
      CALL NUMBER(XRAYNO,YPLT(1),0.14,RAYNO,0.,-1)
```

```
      XPLT(NPT+1)=0.
      YPLT(NPT+1)=0.
      XPLT(NPT+2)=1.
      YPLT(NPT+2)=1.
      CALL LINE(XPLT,YPLT,NPT,1,0,L)
  110 CONTINUE
      CALL PLOT(XMI,0.,-3)
  120 CONTINUE
      CALL PLOT (0.,0.,999)
      WRITE(6,62) NOSETS
      GO TO 12
   10 WRITE(6,64)
      GO TO 12
   11 WRITE(6,65)
   12 STOP
      END

      SUBROUTINE RAYCON(X,Y,A,DEP,M,N)
      COMMON    IPT(200),   D(12),E(6),B1,B2,C0,CXY,DCDH,DCON,DELTAS,DRC,
     .DTGR,DXY,GRINC,HO,IGO,JGO,LIMNPT,NPRINT,NPT,PHX,PHY,RCCO,RHS,RK,
     .SIG,SK,TOP,V,WL,WLO,THETA(200),ET(200),EL(200),STEEP(200),CG(200),
     . PL(200),P(200),IDIR(200),WX(200),WY(200),FACTOR,IWRT,DTHETA(200)
      COMMON/CUMA/XP,YP
      COMMON/COMPLT/XPLT(500),YPLT(500),SCAFAC
      COMMON /KCUNT/ DEPCNT
      DIMENSION DEP(M,N)
      REAL*8 C1,C2
      DATA C1,C2/0.0174532925,57.29577951/
    5 IND=0
      ISW=0
      ANG = A
      A = A*C1
      H = HO
      IGO = 1
      COSA = COS(A)
      SINA = SIN(A)
   10 PX = X
      PY = Y
  101 XX= COSA*GRINC+X
      YY= SINA*GRINC+Y
      CALL DEPTH (XX,YY,DEP,M,N)
      IF (NPT.NE.1) GO TO 500
  400 NWRITE = 1
      X=XX
      Y=YY
      IF (DXY .LE. 0.) GO TO 22
      IF (DXY .LT. DRC) GO TO 11
      NPT = NPT+1
      XPLT(NPT) = X*SCAFAC
      YPLT(NPT) = Y*SCAFAC
      CALL FRICTN
      CALL ENERGY (A,H)
      CALL WRITER (X,Y,ANG,H,NWRITE,IND)
      GO TO (10,11,23), IGO
   11 X = PX
      Y = PY
      CALL CURVE(X,Y,A,FK,DEP,M,N)
   12 NPT = NPT+1
      NWRITE = 1
      CALL REFRAC(X,Y,A,FK,INDEX,DEP,M,N)
      GO TO (19,20,21,22,25), INDEX
   20 NWRITE = 2
      GO TO 19
   21 NWRITE = 3
      GO TO 19
   22 NWRITE = 4
      GO TO 13
   25 NWRITE = 7
   19 CALL HEIGHT(XP,YP,A,H)
      XPLT(NPT) = X*SCAFAC
      YPLT(NPT) = Y*SCAFAC
```

```
      IF (NPT .GT. LIMNPT) NWRITE = 6                                   168
      IF (X .GE. RHS .OR. X .LE. 1.5) NWRITE = 5                        169
      IF (Y .GE. TOP .OR. Y .LE. 1.5) NWRITE = 5                        170
      IF (NWRITE .GT. 1) GO TO 13                                       171


      IF (NPT/NPRINT*NPRINT-NPT .NE. 0) GO TO 14                        172
   13 ANG = A*C2                                                        173
      CALL ENERGY (A,H)
      CALL WRITER (X,Y,ANG,H,NWRITE,IND)
   14 GO TO (10,12,23), IGO                                             175
   23 RETURN                                                            176
  500 TEST=ABS(DXY-DEPCNT)
      IF (TEST.LE.1.0) GO TO 510
      IF (ISW.EQ.1) GO TO 505
      IF (DXY.LT.DEPCNT) GO TO 505
  502 DXYSV=DXY
      GRSV=GRINC
      GRINC=GRINC*2.
      GO TO 101
  505 IF (DXY-DXYSV.EQ.0.) GO TO 502
      ISW=1
      SLOP=(DXY-DXYSV)/(GRINC-GRSV)
      DXYSV=DXY
      GRSV=GRINC
      GRINC=GRINC + (DEPCNT-DXY)/SLOP
      GO TO 101
  510 IF (DXY.LT.DRC) GO TO 400
      IF (DEPCNT.LE.10.) DEPCNT=DEPCNT-1.
      IF (DEPCNT.GE.20.) DEPCNT=DEPCNT-10.
      DXYSV=DXY
      GRSV=0
      GO TO 400
      END


      SUBROUTINE REFRAC(X,Y,A,FK,INDEX,DEP,M,N)
      COMMON   IPT(200),  D(12),E(6),B1,B2,CO,CXY,DCOH,DCON,DELTAS,DRC,      21
     .DTGR,DXY,GRINC,HO,IGO,JGO,LIMNPT,NPRINT,NPT,PHX,PHY,RCCO,RHS,RK,     181
     .SIG,SK,TOP,V,WL,WLO,THETA(200),ET(200),EL(200),STEEP(200),CG(200),
     . PL(200),P(200),IDIR(200),WX(200),WY(200),FACTOR,IWRT,DTHETA(200)
      COMMON /NEWH/ SKPREV,RKPREV,HPREV,DS,HNEW,T
      COMMON /KOUNT/ DEPCNT
      DIMENSION DEP(M,N)
      NCUR = 1                                                          183
      ITS=0
      ISWOK=0
      ISW=0
    5 GO TO (11,12,10), IGO
   11 FKM = FK                                                          185
      IGO = 2                                                           186
   12 DS = CXY*DTGR                                                     187
      IF (DS.GE.DELTAS) GO TO 14
      INDEX=5
      RETURN
   14 RESMAX = 0.00005/DS                                               189
   13 DO 110 I=1,20                                                     190
      DELA = FKM*DS                                                     191
      AA = A+DELA                                                       192
      AM = DELA*0.5+A                                                   193
      XX = COS(AM)*DS+X                                                 194
      YY = SIN(AM)*DS+Y                                                 195
      CALL CURVE(XX,YY,AA,FKK,DEP,M,N)
      GO TO 500
  400 CALL CURV2(XX,YY,AA,FKK,DEP,M,N)
      IF (DXY.GT.0.) GO TO (111, 16), NCUR
      INDEX=4
      RETURN
  111 FKM = (FK+FKK)*0.5                                                199
      IF (I .EQ. 1) GO TO 110                                           200
      IF (RESMAX .GT. ABS(FKP-FKM)) GO TO 16                            201
      IF (I .EQ. 18) FKI8 = FKM                                         202
```

```
      110 FKP = FKM                                                         203
          IF (RESMAX .GT. ABS(FK18-FKM)) GO TO 15                           204
          INDEX=3
          RETURN
       15 FKM = (FKM+FK18)*0.5                                              206
          NCUR = 2                                                          207
          GO TO 13                                                          208
       16 X = XX                                                            209
          Y = YY                                                            210
          A = AA                                                            211
          FK = FKK                                                          212
          IF (NCUR-2) 10, 9, 10
        9 INDEX=2
          RETURN
       10 INDEX=1
          RETURN
      500 IF (ISWOK.EQ.1) GO TO 400
          TEST=ABS(DXY-DEPCNT)
          ITS=ITS+1
          IF (TEST.LE..10) GO TO 510
          IF (ITS.GE.30) GO TO 510
          IF (ISW.EQ.1) GO TO 505


          IF (DXY.LT.DEPCNT) GO TO 505
      502 DXYSV=DXY
          DTSV=DTGR
          DTGR=DTGR*2.
          GO TO 5
      505 IF (DXYSV-DXY.EQ.0.) GO TO 502
          ISW=1
          SLOP=(DXY-DXYSV)/(DTGR-DTSV)
          DXYSV=DXY
          DTSV=DTGR
          DTGR=DTGR + (DEPCNT-DXY) / SLOP
          GO TO 5
      510 IF (DEPCNT.LE.10.)DEPCNT=DEPCNT-1.
          IF (DEPCNT.GE.20.) DEPCNT=DEPCNT-10.
          ISWOK=1
          DXYSV=DXY
          DTSV=0
          ITS=0
          GO TO 400
          END                                                               215



          SUBROUTINE CURVE(X,Y,A,FK,DEP,M,N)
          COMMON   IPT(200),  D(12),E(6),B1,B2,CO,CXY,DCDH,DCON,DELTAS,DRC,    21
         .DTGR,DXY,GRINC,HO,IGO,JGO,LIMNPT,NPRINT,NPT,PHX,PHY,RCCO,RHS,RK,    219
         .SIG,SK,TOP,V,WL,WLO,THETA(200),ET(200),EL(200),STEEP(200),CG(200),
         . PL(200),P(200),IDIR(200),WX(200),WY(200),FACTOR,IWRT,DTHETA(200)
          COMMON/COMA/XP,YP                                                 221
          COMMON /KOUNT/ DEPCNT
          DIMENSION DEP(M,N)
          GO TO (10,11), IGO                                                222
       11 CALL DEPTH(X,Y,DEP,M,N)
          RETURN
          ENTRY CURV2(X,Y,A,FK,DEP,M,N)
          IF (DXY*200. .GT. WL) GO TO 10                                    224
          IF (DXY .LE. 0.) RETURN                                           225
          JGO = 2                                                           226
          ARG = 32.1725*DXY                                                 227
          CXY = SQRT(ARG)                                                   228
          DCDH = 16.08625/CXY                                               229
          GO TO 14                                                          230
       10 CI = CXY                                                          231
          JGO = 1                                                           232
          DO 120 I=1,50                                                     233
          ARG = (DXY*SIG)/CI                                                234
          CXY = CO*TANH(ARC)                                                235
```

```
      RESID = CXY-CI
      IF (ABS(RESID) .LT. 0.001) GO TO 13
  120 CI = (CXY+CI)*0.5
   13 RCCO = CXY/CO
      SCMC = (1.-RCCO*RCCO)*SIG
      V = SCMC*DXY+RCCO*CXY
      DCDH = CXY*SCMC/V
   14 PHX = E(4)*2.*XP+E(5)*YP+E(2)
      PHY = E(6)*2.*YP+E(5)*XP+E(3)
      FK = (SIN(A)*PHX-COS(A)*PHY)*DCDH*DCON/CXY
      RETURN
      END
```

```
      SUBROUTINE DEPTH(X,Y,DEP,M,N)
      COMMON    IPT(200),   D(12),E(6),B1,B2,CO,CXY,DCDH,DCON,DELTAS,DRC,
     .DTGR,DXY,GRINC,HO,IGO,JGO,LIMNPT,NPRINT,NPT,PHX,PHY,RCCO,RHS,RK,
     .SIG,SK,TOP,V,WL,WLO,THETA(200),ET(200),EL(200),STEEP(200),CG(200),
     . PL(200),P(200),IDIR(200),WX(200),WY(200),FACTOR,IWRT,DTHETA(200)
      COMMON/COMA/XP,YP
      DIMENSION DEP(M,N)
      DIMENSION SXY(12,6)
      DATA SXY                           /0.30861241,0.23684207,0.21770331,
     .0.23684207,-0.08492823,2*-0.05143541,-0.08492823,0.00598086,2*0.13
     .038277,0.00598086,0.05322964,0.19677030,0.14413872,0.10586122,0.09
     .031100,-0.06758374,-0.03349283,0.03349282,-0.18241626,-0.34031099,
     .-0.12440190,0.12440190,0.05322964,0.10586122,0.14413872,0.19677030
     .,0.03349282,-0.03349283,-0.06758374,0.09031099,0.12440190,-0.12440
     .191,-0.34031099,-0.18241625,4*-0.12499998,2*0.125,2*0.,2*0.1249999
     .9,2*-0.,0.05263157,-0.05263157,0.05263158,-0.05263157,-0.15789473,
     .2*0.15789474,2*-0.15789473,2*0.15789473,-0.15789473,4*-0.12499998,
     .2*0.,2*0.125,2*-0.,2*0.12499999/
      I = X+1.
      J = Y+1.
      XP = AMOD(X,1.)
      YP = AMOD(Y,1.)
      IF (NPT .EQ. 1) GO TO 11
      IF (IP .NE. I) GO TO 11
      IF (JP .EQ. J) GO TO 14
   11 IP = I
      JP = J
      D(1) = DEP(I,J)
      D(2) = DEP(I+1,J)
      D(3) = DEP(I+1,J+1)
      D(4) = DEP(I,J+1)
      D(5) = DEP(I+2,J)
      D(6) = DEP(I+2,J+1)
      D(7) = DEP(I+1,J+2)
      D(8) = DEP(I,J+2)
      D(9) = DEP(I-1,J+1)
      D(10) = DEP(I-1,J)
      D(11) = DEP(I,J-1)
      D(12) = DEP(I+1,J-1)
      DO 110 K=1,6
      E(K) = 0.
      DO 110 L=1,12
  110 E(K) = E(K)+D(L)*SXY(L,K)
   14 DXY = (E(1)+E(2)*XP+E(3)*YP+E(4)*XP*XP+E(5)*XP*YP+E(6)*YP*YP)*DCON
      RETURN
      END
```

```
      SUBROUTINE HEIGHT(X,Y,A,H)
      COMMON    IPT(200),   D(12),E(6),B1,B2,CO,CXY,DCDH,DCON,DELTAS,DRC,
     .DTGR,DXY,GRINC,HO,IGO,JGO,LIMNPT,NPRINT,NPT,PHX,PHY,RCCO,RHS,RK,
     .SIG,SK,TOP,V,WL,WLO,THETA(200),ET(200),EL(200),STEEP(200),
     .DM1(200), PL(200),DM2(200),IDIR(200),WX(200),WY(200),FACTOR,IWRT,
     . DTHETA(200)
      COMMON /NEWH/ SKPREV,RKPREV,HPREV,DS,HNEW,T
      SKPREV=SK
      RKPREV=RK
```

```
      WL = WLO*RCCO
      GN = 12.56637066144*DXY/WL
      CG = (1.+GN/SINH(GN))*CXY
      SK = SQRT(CO/CG)
      IF (CG .LT. 0.) RETURN
      RK = ABS(1./B2)
      RK = SQRT(RK)
      H = HO*SK*RK
      GO TO (11,12), JGO
   11 U = -2.*SIG*RCCO*CXY/(V*V)
      GO TO 10
   12 U = -0.5/DXY
   10 U = U*DCON
      DCDH = DCDH*DCON
      COSA = COS(A)
      SINA = SIN(A)
      P = -(COSA*PHX+SINA*PHY)*DCDH*DTGR*2.
      Q = ((E(4)*2.+U*PHX*PHX)*SINA*SINA-(E(5)+U*PHX*PHY)*2.*SINA*COSA
     .     +(E(6)*2.+U*PHY*PHY)*COSA*COSA)*DCDH*CXY*DTGR*DTGR*2.
      B3 = ((P-2.)*B1+(4.-Q)*B2)/(P+2.)
      B1 = B2
      B2 = B3
      WRITE (6,1000) SINA,COSA,PHX,PHY,DCDH,DTGR,P,E(4)
      WRITE (6,1000) U,E(5),E(6),CXY,Q,B3,B1,B2
 1000 FORMAT (1X,8E14.6)
      CALL FRICTN
      RETURN
      END


      SUBROUTINE ERROR(FIT,DIFMAX)
      COMMON    IPT(200),  D(12),E(6),B1,B2,CO,CXY,DCDH,DCON,DELTAS,DRC,
     .DTGR,DXY,GRINC,HO,IGO,JGO,LIMNPT,NPRINT,NPT,PHX,PHY,RCCO,RHS,RK,
     .SIG,SK,TOP,V,WL,WLO,THETA(200),ET(200),EL(200),STEEP(200),CG(200),
     . PL(200),P(200),IDIR(200),WX(200),WY(200),FACTOR,IWRT,DTHETA(200)
      DIMENSION DP(4)
      IF (NPT .LT. 3) GO TO 11
      IF (EP .EQ. E(5)) GO TO 12
   11 DP(1) = E(1)
      DP(2) = E(1)+E(2)+E(4)
      DP(3) = E(1)+E(2)+E(3)+E(4)+E(5)+E(6)
      DP(4) = E(1)+E(3)+E(6)
      DIFMAY = 0.
      SUM = 0.
      DO 110 I=1,4
      DIF = ABS(D(I)-DP(I))
      DIFMAY = AMAX1(DIF,DIFMAY)
  110 SUM = DIF*DIF+SUM
      DIFMAY = DIFMAY*DCON
      SUM = SUM*0.33333333
      FIT = SQRT(SUM)
      EP = E(5)
   12 DIFMAX = DIFMAY/DXY*100.
      RETURN
      END


      SUBROUTINE WRITER (X1,Y1,ANG,H,NWRITE,IND)
      COMMON    IPT(200),  D(12),E(6),B1,B2,CO,CXY,DCDH,DCON,DELTAS,DRC,
     .DTGR,DXY,GRINC,HO,IGO,JGO,LIMNPT,NPRINT,NPT,PHX,PHY,RCCO,RHS,RK,
     .SIG,SK,TOP,V,WL,WLO,THETA(200),ET(200),EL(200),STEEP(200),CG(200),
     . PL(200),P(200),IDIR(200),WX(200),WY(200),FACTOR,IWRT,DTHETA(200)
      COMMON /NEWH/ SKPREV,RKPREV,HPREV,DS,HNEW,T
      CALL ERROR(FIT,DIFMAX)
      A  =450. - ANG
      IF (A  .GT.360.) A  =A  -360.
```

```
      X=X1 * FACTOR - FACTOR
      Y=Y1 * FACTOR - FACTOR
      IF (IND.EQ.1) GO TO 10
      WX(IWRT)=X
      WY(IWRT)=Y
      IPT(IWRT)=NPT
      IWRT=IWRT + 1
   10 WRITE (6,62) NPT,X,Y,A   ,DXY,DIFMAX,FIT,WL,CXY,H,RK,SK,HNEW
   62 FORMAT (1H ,I5,3F9.1,F11.2,F8.2,4F9.2,2F10.4,F9.2)
      GO TO (11,20,21,22,23,24,25), NWRITE
   20 WRITE(6,61) NPT
   61 FORMAT(29H  CURVATURE AVERAGED AT POINT, I4)
      GO TO 11
   21 WRITE(6,63)
      CALL WRITE2
      WRITE(6,63)
   63 FORMAT(1H ,42HRAY STOPPED, NO CONVERGENCE FOR CURVATURE.)
      GO TO 12
   22 WRITE(6,64) X,Y
      CALL WRITE2
      WRITE(6,64) X,Y
   64 FORMAT(1H ,32HRAY STOPPED, REACHED SHORE.  X =,F7.2,6H,  Y =,F7.2)
      GO TO 12
   23 WRITE(6,65) X,Y
      CALL WRITE2
      WRITE(6,65) X,Y
   65 FORMAT(1H ,35HRAY STOPPED, REACHED BOUNDARY.  X =,F7.2,6H,  Y =,
     .F7.2)
      GO TO 12
   24 WRITE(6,66) LIMNPT,X,Y
      CALL WRITE2
      WRITE(6,66) LIMNPT,X,Y
   66 FORMAT(1H ,55HRAY STOPPED, NUMBER OF POINTS EXCEEDS MAXIMUM.  LIMI
     .T =,I4,13H POINTS.  X =,F7.2,6H,  Y =,F7.2)
      GO TO 12
   25 WRITE(6,67) DELTAS,X,Y
      CALL WRITE2
      WRITE(6,67) DELTAS,X,Y
   67 FORMAT(1H ,51HRAY STOPPED, INCREMENT DISTANCE ALONG RAY LESS THAN,
     .F6.3,17H GRID UNITS.  X =,F7.2,6H,  Y =,F7.2)
   12 IGO = 3
   11 RETURN
      END

      SUBROUTINE GETDEP(DEP,M,N,GRID,XMAX,YMAX,IOPT)
      COMMON   IPT(200),  D(12),E(6),B1,B2,CO,CXY,DCDH,DCON,DELTAS,DRC,
     .DTGR,DXY,GRINC,HO,IGO,JGO,LIMNPT,NPRINT,NPT,PHX,PHY,RCCO,RHS,RK,
     .SIG,SK,TOP,V,WL,WLO,THETA(200),ET(200),EL(200),STEEP(200),CG(200),
     . PL(200),P(200),IDIR(200),WX(200),WY(200),FACTOR,IWRT,DTHETA(200)
      COMMON /NEW/ NTIT(18),NEWCON,XLIM
      DIMENSION NDATA(251),COORDS(251)
      DIMENSION IA(4)
      DIMENSION DEP(10000)
      DATA IWDBK /4H    /
      EQUIVALENCE(COORDS(1), NDATA(1))
      NEWCON=1
C
C     **  READ TAPE FROM DIGITIZER (TAPE IS BINARY)
C
      READ (1)  ICODE, NWORDS, (NDATA(I),I=1,NWORDS)
C
C     **  ICODE=0 RECORD IS ID, SCALING, OR COMMENT
C         ICODE=1 RECORD IS X AND Y COORDINATES FROM CONTOUR MAP
C         NWORDS = NUMBER OF WORDS IN RECORD
      IF (NWORDS.GT.18) NWORDS=18
      DO 10 I=1,NWORDS
   10 NTIT(I)=NDATA(I)
      IF (NWORDS.EQ.18) GO TO 15
      DO 12 I=NWORDS,18
   12 NTIT(I)=IWDBK
C
```

```
C      **  FILL DEP ARRAY WITH 1.E20 **
C
    15 DO 20 I=1,10000
    20 DEP(I)=1.E20
C
C      **  COMPUTE SIZE OF GRID  **
C      **  GRID IS SIZE OF GRID INTERVAL
C      **  M IS NO. OF COLUMNS  **
C      **  M IS NO. OF ROWS  **
       GRID =SQRT(XMAX*YMAX/10000.)
       XM=XMAX/GRID
       M=XM
       YN=YMAX/GRID
       N=YN
C      **  FIRST TIME SWITCH  **
       ISW=1
    30 READ(1,END=50) ICODE,NWORDS,(NDATA(I),I=1,NWORDS)
       IF (ISW.EQ.0) GO TO 35
C
       IF (ICODE.NE.0) GO TO 30
       ISW=0
    35 IF (ICODE.NE.0) GO TO 40
C
C      **  UNPACK DEPTH IN COMMENT FROM DIGITIZER TAPE  **
C
       CALL UNPACK (NDATA,  IA   )
C
       CALL CONVRT (IA,DEPTH)
C
       GO TO 30
C


    40 CALL BLDDEP (DEP,M,N,NWORDS,COORDS,DEPTH,GRID)
       GO TO 30
C
    50 CONTINUE
       CALL PLOT (XLIM+1.,0.,-3)
       IF (IOPT.EQ.1) CALL WRTDEP (DEP,M,N)
       CALL INTERP(DEP,M,N)
       IF (IOPT.EQ.1) CALL WRTDEP (DEP,M,N)
C
C
       RETURN
       END



       SUBROUTINE INTERP (D,IX,IY)
C      **  THIS SUBROUTINE DOES 3-DIMENSIONAL INTERPOLATION  **
C      **  D = DOUBLE SUBSCRIPTED ARRAY OF FUNCTIONAL VALUES
C              MUST BE PADDED WITH NO.'S LARGER THAN 1.E20
C          IX = NO. OF COLUMNS IN ARRAY
C          IY = NO.OF ROWS IN ARRAY
C
       COMMON /KOUNT/ DEPCNT
       DIMENSION D(IX,IY)
       LOGICAL NO1,NO2,NO3,NO4
       DO 300 J=1,IY
       DO 300 I=1,IX
C      **  IS FUNCTIONAL VALUE AT I,J KNOWN  **
       IF (D(I,J).LT.1.E20) GO TO 300
C      **  SEARCH FOR KNOWN VALUES ON EACH SIDE OF VALUE WANTED  **
C      **  SEARCH IN NEGATIVE X DIRECTION  **
       N=I-1
       IF (N.LT.1) GO TO 20
       DO 10 K=1,N
       NX1=I-K
       ID1=D(NX1,J)/10
       D1=ID1*10
       IF (D1.EQ.D(NX1,J)) GO TO 30
    10 CONTINUE
```

```
   20 NX1=0
C     **  SEARCH IN POSITIVE X DIRECTION
   30 N=I+1
      IF (N.GT.IX) GO TO 50
      DO 40 K=N,IX
      NX2=K
      IF (D(NX2,J).LT.1.E20) GO TO 90
   40 CONTINUE
   50 NX2=0
C     **  INTERPOLATION IN X DIRECTION  **
C     **  SEARCH IN NEGATIVE Y DIRECTION  **
   90 N=J-1
      IF (N.LT.1) GO TO 110
      DO 100 K=1,N
      NX3=J-K
      ID1=D(I,NX3)/10
      D1=ID1*10
      IF (D1.EQ.D(I,NX3)) GO TO 120
  100 CONTINUE
  110 NX3=0
C  **  SEARCH IN POSITIVE Y DIRECTION
  120 N=J+1
      IF (N.GT.IY) GO TO 140
      DO 130 K=N,IY
      NX4=K
      IF (D(I,NX4).LT.1.E20) GO TO 150
  130 CONTINUE
  140 NX4=0
C     **  INTERPOLATION IN Y DIRECTION  **
  150 IF(NX1.EQ.0.AND.NX2.EQ.0.AND.NX3.EQ.0.AND.NX4.EQ.0) GO TO 300
      IF (NX1.EQ.0.AND.NX2.EQ.0) GO TO 180
      IF (NX3.EQ.0.AND.NX4.EQ.0) GO TO 170
      IF (NX1.EQ.0.OR.NX2.EQ.0.OR.NX3.EQ.0.OR.NX4.EQ.0) GO TO 190
      NXDIS=NX2-NX1


      NYDIS=NX4-NX3
      IF (NXDIS.LE.NYDIS) GO TO 155
      D(I,J)=D(I,J-1) + (D(I,NX4)-D(I,NX3))/(NX4-NX3)
      GO TO 200
  155 D(I,J)=D(I-1,J)+(D(NX2,J)- D(NX1,J))/(NX2-NX1)
      GO TO 200
  170 IF (NX1.EQ.0) GO TO 210
      IF (NX2.EQ.0) GO TO 220
      D(I,J)=D(I-1,J) + (D(NX2,J)-D(NX1,J))/(NX2-NX1)
      GO TO 200
  180 IF (NX3.EQ.0) GO TO 230
      IF (NX4.EQ.0) GO TO 240
      D(I,J)=D(I,J-1)  +  (D(I,NX4)  -  D(I,NX3))/ (NX4-NX3)
      GO TO 200
  190 NO1=.FALSE.
      NO2=.FALSE.
      NO3=.FALSE.
      NO4=.FALSE.
      IF (NX1.NE.0) NO1=.TRUE.
      IF (NX2.NE.0) NO2=.TRUE.
      IF (NX3.NE.0) NO3=.TRUE.
      IF (NX4.NE.0) NO4=.TRUE.
C     IF TWO VALUES FOUND IN SAME DIRECTION,INTERPOLATE ALONG THAT AXIS
      IF (NO1.AND.NO2) GO TO 155
      IF (NO3.AND.NO4) GO TO 180
C     IF TWO VALUES FOUND, NOT IN SAME DIREDTION, CHOSE VALUE CLOSEST
C     TO SURROUNDING VALUES
      IF (NO1.AND.NO3) GO TO 250
      IF (NO1.AND.NO4) GO TO 260
      IF (NO2.AND.NO3) GO TO 270
      IF(NO2.AND.NO4) GO TO 280
C     IF ONLY ONE VALUE FOUND USE IT
      IF (NO1) D(I,J)=D(NX1,J)
      IF (NO2) D(I,J)=D(NX2,J)
      IF (NO3) D(I,J)=D(I,NX3)
      IF (NO4) D(I,J)=D(I,NX4)
```

```
  200 IDI=D(I,J)/10
      DI=IDI*10
      IF(DI.EQ.D(I,J))D(I,J)=D(I,J)-.001
  300 CONTINUE
      DO 400J=1,IY
      DO 400 I=1,IX
      IF (D(I,J).GE.1.E20)  D(I,J)=DEPCNT+10.
  400 CONTINUE
      RETURN
  210 D(I,J)=D(NX2,J)
      GO TO 200
  220 D(I,J)=D(NX1,J)
      GO TO 200
  230 D(I,J)=D(I,NX4)
      GO TO 200
  240 D(I,J)=D(I,NX3)
      GO TO 200
  250 CALL CLOSE (NX1,NX3,D,IX,IY,I,J)
      GO TO 200
  260 CALL CLOSE (NX1,NX4,D,IX,IY,I,J)
      GO TO 200
  270 CALL CLOSE (NX2,NX3,D,IX,IY,I,J)

      GO TO 200
  280 CALL CLOSE (NX2,NX4,D,IX,IY,I,J)
      GO TO 200
 1001 FORMAT (1H ,4I5,E14.7)
      END
```

```
      SUBROUTINE CLOSE (I1,J1,D,M,N,I,J)
      DIMENSION D(M,N)
      IF (D(I1,J).NE.D(I,J1))GO TO 10
      D(I,J)=D(I1,J)
      RETURN
   10 IF (J-1.LE.0) GO TO 50
      VAL1=D(I1,J)-D(I,J-1)
      VAL2=D(I,J1)-D(I,J-1)
   30 IF (ABS(VAL1).GT.ABS(VAL2)) GO TO 40
      D(I,J)=D(I1,J)
      RETURN
   40 D(I,J)=D(I,J1)
      RETURN
   50 VAL1=D(I1,J)-D(I-1,J)
      VAL2=D(I,J1)-D(I-1,J)
      GO TO 30
      END
```

```
      SUBROUTINE BLDDEP (DEP,M,N,NWORDS,COORDS,DEPTH,GRID)
      DIMENSION COORDS(NWORDS), DEP(M,N)
    1 CONTINUE
      LIMIT=NWORDS-1
      DO 10 I=1,LIMIT,2
      IY=COORDS(I+1)/GRID+1
      IX=COORDS(I)/GRID+1
      YY=COORDS(I+1)/GRID+1
      XX=COORDS(I)/GRID+1
      CALL PLTCON (DEP,M,N,XX,YY)
      IF (IX.GT.M.OR.IY.GT.N) GO TO 50
   10 DEP(IX,IY)=DEPTH
      RETURN
   50 WRITE (6,100) IY,COORDS(I+1)
      WRITE (6,100) IX,COORDS(I)
  100 FORMAT (1H ,I5,E14.7)
      GO TO 10
      END
```

```
      SUBROUTINE UNPACK (IALPH,  ISEP  )
C
C     **  THIS SUBROUTIN UNPACKS ALPHA INFORMATION, PUTTING EADH CHARACTER
C     **  IN A WORD BY ITSELF  **
C
      M=4
      DIMENSION ISEP(4)
      REWIND 2
      WRITE (2,101 )  IALPH
      REWIND 2
      READ (2,102 ) (ISEP(I),I=1,M)
      RETURN
  101 FORMAT (A4)
  102 FORMAT (4A1)
      END
```

```
      SUBROUTINE CONVRT (IA,DEPTH)
      DIMENSION IA(4),INT(4)
      DATA IAMP /1H&/
      DATA MINUS /1H-/
      DATA IBLNK/1H /
      DATA MT24/Z1000000/
      DO 10 I=1,4
      J=4-I+1
      IF (IA(J).NE.IBLNK) GO TO 20
   10 CONTINUE
   20 IF (IA(1).EQ.MINUS) ISGN=1
      IF (IA(1).NE.MINUS) ISGN=-1
      IF (IA(1).EQ.IAMP) GO TO 65
      DO 40 I=1,J
      K=J-I+1
      IF (IA(K).EQ.MINUS) GO TO 25
      INT(I)=IA(K)/MT24
      IF (INT(I).LT.0) GO TO 30
      IGO=INT(I)/10
      INT(I)=INT(I)-IGO*10+8
      GO TO 40
   25 INT(4)=0
      GO TO 60
   30 INT(I)=INT(I)+127
      INT(I)=INT(I)-112
   40 CONTINUE
      IF (J.EQ.4) GO TO 50
      L=J+1
      DO 50 I=L,4
   50 INT(I)=0
   60 LAST=ISGN*(INT(1) + INT(2)*10 + INT(3)*100 + INT(4)*1000)
      DEPTH=LAST
      RETURN
   65 LAST=100
      DEPTH=LAST
      RETURN
      END
```

```
      SUBROUTINE WRTDEP(DEP,M,N)
      COMMON /NEW/ NTIT(18)
      DIMENSION DEP(M,N)
      NSAVC=1
      NSAVR=1
   10 NROW=NSAVR
      NROWS=NROW+9
      IF (NROW.GT.M) RETURN
      IF (NROWS.GT.M) NROWS=M
   20 NCOL=NSAVC
      NCOLS=NCOL+49
      IF (NCOL.GT.N) GO TO 40
      IF (NCOLS.GT.N) NCOLS=N
      WRITE (6,900) (NTIT(I),I=1,18)
      WRITE (6,1000) (I,I=NROW,NROWS)
      DO 30 J=NCOL,NCOLS
      WRITE (6,1001) J,(DEP (I,J),I=NROW,NROWS)
   30 CONTINUE
      NSAVC=NCOLS+1
      GO TO 20
   40 NSAVC=1
      NSAVR=NROWS+1
      GO TO 10
  900 FORMAT (1H1,18A4)
 1000 FORMAT (1H0,8X,10(5H COL ,I3,4X), 4X)
 1001 FORMAT (5H ROW ,I3,10F12.4,4X)
      END
```

```
      SUBROUTINE WRITE2
      COMMON    IPT(200),  D(12),E(6),B1,B2,CO,CXY,DCDH,DCON,DELTAS,DRC,     21
     .DTGR,DXY,GRINC,HO,IGO,JGO,LIMNPT,NPRINT,NPT,PHX,PHY,RCCO,RHS,RK,       22
     .SIG,SK,TOP,V,WL,WLO,THETA(200),ET(200),EL(200),STEEP(200),CG(200),
     . PL(200),P(200),IDIR(200),WX(200),WY(200),FACTOR,IWRT,DTHETA(200)
      COMMON /RAYNUM/ NORAY
      WRITE (6,100)
  100 FORMAT (1H1,5HPOINT,5X,1HX,8X,1HY,5X,4HIDIR,3X,5HTHETA,3X,
     1 6HDTHETA,9X,2HET,12X,2HEL,9X,5HSTEEP,12X,2HCG,12X,2HPL,13X,1HP//
     2 )
      K=IWRT-1
      DO 10 I=1,K
   10 WRITE (6,101) IPT(I),WX(I),WY(I),IDIR(I),THETA(I),DTHETA(I),
     1 ET(I),EL(I),STEEP(I),CG(I),PL(I),P(I)
      IF (NORAY.EQ.1) GO TO 20
      PDIF=PPREV-P(K-1)
      PLDIF=PLPREV - PL(K-1)
      DIS=SQRT ((XPREV-WX(K-1))**2 + (YPREV - WY(K-1))**2)
      PG=PDIF/DIS
      PLG=PLDIF/DIS
      WRITE (6,102) PG,PLG,DIS
  102 FORMAT (1H0,17HPOWER GRADIENT = ,E15.6,28H LONGSHORE POWER GRADIEN
     1T = ,F15.6,7H DIS = ,E15.6)
   20 PPREV=P(K-1)
      PLPREV=PL(K-1)
      XPREV=WX(K-1)
      YPREV=WY(K-1)
  101 FORMAT (1H ,I5,2F9.1,A4,2F10.3,6E14.5)
      IWRT=1
      RETURN
      END
```

```
      SUBROUTINE FRICTN
      COMMON    IPT(200),  D(12),E(6),B1,B2,CO,CXY,DCDH,DCON,DELTAS,DRC,     21
     .DTGR,DXY,GRINC,HO,IGO,JGO,LIMNPT,NPRINT,NPT,PHX,PHY,RCCO,RHS,RK,       22
     .SIG,SK,TOP,V,WL,WLO,THETA(200),ET(200),EL(200),STEEP(200),CG(200),
     . PL(200),P(200),IDIR(200),WX(200),WY(200),FACTOR,IWRT,DTHETA(200)
      COMMON /NEWH/ SKPREV,RKPREV,HPREV,DS,HNEW,T
```

```
      DX=DS * FACTOR * 5280.
      OH=HPREV *(SK / SKPREV)*(RK / RKPREV)
      ARG=6.2830 * DXY / WL
      PHI=.6391 * ((SK / SINH(ARG))   **3)
      HNEW=OH    / ((.02 * OH     * PHI * DX) / (SK * T**4) + 1.)
      HPREV=HNEW
      RETURN
      END
```

```
      SUBROUTINE PLTCON (DEP,M,N,XX,YY)
      DATA IND /0/
      COMMON /NEW/ NTIT(18),NEWCON,XLIM
      COMMON /COMPLT/ XPLT(500),YPLT(500),SCAFAC
      DIMENSION DATA (1024), DEP(M,N)
      IF (IND.EQ.1) GO TO 200
  100 IND=1
      NEWCON=1
      XLIM=M-1
      YLIM=N-1
      SCAFAC = 10./YLIM
       XLIM=XLIM * SCAFAC
      NOX=AMAX1 (11.0,XLIM+1.5)
      XLIM=XLIM + 6.
      CALL PLOTS (DATA(1),1024)
      DO 10 I=1,NOX
      XPLT(I)=I-1
   10 YPLT(I)=0.
      CALL SYMBOL (0.21,0.,0.21,NTIT,90.,55)
      CALL PLOT (1.,0.,-3)
      XPLT(NOX+1)=0.
      YPLT(NOX+1)=0.
      XPLT(NOX+2)=1.
      YPLT (NOX+2)=1.
      CALL LINE (XPLT,YPLT,NOX,1,-1,3)
      XPLT(12)=0.
      YPLT(12)=0.
      XPLT(13)=1.
      YPLT(13)=1.
      CALL LINE (YPLT,XPLT,11,1,-1,3)
  200 IF (NEWCON.EQ.1) GO TO 210
      IC=+2
  205 X=XX * SCAFAC
      Y=YY * SCAFAC
      CALL PLOT (X,Y,IC)
      RETURN
  210 IC=+3
      NEWCON=0
      GO TO 205
      END
```

```
      SUBROUTINE ENERGY (A,H)
      COMMON    IPT(200),   D(12),E(6),B1,B2,CO,CXY,DCDH,DCON,DELTAS,DRC,      21
     .DTGR,DXY,GRINC,HO,IGO,JGO,LIMNPT,NPRINT,NPT,PHX,PHY,RCCO,RHS,RK,         22
     .SIG,SK,TOP,V,WL,WLO,THETA(200),ET(200),EL(200),STEEP(200),CG(200),
     . PL(200),P(200),IDIR(200),WX(200),WY(200),FACTOR,IWRT,DTHETA(200)
      COMMON /NEWH/ SKPREV,RKPREV,HPREV,DS,HNEW,T
      DATA IRIGHT /4H   R/
      DATA LEFT /4H   L/
      IF (PHY.EQ.0.) GO TO 20
      THETA(IWRT)=  ATAN (PHX/PHY) + 3.14159265/2.
   10 DTHETA(IWRT)=THETA(IWRT) - A
      IF (DTHETA(IWRT).LT.C.0) IDIR(IWRT)=LEFT
      IF (DTHETA(IWRT).GT.C.0) IDIR(IWRT)=IRIGHT
      DX=DS*FACTOR*5280.
      ET(IWRT)=8. * HNEW * HNEW * WL
```

```
      ATHETA=DTHETA(IWRT)
      ATHETA=ABS(ATHETA)
      DTHETA(IWRT) = ABS(ATHETA)
      EL(IWRT)=ET(IWRT) * SIN(ATHETA) * COS(ATHETA)
      STEEP(IWRT)=HNEW/WL
      DLR=4. * 3.14159265 * DXY /WL
      SDLR=SINH(DLR)
      IF (SINH(DLR).LT.1.E-10) SDLR=1.E-10
      CG(IWRT)=.5 * CXY * (1. + DLR/SDLR)
      P(IWRT)=8. * HNEW * HNEW * CG(IWRT)
      PL(IWRT)=P(IWRT) * SIN(ATHETA) * COS(ATHETA)
      RETURN
   20 THETA(IWRT)=3.14159
      GO TO 10
      END
```

Sample Output for Wave Program

NIGER PERIOD=6,ANG=0,HT=5

SET NO. 1, PERIOD = 6.00 SECS., RAY NO. 3, TIME STEP =221.2698SECS./

POINT	X	Y	ANGLE	DEPTH	MAX DIF	FIT	LENGTH	SPEED	HEIGHT	KR	KS	NEWH
1	46.1	24.0	90.0				184.33	30.72	5.00			
2	45.0	21.8	90.0	100.67	1.30	0.95	183.95	30.66	4.97	1.0000	0.9940	4.97
3	46.1	21.8	90.0	99.94	1.30	0.95	183.94	30.66	4.97	1.0000	0.9938	4.97
4	47.3	21.8	90.0	99.59	2.10	1.60	183.93	30.65	4.97	1.0000	0.9936	4.97
5	48.4	21.8	90.0	96.51	2.17	1.60	183.83	30.64	4.96	0.9999	0.9925	4.96
6	49.5	21.8	89.9	92.03	3.46	2.83	183.66	30.61	4.95	0.9998	0.9904	4.95
7	50.6	21.8	89.9	88.10	3.61	2.83	183.45	30.58	4.94	0.9995	0.9882	4.93
8	51.7	21.8	89.8	81.29	5.03	3.52	182.95	30.49	4.91	0.9990	0.9833	4.91
9	52.8	21.8	89.8	77.36	5.29	3.52	182.55	30.42	4.89	0.9985	0.9798	4.88
10	53.9	21.8	89.6	76.34	6.99	4.10	182.43	30.40	4.88	0.9978	0.9788	4.87
11	55.0	21.8	89.5	72.76	7.33	4.10	181.93	30.32	4.86	0.9965	0.9749	4.84
12	56.1	21.8	89.2	70.56	2.58	2.10	181.56	30.26	4.83	0.9941	0.9723	4.81
13	57.2	21.8	88.9	67.69	2.69	2.10	181.01	30.17	4.80	0.9903	0.9686	4.76
14	58.3	21.9	88.5	60.35	4.32	1.74	179.07	29.85	4.72	0.9849	0.9575	4.66
15	59.4	21.9	88.0	56.50	4.62	1.74	177.68	29.61	4.66	0.9793	0.9510	4.58
16	60.5	21.9	87.6	53.02	7.90	3.11	176.13	29.36	4.60	0.9737	0.9449	4.50
17	61.6	22.0	87.1	49.48	8.46	3.11	174.22	29.04	4.54	0.9686	0.9384	4.40
18	62.6	22.1	86.5	47.08	7.80	3.30	172.72	28.79	4.50	0.9638	0.9341	4.32
19	63.7	22.1	86.0	44.97	8.17	3.30	171.23	28.54	4.46	0.9595	0.9304	4.23
20	64.7	22.2	85.4	42.89	8.56	3.30	169.59	28.26	4.43	0.9558	0.9268	4.13
21	65.7	22.3	84.7	40.09	9.16	3.30	167.10	27.85	4.39	0.9529	0.9224	4.02
22	66.7	22.4	84.1	37.75	8.37	3.65	164.73	27.46	4.37	0.9509	0.9192	3.91
23	67.7	22.5	83.5	35.49	8.90	3.65	162.18	27.03	4.35	0.9484	0.9165	3.79
24	68.7	22.6	82.6	33.51	9.42	3.65	159.70	26.62	4.33	0.9459	0.9147	3.66
25	69.7	22.8	81.3	31.05	11.83	3.30	156.28	26.05	4.31	0.9430	0.9133	3.51
26	70.6	22.9	79.7	28.52	12.88	3.30	152.32	25.39	4.29	0.9404	0.9131	3.35
27	71.5	23.1	78.2	26.06	14.09	3.30	147.98	24.66	4.29	0.9382	0.9143	3.17
28	72.4	23.3	76.6	23.43	15.67	3.30	142.75	23.79	4.30	0.9368	0.9178	2.97
29	73.2	23.5	74.8	20.77	17.68	3.30	136.74	22.79	4.33	0.9371	0.9241	2.76
30	74.0	23.7	72.6	19.69	24.17	3.36	134.07	22.34	4.36	0.9392	0.9277	2.55
31	74.8	24.0	69.7	16.25	29.31	3.36	124.45	20.74	4.43	0.9385	0.9443	2.30
32	75.5	24.3	65.8	12.33	38.61	3.36	111.09	18.52	4.57	0.9349	0.9774	1.97
33	76.1	24.6	60.2	6.88	58.33	3.04	85.74	14.29	5.01	0.9288	1.0783	1.34
34	76.1	24.6	60.2	0.99	713.80	5.47	33.59	5.60	7.68	0.9227	1.6657	0.08

RAY STOPPED, NO CONVERGENCE FOR CURVATURE.

POINT	X	Y	IDIR	THETA	DTHETA	ET	EL	STEEP	CG	PL	P
2	45.0	21.8	R	0.137	0.137	0.36346E 05	0.49334E 04	0.27016E-01	0.15547E 02	0.41695E 03	0.30718E 04
3	46.1	21.8	R	2.832	2.832	0.36318E 05	-0.10545E 05	0.27010E-01	0.15555E 02	-0.89176E 03	0.30713E 04
4	47.3	21.8	R	2.699	2.699	0.36301E 05	-0.14047E 05	0.27005E-01	0.15558E 02	-0.11882E 04	0.30708E 04
5	48.4	21.8	R	2.553	2.552	0.36185E 05	-0.16721E 05	0.26983E-01	0.15595E 02	-0.14185E 04	0.30697E 04
6	49.5	21.8	R	2.445	2.444	0.35978E 05	-0.17710E 05	0.26944E-01	0.15660E 02	-0.15101E 04	0.30677E 04
7	50.6	21.8	R	2.522	2.520	0.35739E 05	-0.16921E 05	0.26899E-01	0.15730E 02	-0.14508E 04	0.30643E 04
8	51.7	21.8	R	2.680	2.677	0.35219E 05	-0.14115E 05	0.26812E-01	0.15886E 02	-0.12257E 04	0.30582E 04
9	52.8	21.8	R	2.542	2.538	0.34798E 05	-0.16267E 05	0.26740E-01	0.16001E 02	-0.14258E 04	0.30501E 04
10	53.9	21.8	R	2.344	2.338	0.34600E 05	-0.17289E 05	0.26691E-01	0.16034E 02	-0.15195E 04	0.30411E 04
11	55.0	21.8	R	2.248	2.239	0.34064E 05	-0.16565E 05	0.26592E-01	0.16161E 02	-0.14715E 04	0.30260E 04
12	56.1	21.8	R	1.942	1.928	0.33559E 05	-0.11004E 05	0.26474E-01	0.16249E 02	-0.98482E 03	0.30034E 04

13	57.2	21.8	R	2.115	2.095	0.32828E 05	-0.14226E 05	0.26304E-01	0.16375E 02	-0.12869E 04	0.29697E 04
14	58.3	21.9	R	2.330	2.303	0.31172E 05	-0.15498E 05	0.26050E-01	0.16753E 02	-0.14499E 04	0.29164E 04
15	59.4	21.9	R	2.346	2.312	0.29866E 05	-0.14874E 05	0.25798E-01	0.16983E 02	-0.14217E 04	0.28547E 04
16	60.5	21.9	R	2.462	2.420	0.28510E 05	-0.14138E 05	0.25539E-01	0.17206E 02	-0.13811E 04	0.27851E 04
17	61.6	22.0	R	2.404	2.353	0.27035E 05	-0.13517E 05	0.25279E-01	0.17443E 02	-0.13533E 04	0.27067E 04
18	62.6	22.1	R	2.180	2.119	0.25736E 05	-0.11450E 05	0.24987E-01	0.17604E 02	-0.11670E 04	0.26231E 04
19	63.7	22.1	R	2.223	2.153	0.24454E 05	-0.11229E 05	0.24676E-01	0.17746E 02	-0.11638E 04	0.25344E 04
20	64.7	22.2	R	2.274	2.193	0.23148E 05	-0.10964E 05	0.24357E-01	0.17882E 02	-0.11561E 04	0.24407E 04
21	65.7	22.3	R	2.435	2.343	0.21626E 05	-0.10809E 05	0.24071E-01	0.18053E 02	-0.11678E 04	0.23365E 04
22	66.7	22.4	R	2.565	2.462	0.20162E 05	-0.98552E 04	0.23744E-01	0.18182E 02	-0.10877E 04	0.22253E 04
23	67.7	22.5	R	2.283	2.169	0.18620E 05	-0.86654E 04	0.23358E-01	0.18287E 02	-0.97708E 03	0.20995E 04
24	68.7	22.6	R	2.189	2.060	0.17091E 05	-0.70858E 04	0.22902E-01	0.18359E 02	-0.81457E 03	0.19647E 04
25	69.7	22.8	R	2.146	1.994	0.15398E 05	-0.57628E 04	0.22455E-01	0.18416E 02	-0.67908E 03	0.18144E 04
26	70.6	22.9	R	2.179	1.999	0.13642E 05	-0.51528E 04	0.21967E-01	0.18425E 02	-0.62333E 03	0.16502E 04
27	71.5	23.1	R	2.215	2.009	0.11883E 05	-0.45633E 04	0.21410E-01	0.18374E 02	-0.56661E 03	0.14755E 04
28	72.4	23.3	R	2.265	2.030	0.10091E 05	-0.40101E 04	0.20825E-01	0.18237E 02	-0.51231E 03	0.12892E 04
29	73.2	23.5	R	2.262	1.996	0.83273E 04	-0.31309E 04	0.20178E-01	0.17989E 02	-0.41189E 03	0.10955E 04
30	74.0	23.7	R	2.212	1.908	0.69983E 04	-0.21863E 04	0.19054E-01	0.17851E 02	-0.29111E 03	0.93181E 03
31	74.8	24.0	R	2.220	1.866	0.52831E 04	-0.14685E 04	0.18509E-01	0.17227E 02	-0.20327E 03	0.73129E 03
32	75.5	24.3	R	2.228	1.806	0.34414E 04	-0.77935E 03	0.17713E-01	0.16079E 02	-0.11280E 03	0.49808E 03
33	76.1	24.6	R	2.138	1.618	0.12363E 04	-0.57772E 02	0.15657E-01	0.13211E 02	-C.89010E 01	0.19047E 03
34	76.1	24.6	R	2.304	1.783	0.17801E 01	-0.36662E 00	0.24227E-02	0.55365E 01	-0.60422E-01	0.29338E 00

POWER GRADIENT = -0.444677E 02 LONGSHORE POWER GRADIENT = 0.209132E 01 DIS = 0.428085E 01
RAY STOPPED, NO CONVERGENCE FOR CURVATURE.